Stéphane Monteil, monteil@in2p3.fr

Clermont University – IN2P3 / CNRS

Some authoritative literature about the lecture :

- BaBar physics book: http://www.slac.stanford.edu/pubs/slacreports/slac-r-504.html
- LHCb performance TDR: http://cdsweb.cern.ch/record/630827?ln=en
- A. Höcker and Z. Ligeti: CP Violation and the CKM Matrix. hep-ph/0605217
- To come next: the Belle II Physics TDR.

World Averages and Global Fits:

- Heavy Flavour Averaging Group: http://www.slac.stanford.edu/xorg/hfag/
- CKMfitter: http://ckmfitter.in2p3.fr/
- UTFit: http://www.utfit.org/

Disclaimers

- This is an experimentalist point of view on a subject which is all about intrications between experiment and theory.

- I won’t discuss (at all) CP violation in the lepton sector.

- The main machines in question here are the, PEPII (SLAC, US), KEKB (KEK, Japan) and LHC (CERN, EU). Former experiments played a pioneering role: LEP (CERN, EU), CLEO (CESR, US) and TeVatron (Fermilab, US).

- Most of the material concerning global tests of the SM and above is taken from the CKMfitter group results (assumed bias) and Heavy Flavour Averaging Group (and hence the experiments themselves). I borrowed materials in presentations from colleagues which I tried to cite correctly.

Motivation

- In any HEP physics conference summary talk, you will find this plot, stating that (heavy) flavours and *CP* violation physics is a pillar of the Standard Model.

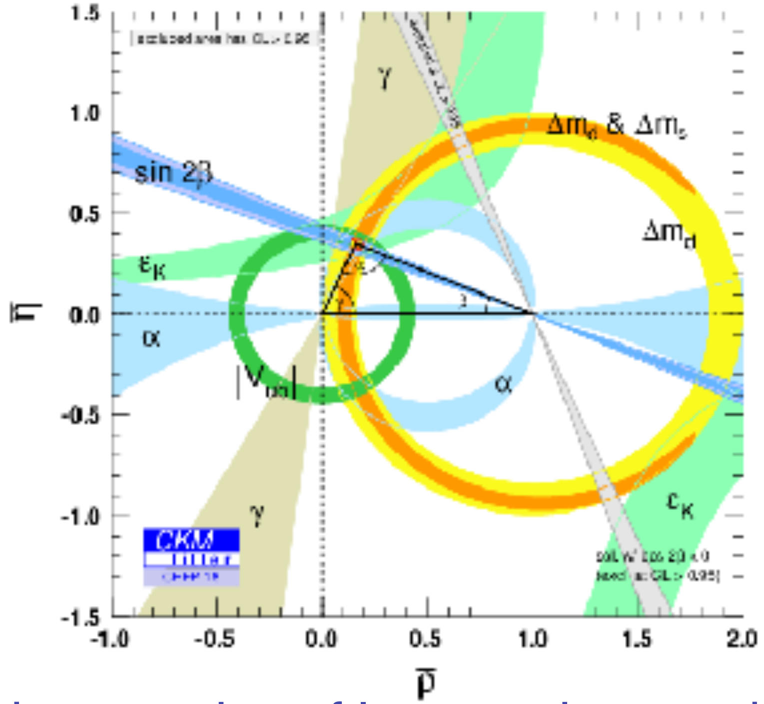

- One objective of these series of lectures is to undress this plot.

A more detailed outline

1. Introduction: setting the scene. History and recent past of the parity violation experiments. The discovery of the *CP* violation.

2. Few elements about CKM. Machine and experiments. Main observables and measurements relevant to study *CP* violation.

3. The global fit of the SM: CKM profile.

4. New Physics exploration with current data: two examples.

Outline of the second chapter

1. Elements of the Kobayashi-Maskawa paradigm
2. Machine and experiments. Main observables and measurements relevant to study *CP* violation.
3. The global fit of the SM: CKM profile.
4. New Physics exploration with current data: two examples.

2.1 Introduction: the unitarity triangle.

•You have been taught by Sébastien that the Higgs field gives mass to bosons and fermions (quarks and leptons) through the Yukawa couplings but this is not the end of the story:

$$\mathcal{L}_{cc}^{\text{quarks}} = \frac{g}{2\sqrt{2}} W_\mu^\dagger \Big[\sum_{ij} \bar{u}_i(q_2)\gamma^\mu(1-\gamma^5) V_{ij} d_j\Big] + \text{h.c}$$

• After spontaneous symmetry breaking, and once the mass matrices are diagonalised, it determines also how the mass and weak eigenstates are related. This is the CKM matrix. As for the (fermion) masses, nothing is predicted except the mass matrix must be unitary and complex.

$$\begin{pmatrix} u \\ s \\ b \end{pmatrix}_{EW} = \begin{pmatrix} V_{ud} & V_{us} & V_{ub} \\ V_{cd} & V_{cs} & V_{cb} \\ V_{td} & V_{ts} & V_{tb} \end{pmatrix} \begin{pmatrix} u \\ s \\ b \end{pmatrix}_{MASS}$$

2.1 Introduction: the unitarity triangle.

- Weak eigenstates are therefore a mixture of mass eigenstates, controlled by the Cabibbo-Kobayashi-Maskawa elements V_{ij}: flavour changing charged currents between quark generations.

- This matrix is a 3X3, unitary, complex, and hence described by means of four parameters: 3 rotation angles and a phase. The latter makes possible the CP symmetry violation in the Standard Model.

- These four parameters are free parameters of the SM. As for electroweak gauge precision tests, they must be measured with some redundancy and the SM hypothesis is to be falsified by a consistency test. We will review in this lecture this overall test. But let’s define first the parameters.

2.1 Introduction: the unitarity triangle.

- *Homework 2:*

Prove that a 3x3 unitary complex quark mixing matrix is described by four parameters: three real parameters, one complex.

Hint: the phase of each quark field can/must be redefined relative to a global phase. You can advantageously start by showing that a 2x2 unitary matrix is described by one single real parameter.

2.1 Introduction: the unitarity triangle. Parameterisation

$$V_{\mathrm{CKM}} = \begin{pmatrix} V_{ud} & V_{us} & V_{ub} \\ V_{cd} & V_{cs} & V_{cb} \\ V_{td} & V_{ts} & V_{tb} \end{pmatrix}$$

Consider the Wolfenstein parametrization as in EPJ C41:1-131,2005 : unitary-exact at each order and phase- convention independent:

$$\lambda^2 = \frac{|V_{us}|^2}{|V_{ud}|^2 + |V_{us}|^2}, \quad A^2\lambda^4 = \frac{|V_{cb}|^2}{|V_{ud}|^2 + |V_{us}|^2} \quad \text{and} \quad \bar{\rho} + i\bar{\eta} = -\frac{V_{ud}V_{ub}^*}{V_{cd}V_{cb}^*}$$

- λ is measured from $|V_{ud}|$ and $|V_{us}|$ in superallowed beta decays and semileptonic kaon decays, respectively.

- *A* is further determined from $|V_{cb}|$, measured from semileptonic charmed *B* decays.

- The last two parameters are to be determined from angles and sides measurements of the CKM unitarity triangle.

2.1 Introduction: the unitarity triangle. Parameterisation

$$V_{\mathrm{CKM}} = \begin{pmatrix} V_{ud} & V_{us} & V_{ub} \\ V_{cd} & V_{cs} & V_{cb} \\ V_{td} & V_{ts} & V_{tb} \end{pmatrix}$$

$$\lambda^2 = \frac{|V_{us}|^2}{|V_{ud}|^2 + |V_{us}|^2} \;, \quad A^2\lambda^4 = \frac{|V_{cb}|^2}{|V_{ud}|^2 + |V_{us}|^2} \quad \text{and} \quad \bar{\rho} + i\bar{\eta} = -\frac{V_{ud}V_{ub}^*}{V_{cd}V_{cb}^*}$$

$$V_{\mathrm{CKM}} = \begin{pmatrix} 1-\lambda^2/2 & \lambda & A\lambda^3(\rho - i\eta) \\ -\lambda & 1-\lambda^2/2 & A\lambda^2 \\ A\lambda^3(1-\rho-i\eta) & -A\lambda^2 & 1 \end{pmatrix} + \mathcal{O}(\lambda^4).$$

2.1 Introduction: the unitarity triangle. Representation

- An elegant way to represent the unitarity relations is to display them in the complex plane.

- $$\frac{V_{ud}V_{ub}^*}{V_{cd}V_{cb}^*} + \frac{V_{cd}V_{cb}^*}{V_{cd}V_{cb}^*} + \frac{V_{td}V_{tb}^*}{V_{cd}V_{cb}^*} = 0.$$

- The area of the triangle is half the Jarlskog invariant and measures the magnitude of the *CP* violation:

$$J \sum_{\sigma\gamma=1}^{3} \epsilon_{\mu\nu\sigma}\epsilon_{\alpha\beta\gamma} = \mathrm{Im}(V_{\mu\alpha}V_{\nu\beta}V_{\mu\beta}^*V_{\nu\alpha}^*) \,,$$

$$J = A^2\lambda^6\eta(1-\lambda^2/2) \simeq 10^{-5}$$

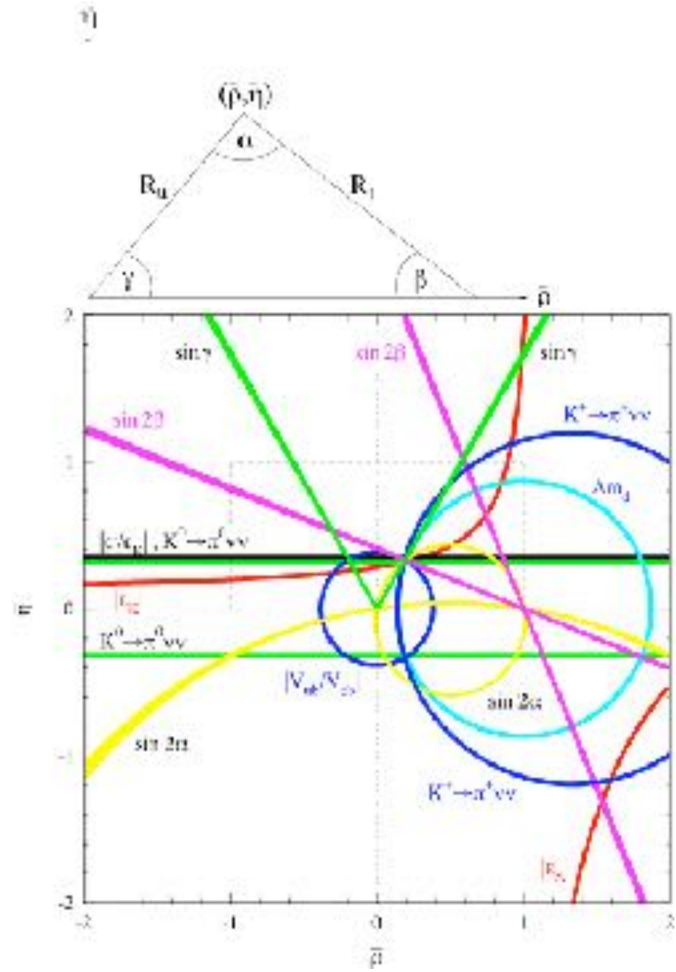

2.1 Introduction: the unitarity triangle. Definitions.

- Sides and angles of the unitarity triangle.

- Normalization given by the matrix element $V_{cd} \cdot V_{cb}^*$.

$$R_u = \left| \frac{V_{ud} V_{ub}^*}{V_{cd} V_{cb}^*} \right| = \sqrt{\bar{\rho}^2 + \bar{\eta}^2} \,,$$
$$R_t = \left| \frac{V_{td} V_{tb}^*}{V_{cd} V_{cb}^*} \right| = \sqrt{(1-\bar{\rho})^2 + \bar{\eta}^2} \,.$$

$$\alpha = \arg\left(- \frac{V_{td} V_{tb}^*}{V_{ud} V_{ub}^*} \right),$$
$$\beta = \pi - \arg\left(\frac{V_{td} V_{tb}^*}{V_{cd} V_{cb}^*} \right),$$
$$\gamma = \arg\left(- \frac{V_{ud} V_{ub}^*}{V_{cd} V_{cb}^*} \right).$$

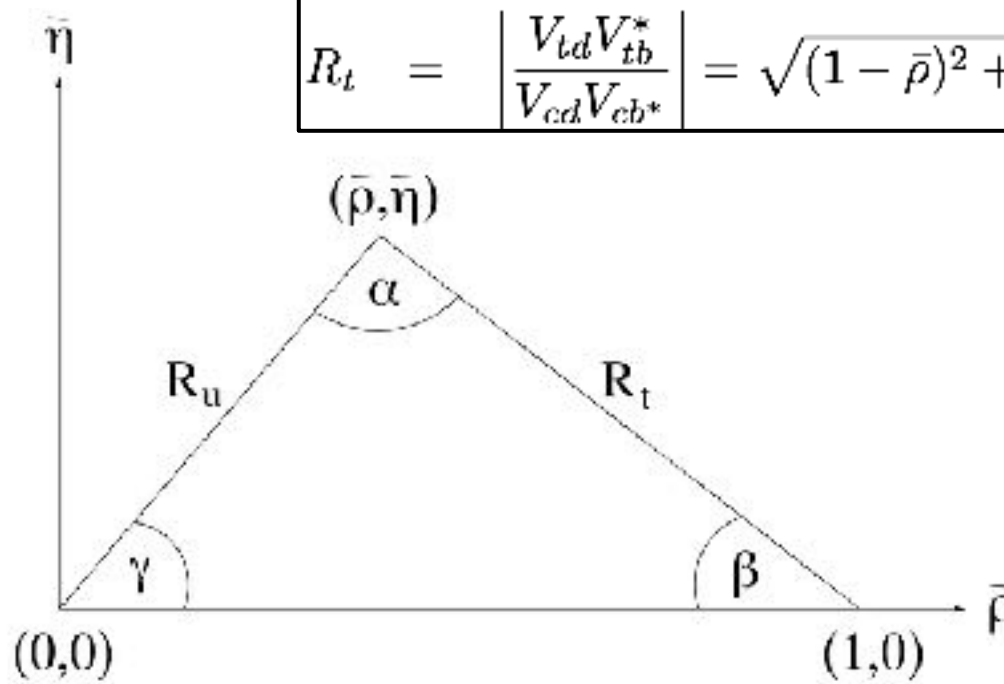

2.1 Introduction: the unitarity triangle. Definitions.

- Sides of the unitarity triangle. Towards the experimental constraints:

$$R_u = \left| \frac{V_{ud}V_{ub}^*}{V_{cd}V_{cb^*}} \right| = \sqrt{\bar{\rho}^2 + \bar{\eta}^2} \, ,$$

$$R_t = \left| \frac{V_{td}V_{tb}^*}{V_{cd}V_{cb^*}} \right| = \sqrt{(1-\bar{\rho})^2 + \bar{\eta}^2} \, .$$

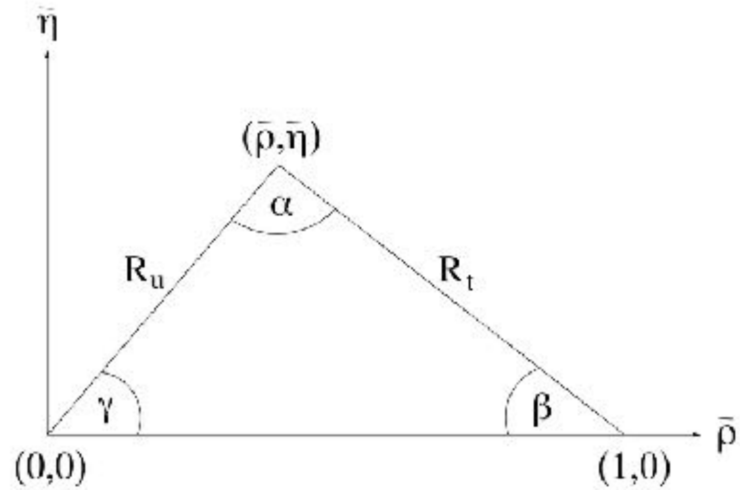

  - R_u is measured by the matrix elements V_{ub} and V_{cb} determined from the semileptonic decays of *b*-hadrons.

  - R_t implies the matrix element V_{td} and hence can be measured from the mixing of B^0 mesons.

2.1 Introduction: the unitarity triangle. Definitions.

- Angles of the unitarity triangle. Towards the experimental constraints:

$$\alpha = \arg\left(-\frac{V_{td}V_{tb}^*}{V_{ud}V_{ub}^*}\right),$$

$$\beta = \pi - \arg\left(\frac{V_{td}V_{tb}^*}{V_{cd}V_{cb}^*}\right),$$

$$\gamma = \arg\left(-\frac{V_{ud}V_{ub}^*}{V_{cd}V_{cb}^*}\right)$$

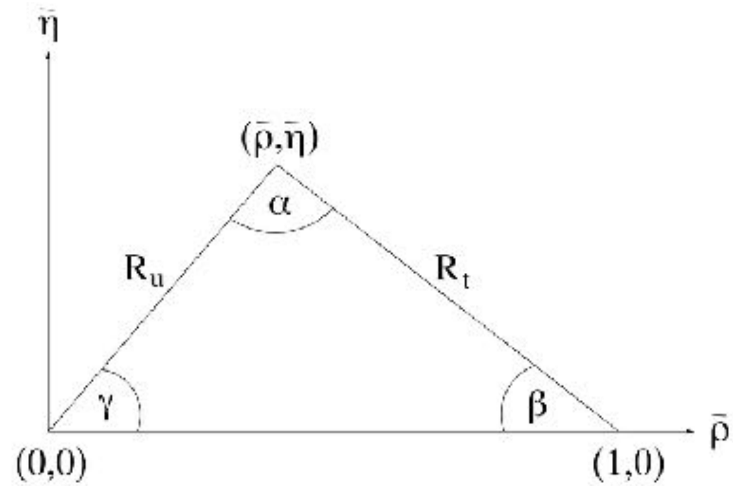

- The angle β is directly the weak mixing phase of the of B^0 mixing.
- The angle γ is the weak phase at work in the charmless *b*-hadrons decays.
- The angle α is nothing else than $(\pi-\beta-\gamma)$ and can be exhibited in processes where both charmless decays and mixing are present.

Note: a phase is not an observable. Only phase differences can be measured.

2.1 Introduction: the unitarity triangle. Experiments.

- Summary:

CP asymmetry in mixing and charmless b-hadron decays

Semileptonic b-hadron decays (LHCb in)

B meson mixing (LHCb in)

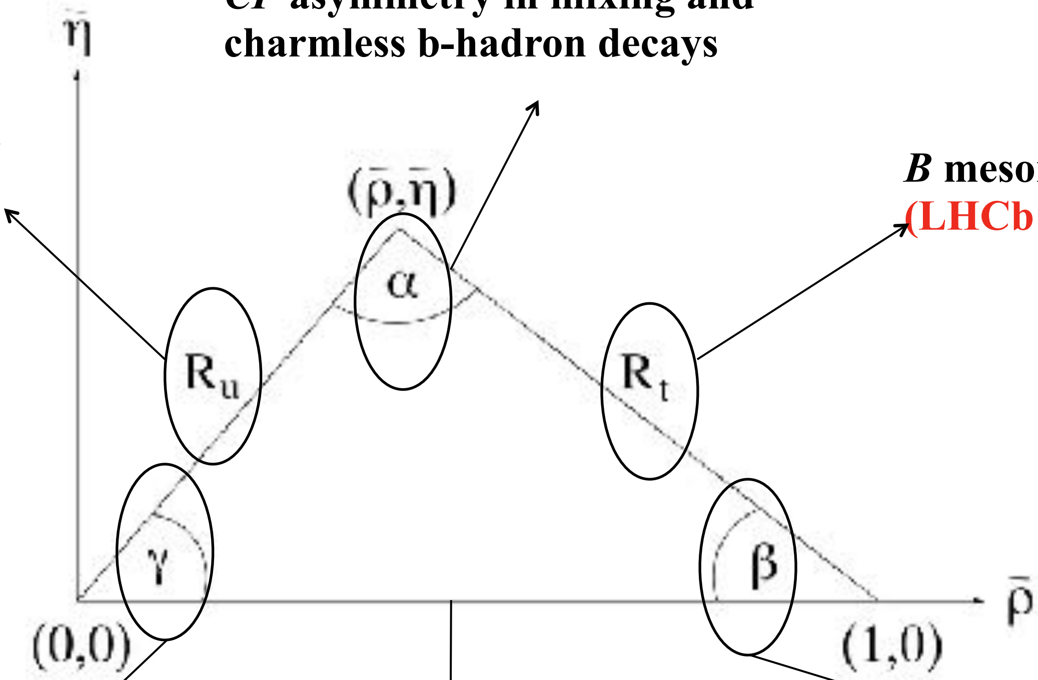

CP asymmetry in $b \rightarrow u$ *b*-hadron decays (LHCb in)

Overall normalisation given by $|V_{cd}V^{*}_{cb}|$, hence semileptonic *b* decays

CP asymmetry in mixing processes (LHCb in)

2.2 Machines and experiments.

There are many machines and experiments which are interested in the Flavour Physics and *CP* violation. As for their pioneering role, we'll mention ARGUS (DESY, Ge), CLEO (Cornell, US) and LEP (CERN, EU) experiments. The kaon sector is not in the scope of this lecture. Major results came from NA48 (CERN, EU) and KTeV (FNAL, US) though. Japan and Cern projects for kaon physics should bring extremely valuable results. Tevatron used to provide as well world class measurements in heavy flavours physics.

But the *B*-factories (now Belle II) and the LHCb experiment at LHC definitely dominate the landscape. Let's concentrate on this.

CP violation

2.2 Machines and experiments.

1. Coherent *b* quarks pair production: the *B*-factories.

2. Incoherent *b* quarks pair production: the Tevatron, LEP and LHC experiments.

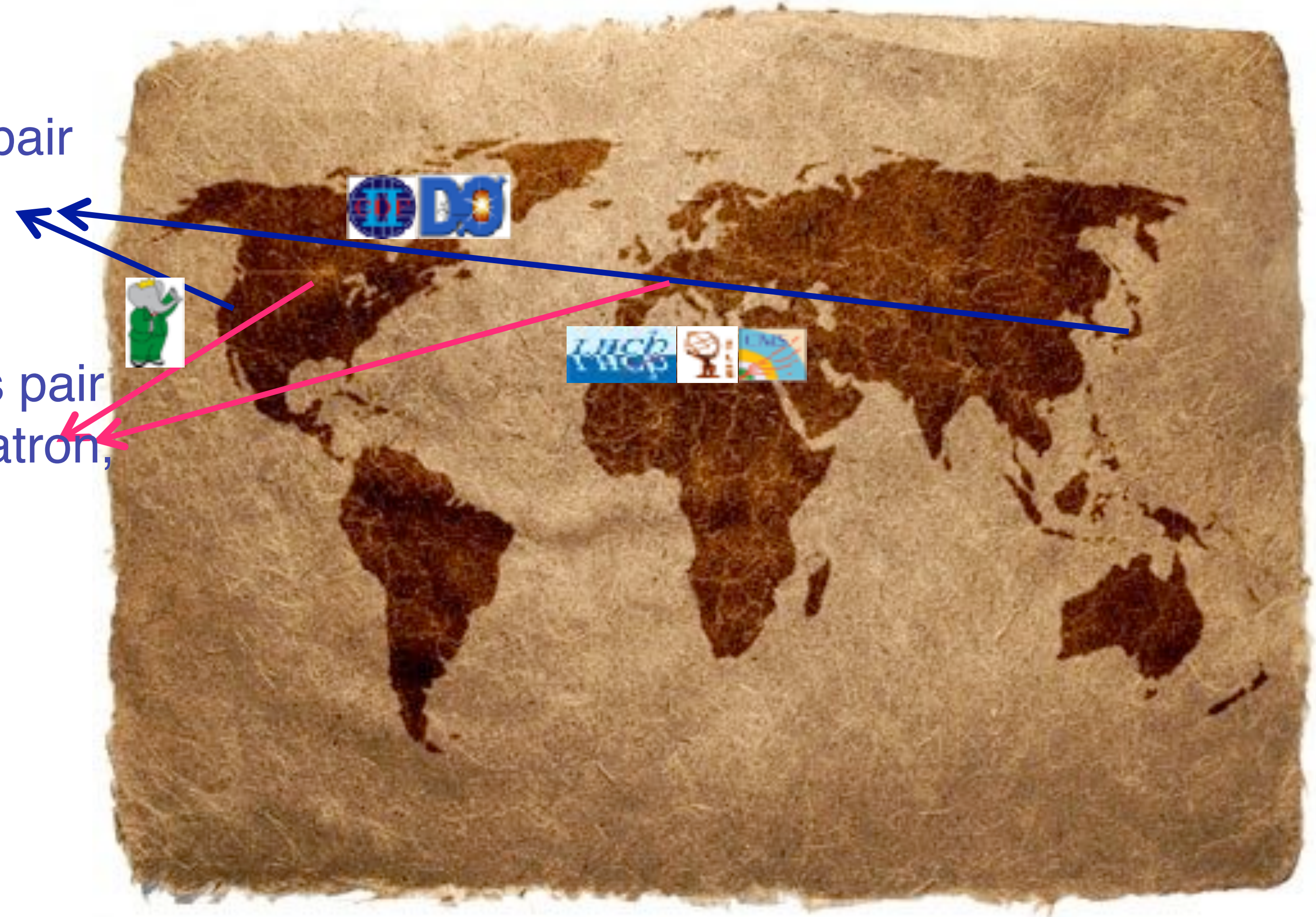

2.2 Machines and experiments: *B*-factories

The physics characteristics of the B factories at the Υ(4s):

- The series of Υ contains the Υ(4s), above the production threshold of *BB* pairs. Almost all (~96%) of the Υ(4s) decays.
- Coherent *B*-anti(*B*) production: when one decays, you know the flavour of the other at the same time. Ideal flavour tagging.
- Beams are asymmetric. The Υ(4s) is boosted allowing time separation between the two *B* mesons.
- No hadronisation. Very clean experimental environment.

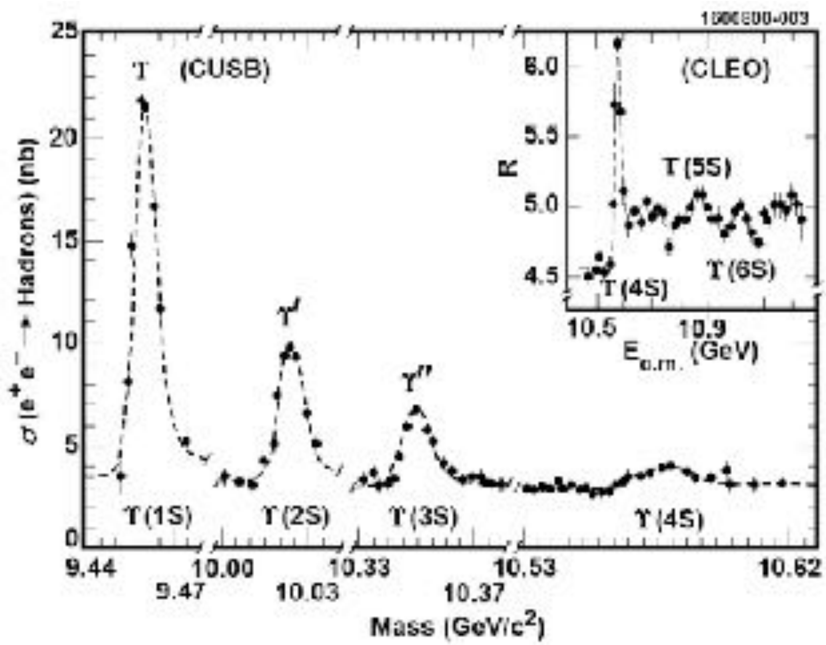

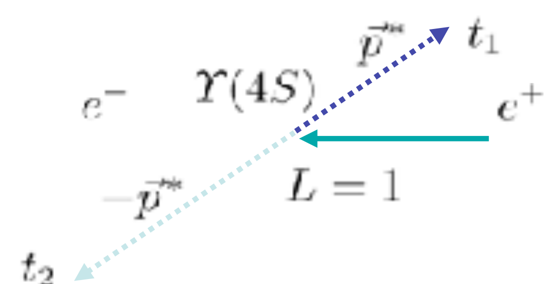

2.2 Machines and experiments: *B*-factories

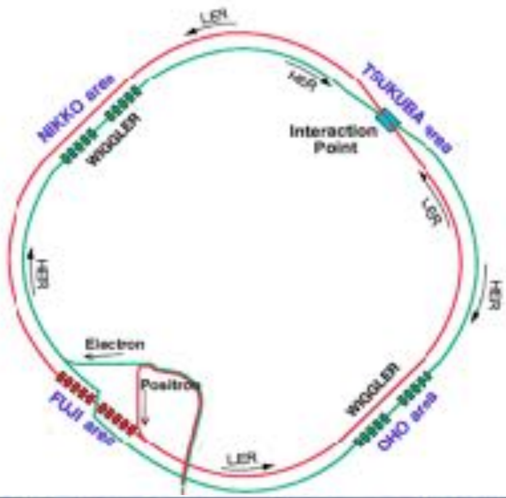

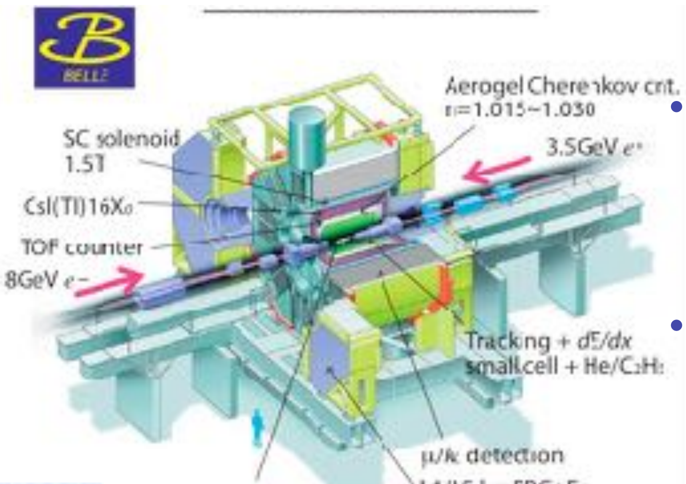

- KEKB – Belle – Japan.
  8 vs 3.5 GeV. βγ=0.425
- PEPII – BaBar – US.
  9 vs 3.1 GeV. βγ=0.56.

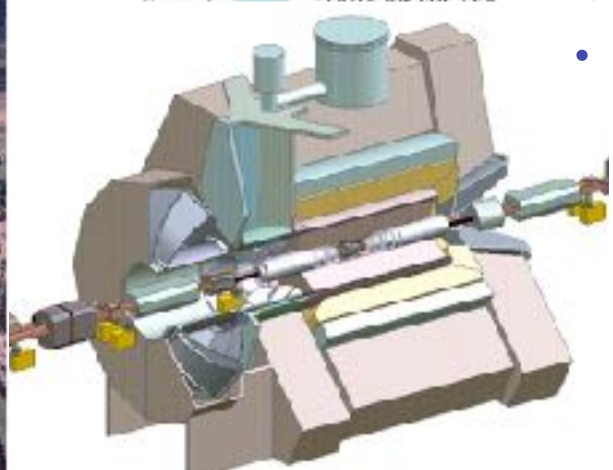

- Common detector characteristics:
  excellent vertexing and particle identification w/ Cerenkov imaging detectors.

2.2 Machines and experiments: *B*-factories

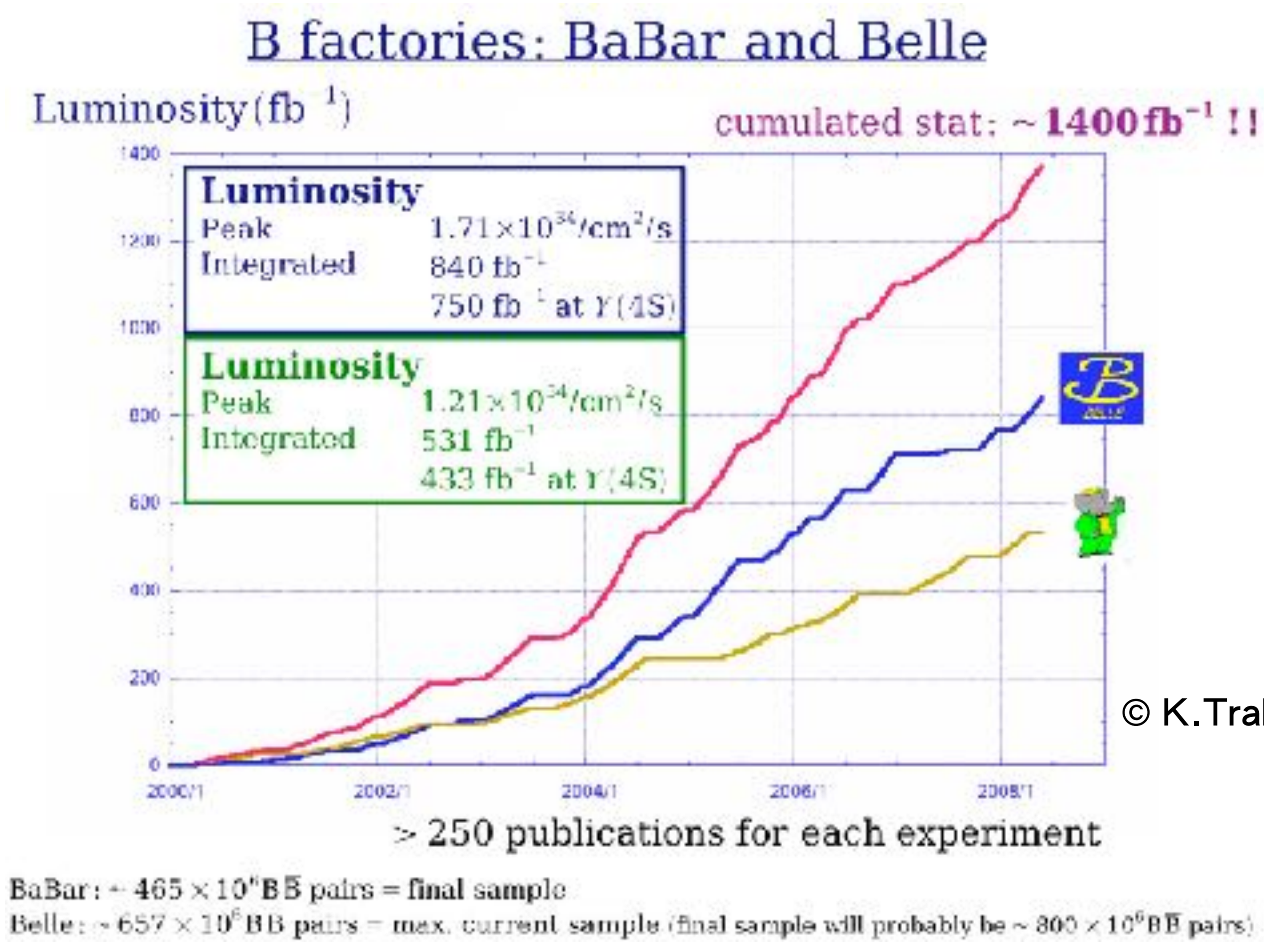

© K.Trabelsi

2.2 Machines and experiments: *hadron colliders*

The physics characteristics of the hadron colliders at high energy (some are playing at electron colliders):

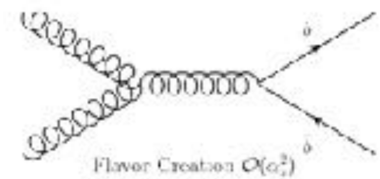

- There is hadronisation. Busy hadronic environment.

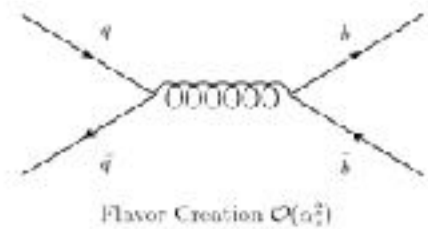

- Incoherent *b* quarks pair production. Flavour tagging is (much) less efficient than at *B*-factories.
- All the *b*-hadrons species can be produced. Unique laboratory for *b*-baryons and charm *B* meson.

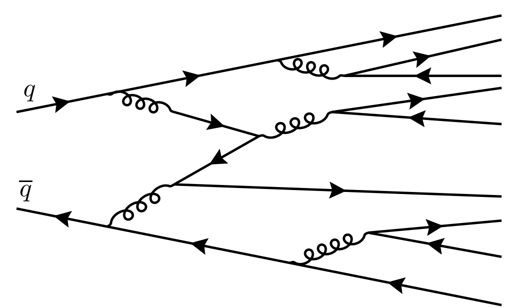

- High production cross-sections and hence high statistics (but a trigger strategy is required).
- Energy: *b*-hadrons do receive an important boost. Facilitates vertexing capability to identify the b-hadron decay vertex.

2.2 Machines and experiments: *ppbar colliders*

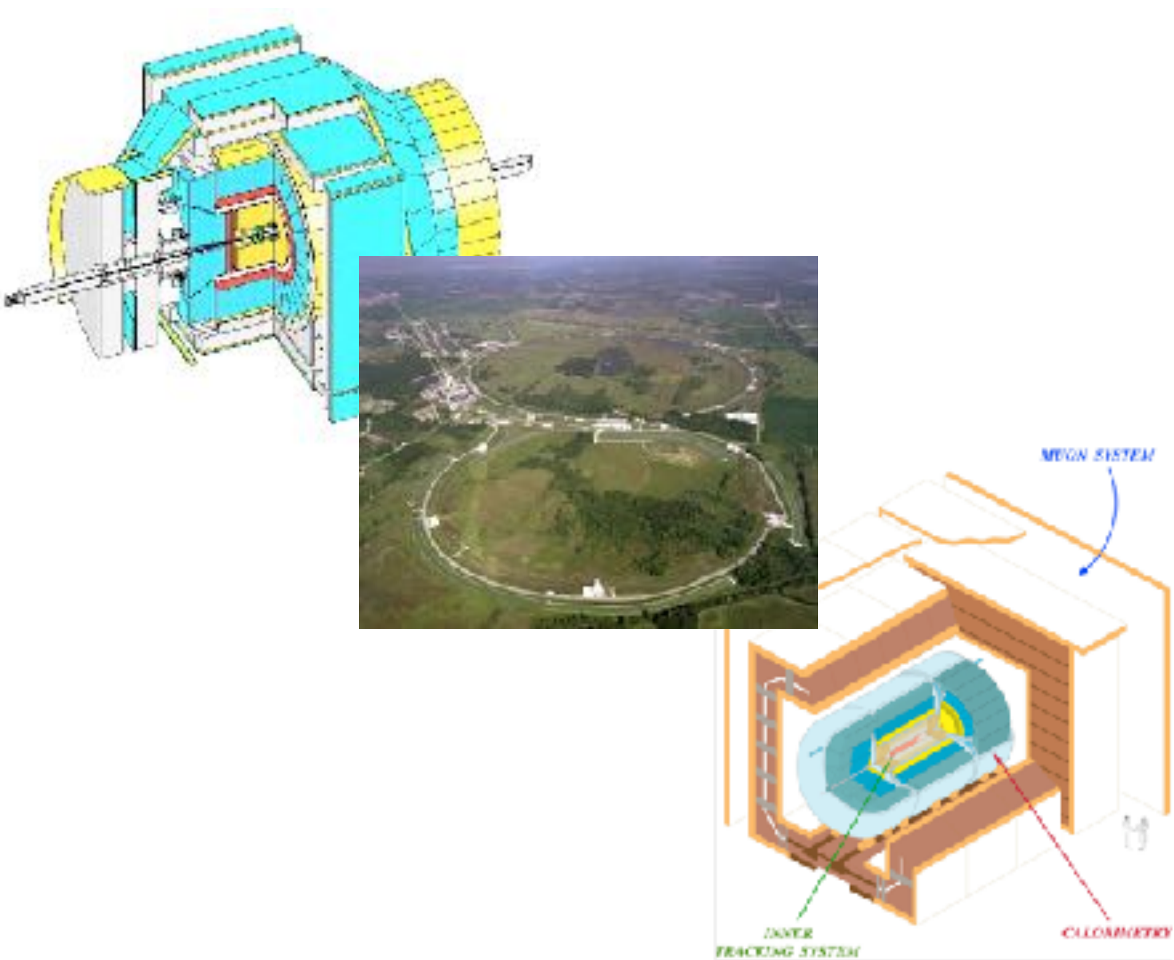

- CDF and D0 are multipurpose experiments.
- D0 has an excellent muon coverage.
- CDF has a flexible trigger and excellent tracking for *b*-hadron Physics.

2.2 Machines and experiments: the *large gluon collider*

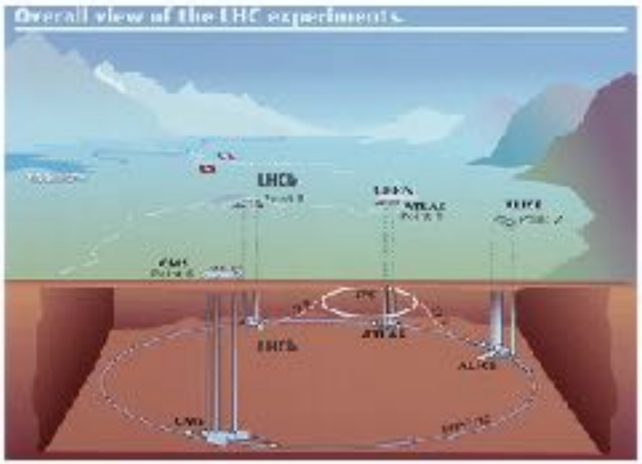

- ATLAS and CMS are general purpose experiments w/ 4π coverage. Flavour physics program however.
- LHCb is on the contrary a spectrometer. The shape of it is driven by the angular distribution of the bea

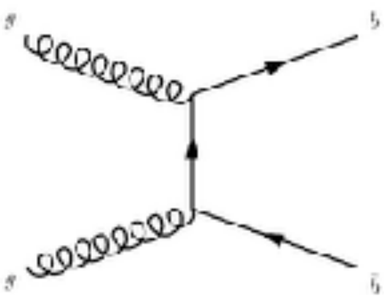

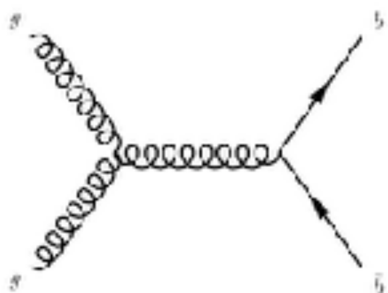

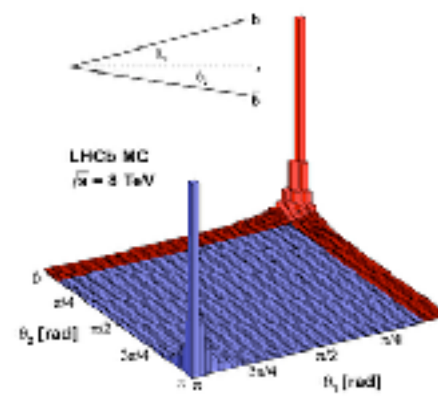

2.2 Machines and experiments: the *large gluon collider*

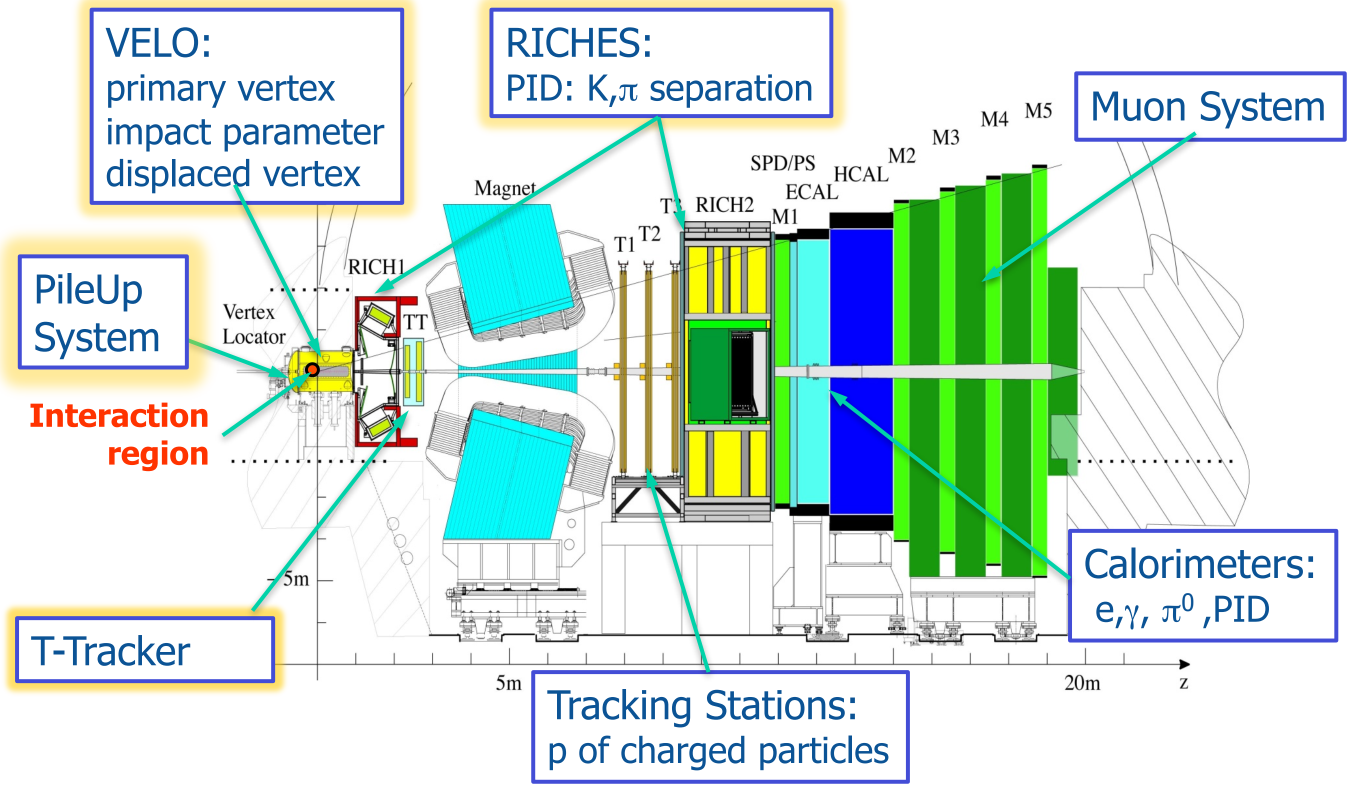

Design: excellent vertexing, excellent particle identification, flexible trigger. All this advertised in the success story relation prepared by M. Teklyshlin.

2.2 Machines and experiments: the *large gluon collider*

For those of you working on Atlas and CMS, the luminosity is lowered in LHCb by displacing the beams. On another hand the luminosity is levelled constantly. Ideas to generalise this to all LHC experiments in 2015.

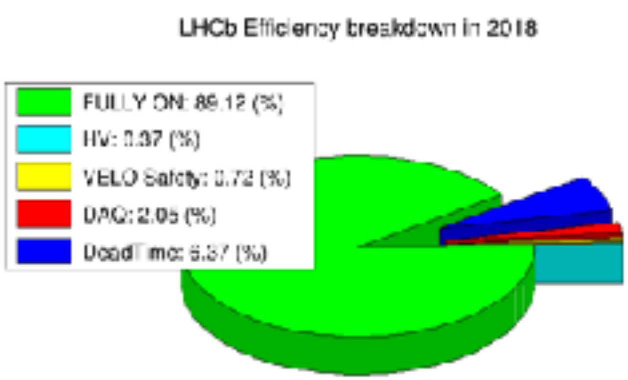

2.2 Machines and experiments: the *large gluon collider*

For those of you working on Atlas and CMS, the luminosity is lowered in LHCb by displacing the beams. On another hand the luminosity is levelled constantly. Ideas to generalise this to all LHC experiments in 2015.

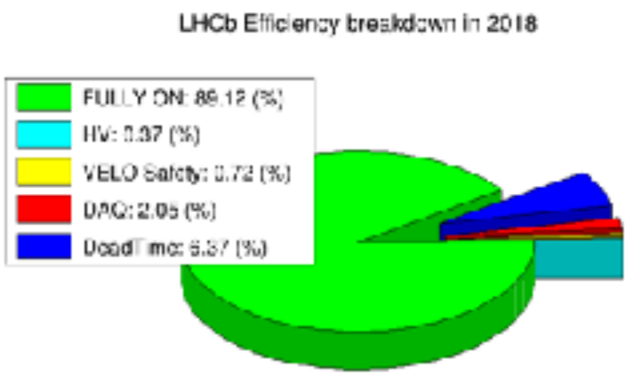

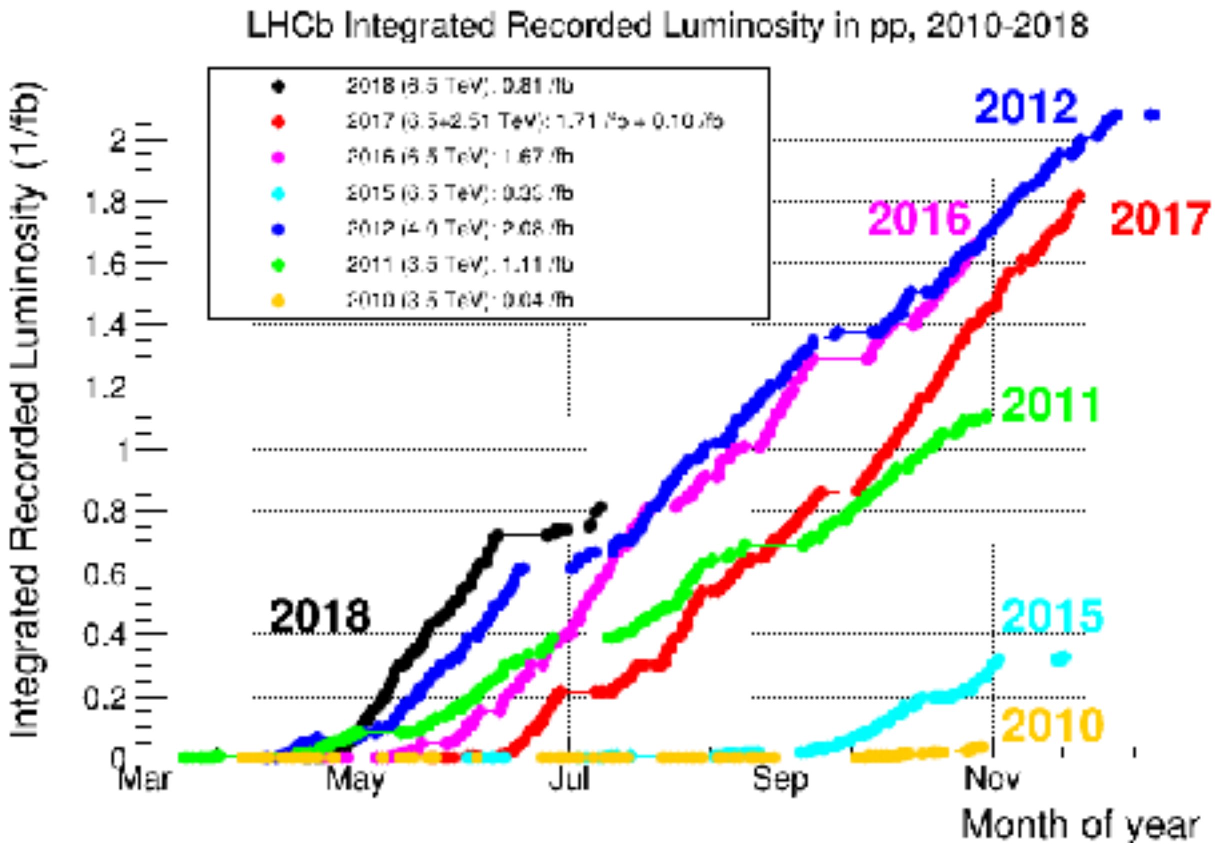

2.2 Machines and experiments: the *large gluon collider*

For those of you working on Atlas and CMS, the luminosity is lowered in LHCb by displacing the beams. On another hand the luminosity is levelled constantly. Ideas to generalise this to all LHC experiments in 2015.

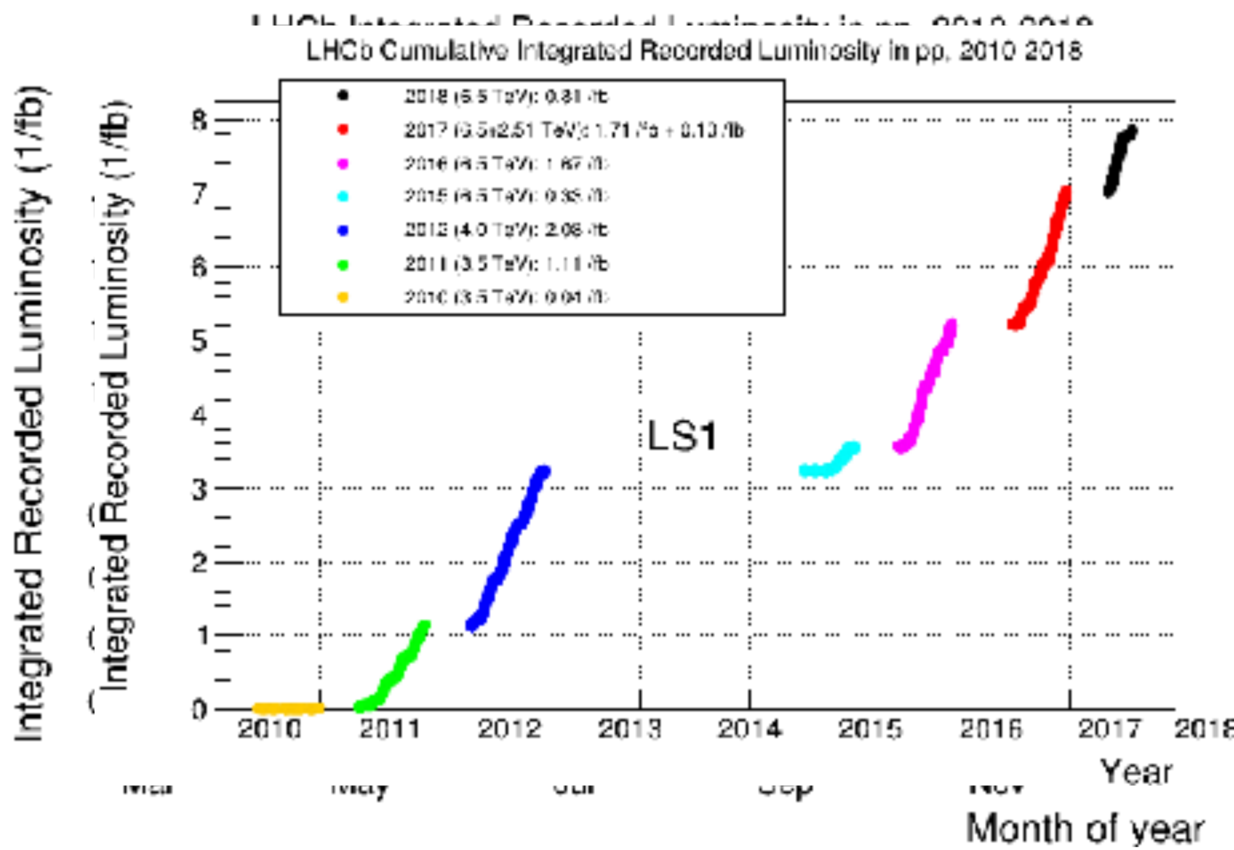

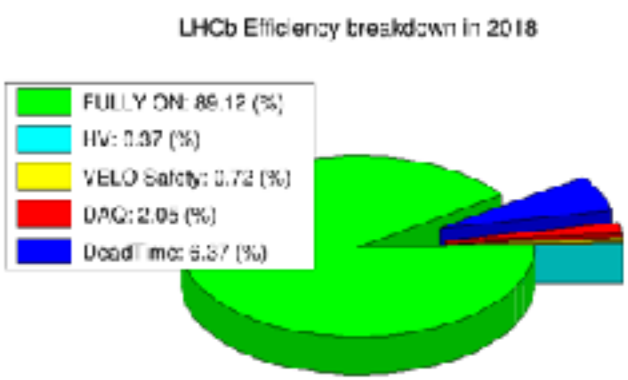

We move now towards the description of the observables, *CP*-violating but also *CP*-conserving, useful to constrain the CKM SM paradigm.

2.3 CP-conserving Observables

- Magnitudes of the matrix elements:
  - **$|V_{ud}|$ and $|V_{us}|$.**
  - **2.3.1 $|V_{ub}|$ and $|V_{cb}|$.**
- Frequency of B^0 oscillations:
  - **2.3.2 Δm_d and Δm_s.**
- These are all *CP*-conserving quantities. But they do bring information on CP violation.

2.3.1 The Semileptonic branching ratios: the $|V_{ub}|$ and $|V_{cb}|$ matrix elements.

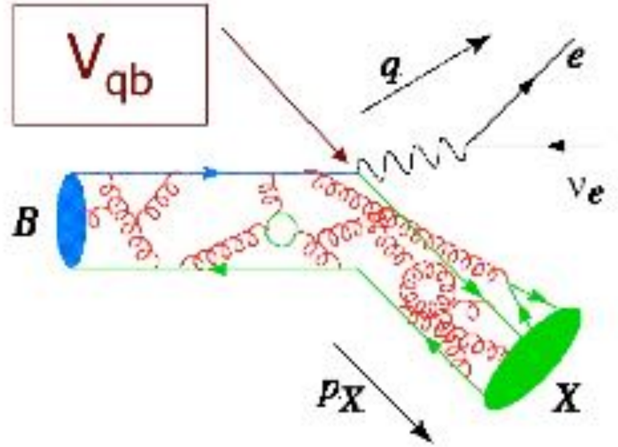

- The magnitude $|V_{ub}|$ is a key observable in constraining the CKM profile. It basically determines the side R_u of the CKM triangle.

- Pioneered in CLEO and LEP experiments. Nowadays *B* factories results dominate but LHCb entered the game.

- The matrix element V_{cb} enters everywhere in the triangle: as a normalisation and in dependencies in some observables.

- There are two ways to access the matrix elements: the inclusive (whatever the charmless *X* is) and exclusive (specific decays – mainly [B → π l ν]]) decay rates.

$$R_u = \left|\frac{V_{ud}V^*_{ub}}{V_{cd}V_{cb^*}}\right| = \sqrt{\bar{\rho}^2 + \bar{\eta}^2}\,,$$

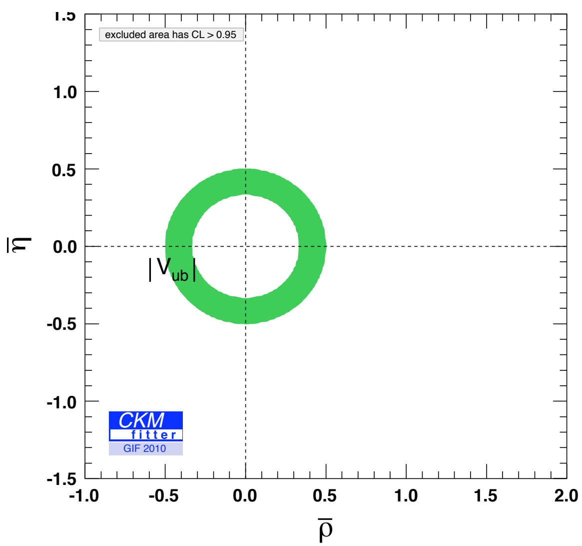

2.3.1 The Semileptonic branching ratios: the $|V_{ub}|$ and $|V_{cb}|$ matrix elements.

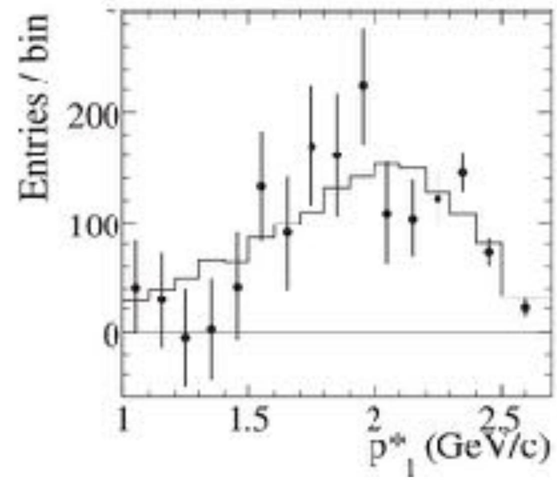

- The experimental technique shared by most of the analyses is to fully reconstruct one *B* decay (hadronic mode) and look at the other *B* of the event.

- Though the branching fractions of the fully reconstructed mode is small, the full kinematics of the other decay is constrained.

- Apply to exclusive and inclusive modes.

- It's in general crucial (at least for V_{ub}) that the background is measured in off-peak data.

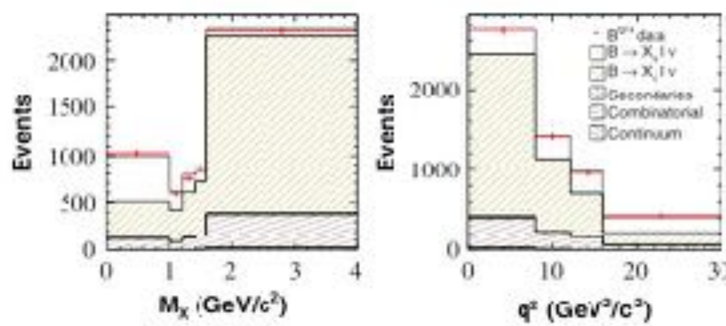

2.3.1 The Semileptonic branching ratios: the $|V_{ub}|$ and $|V_{cb}|$ matrix elements.

- The measurement of the branching fraction relies on the lepton detection and identification above a given threshold.

- To relate the measurements to the theoretical prediction, one has to extrapolate the experimental spectra and hence rely on models.

- As suggested by the diagram on the right, the hadronic content of the decay is rich. Several theoretical techniques compete.

- From the experimental point of view, charmless semileptonic are very difficult to separate from charm (in a ratio 1/150) .

- Very intense activity in this field of theory/ experiment collaboration.

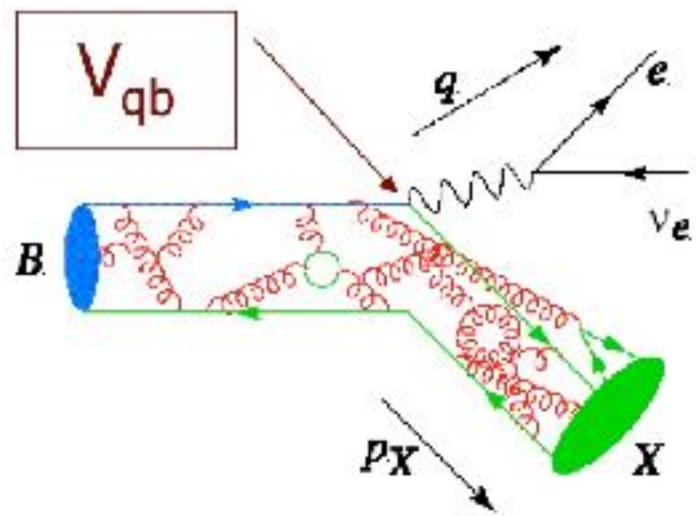

$$\Gamma_0 = \Gamma\left(b \to c[u] \ell \bar{\nu}\right) = \frac{G_F^2 |V_{c[u]b}|^2}{192\pi^3} m_b^5$$

$$\frac{\partial^3 \Gamma}{\partial E_\ell \partial q^2 \partial m_X} = \underbrace{\Gamma_0}_{\text{free quark decay}} \times f(E_\ell, q^2, m_X) \times \underbrace{\left[1 + \sum_n C_n \left(\frac{\Lambda_{QCD}}{m_b}\right)^n\right]}_{\text{Perturbative + non-perturbative corrections}}$$

2.3.1 The Semileptonic branching ratios: the $|V_{ub}|$ and $|V_{cb}|$ matrix elements.

- Inclusive $|V_{ub}|$ measurements: lepton endpoint.
- It's tempting to consider the pure $b \rightarrow u$ region.
- But for higher signal efficiency, the theoretical error is smaller. Get a compromise. Typically the cut is defined larger than 2 GeV.
- 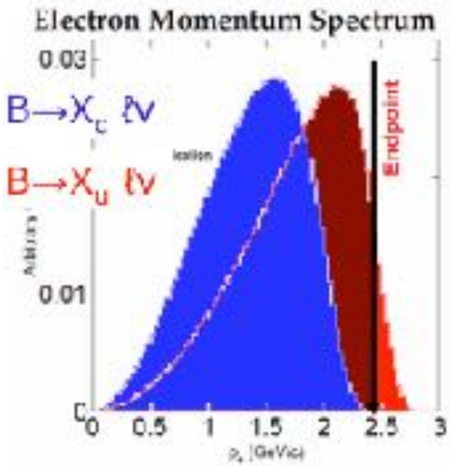

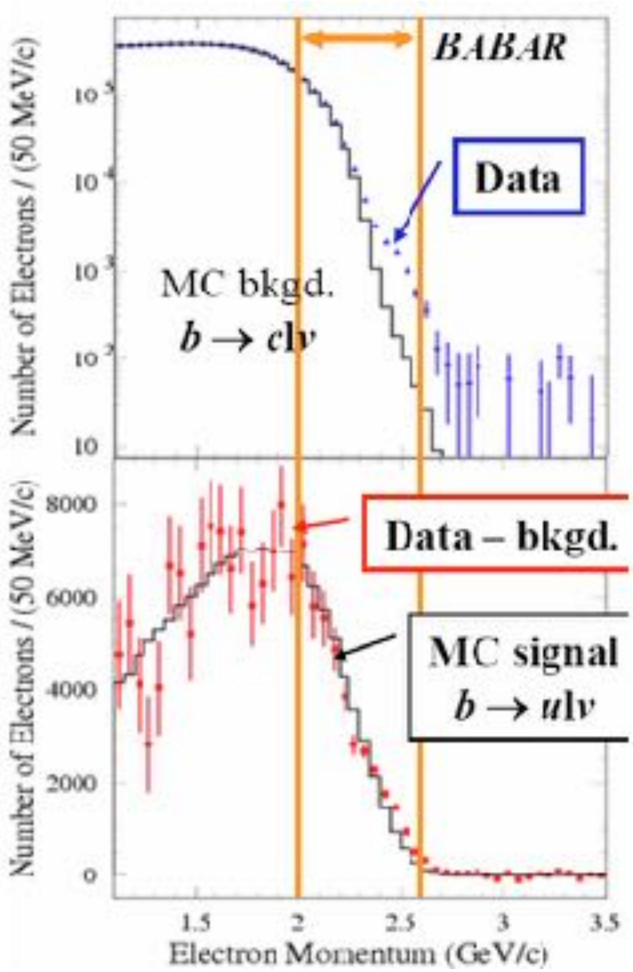

2.3.1 The Semileptonic branching ratios: the $|V_{ub}|$ and $|V_{cb}|$ matrix elements.

- Summary of inclusive $|V_{ub}|$ determinations:

- Shown are the extrapolation within the BLNP scheme. BLNP PRD 72 (2005), DGE arXiv:0806.4524, GGOU JHEP 0710 (2007) 058, ADFR Eur Phys J C 59 (2009) 831

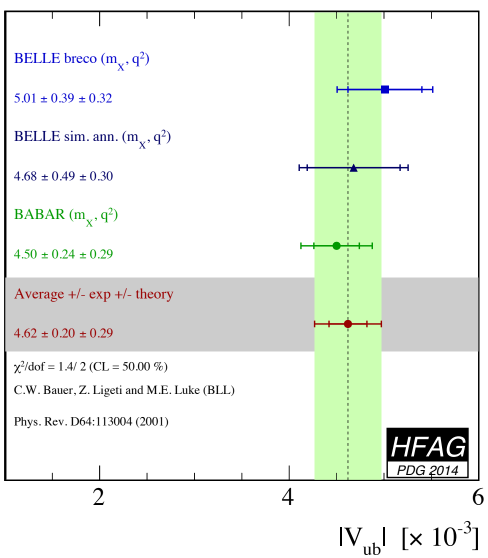

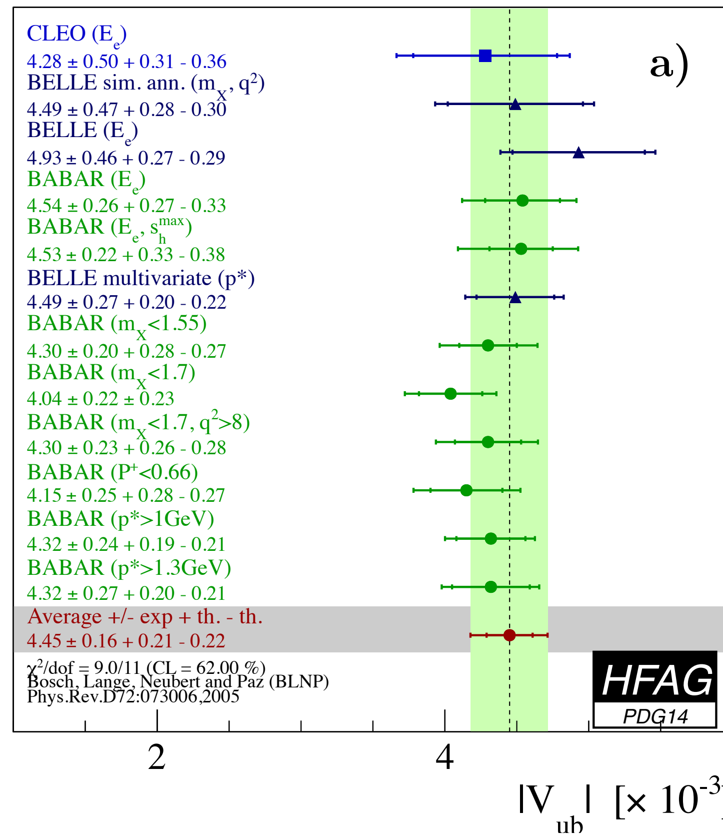

2.3.1 The Semileptonic branching ratios: the $|V_{ub}|$ and $|V_{cb}|$ matrix elements.

- Summary of exclusive $|V_{ub}|$ determinations:

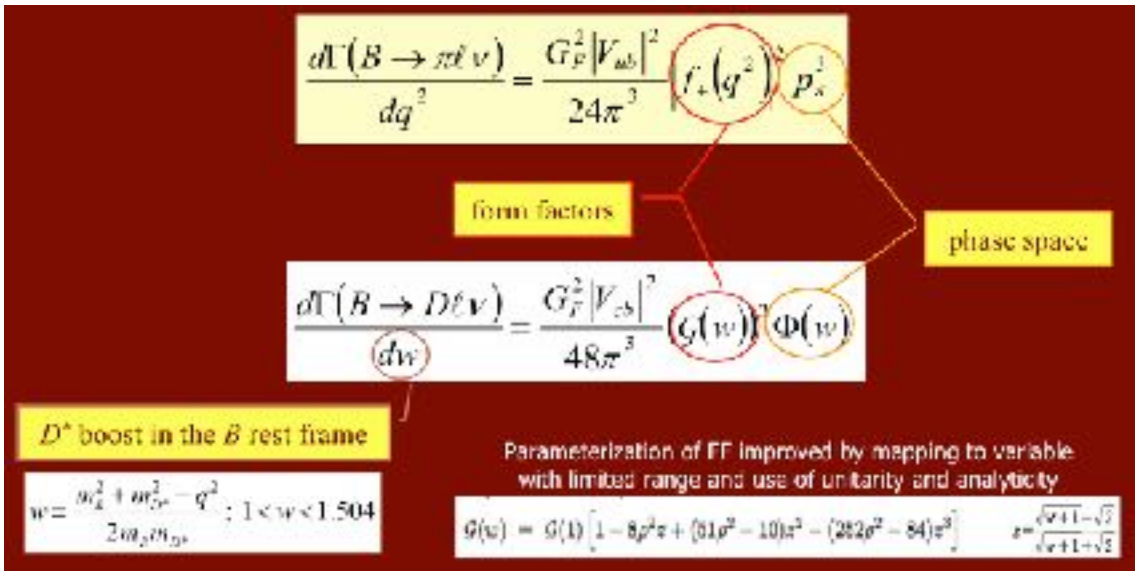

© R.Kowaleski

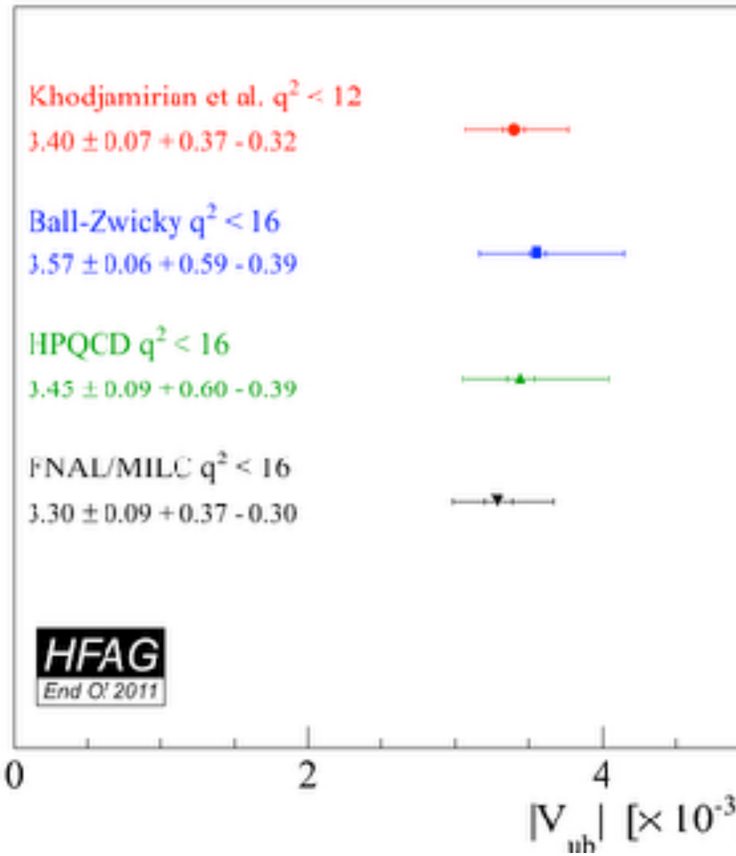

- FF can be as well calculated on the lattice. Significant progresses made recently.

2.3.1 The Semileptonic branching ratios: the $|V_{ub}|$ and $|V_{cb}|$ matrix elements.

- Since the last couple of years, the exclusive $|V_{ub}|$ determinations dominate the average. The most striking example is the 2015 measurement by LHCb collaboration. The progresses are made from a subtle intrication of FF calculations from the lattice in presence of a larger boost of the *b*-hadron particle.

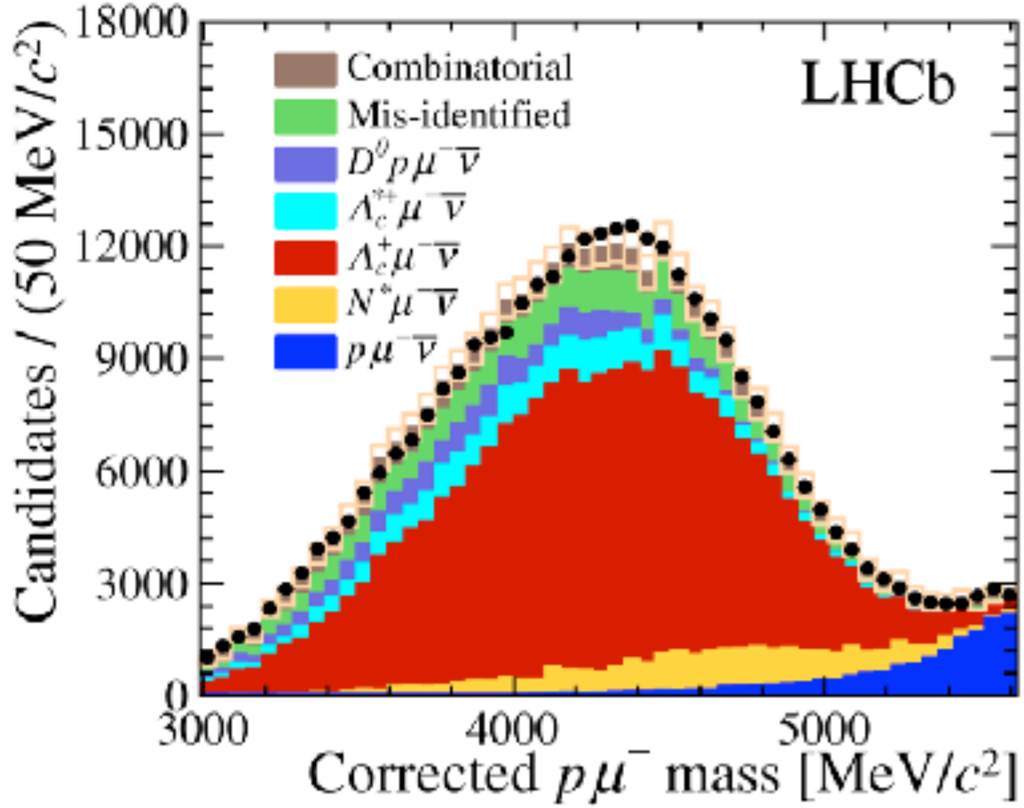

2.3.1 The Semileptonic branching ratios: the $|V_{ub}|$ and $|V_{cb}|$ matrix elements.

- Summary of inclusive and exclusive $|V_{cb}|$ determinations:

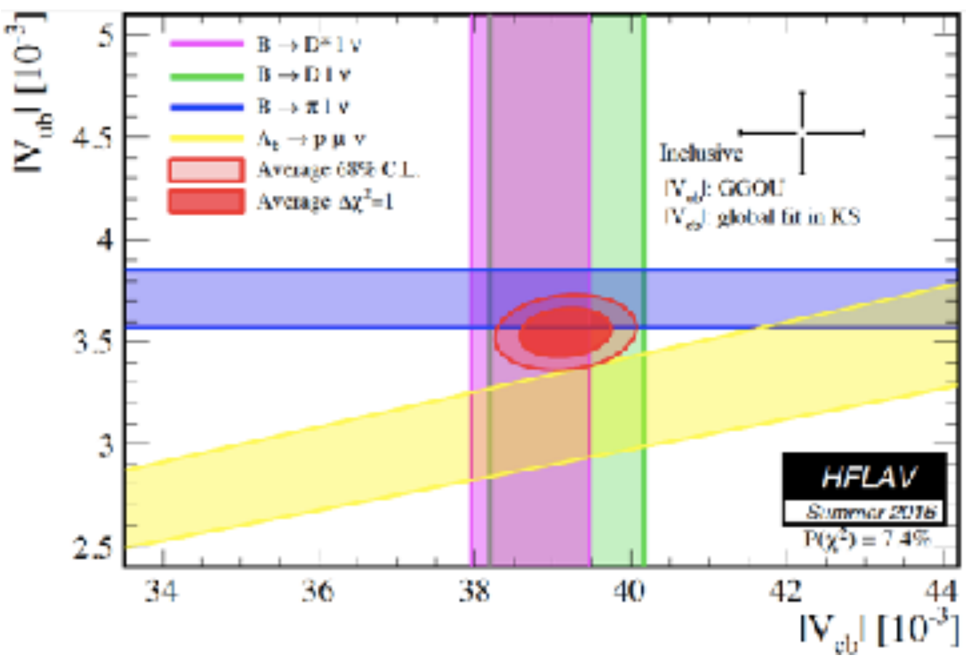

© E. Waheed, ICHEP' 18

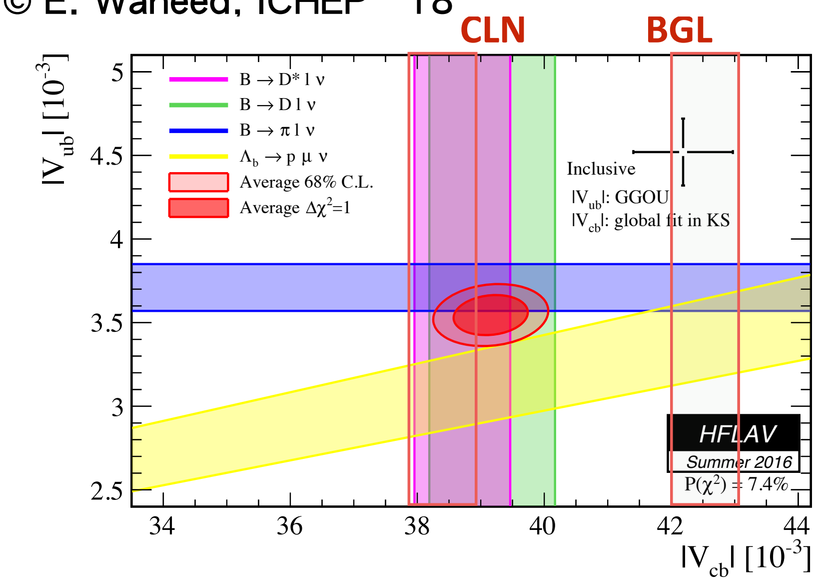

- A longstanding puzzle possibly solved: the two determinations seem reconciled

2.3.1 The Semileptonic branching ratios: the $|V_{ub}|$ and $|V_{cb}|$ matrix elements. The big picture.

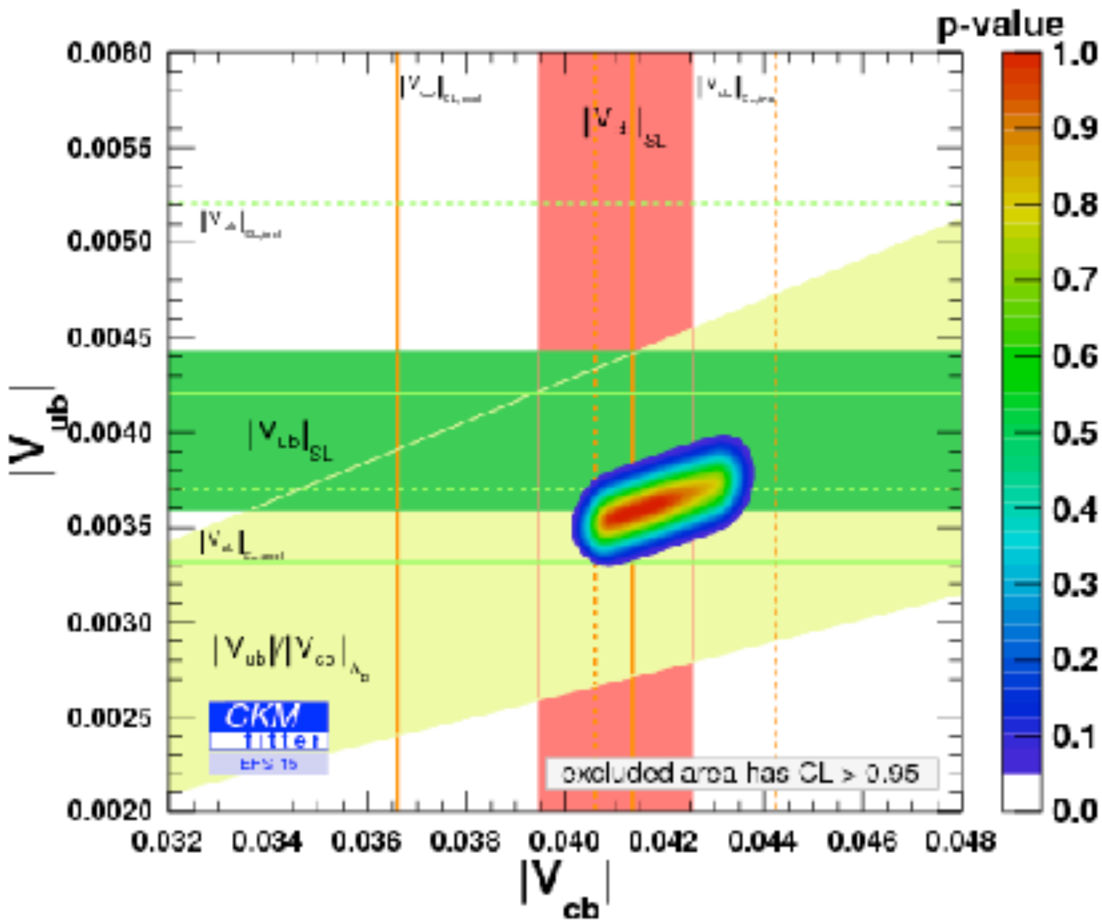

2.3.2 The oscillation frequencies: Δm_d and Δm_s.

- Weakly decaying neutral mesons can mix.
- The B^0 mixing first observation was in 1987 by the ARGUS collaboration:

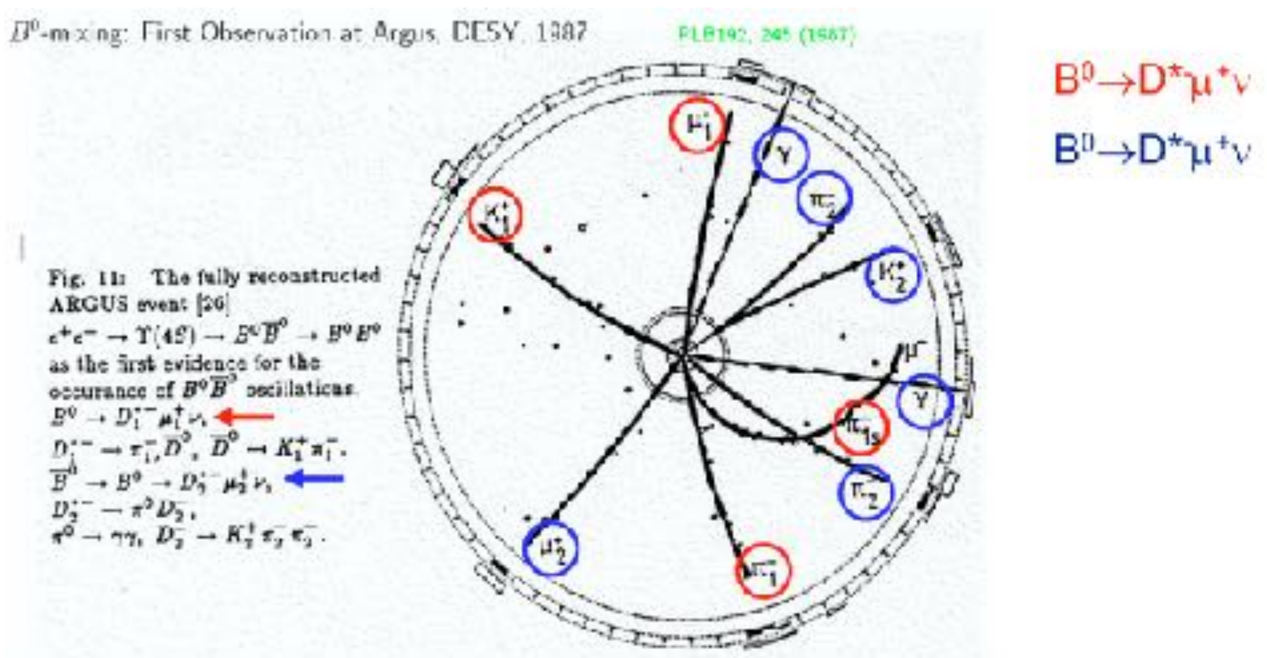

2.3.2 The oscillation frequencies: Δm_d and Δm_s.

• In the case of weakly decaying neutral mesons (K^0, D^0, B^0, B_s), the mass eigenstates (which propagate) are a superposition of the flavour states. The example of the B^0 in presence of CP violation:

$$|B_L\rangle = \frac{1}{\sqrt{2}}(p|B^0\rangle + q|\bar{B}^0\rangle)$$

$$|B_H\rangle = \frac{1}{\sqrt{2}}(p|B^0\rangle - q|\bar{B}^0\rangle)$$

• The time evolution of these mass states is derived by solving the Schrödinger equation for the hamiltonian $H = M - i\Gamma/2$:

$$|B_{L,H}\rangle = e^{-i(M_{L,H} - i\frac{\Gamma_{L,H}}{2})t} \cdot |B_{L,H}(t=0)\rangle$$

2.3.2 The oscillation frequencies: Δm_d and Δm_s.

- Intermediate calculation and definitions:

$$|B^0(t)\rangle = (g_+(t)|B^0\rangle + \frac{q}{p} g_-(t)|\bar{B}^0\rangle)$$
$$|B^0(t)\rangle = (\frac{p}{q} g_-(t)|B^0\rangle + g_+(t)|\bar{B}^0\rangle)$$

$$g_+(t) = e^{-i(m_B - i\frac{\Gamma_B}{2})t}\left[\cosh\frac{\Delta\Gamma_B t}{4}\cos\frac{\Delta m_B t}{2} - i\,\sinh\frac{\Delta\Gamma_B t}{4}\sin\frac{\Delta m_B t}{2}\right],$$
$$g_-(t) = e^{-i(m_B - i\frac{\Gamma_B}{2})t}\left[-\sinh\frac{\Delta\Gamma_B t}{4}\cos\frac{\Delta m_B t}{2} + i\,\cosh\frac{\Delta\Gamma_B t}{4}\sin\frac{\Delta m_B t}{2}\right]$$

- We defined here the mass difference $\Delta m_d = M_H - M_L$ and width (lifetime) difference $\Delta\Gamma_d = \Gamma_H - \Gamma_L$. Δm_B governs the speed of the oscillations.

2.3.2 The oscillation frequencies: Δm_d and Δm_s.

• The master formulae to get a B^0 produced at t=0 decaying in a final state f (neglecting $\Delta\Gamma$ in case of the B^0):

$$
\begin{aligned}
P(B^0(0) \to f) &= \frac{e^{-\Gamma\tau}}{2}[(1+\cos\Delta mt)\,|\langle f\,|H|\,B^0\rangle|^2) \\
&+ (1-\cos\Delta mt)\left|\frac{q}{p}\right|^2 |\langle f\,|H|\,\bar{B}^0\rangle|^2) \\
&- 2\sin\Delta mt\cdot\mathcal{Im}(\left|\frac{q}{p}\right| |\langle f\,|H|\,B^0\rangle|\cdot|\langle f\,|H|\,\bar{B}^0\rangle|^*)].
\end{aligned}
$$

$$
\begin{aligned}
P(\bar{B}^0(0) \to f) &= \frac{e^{-\Gamma\tau}}{2}[(1+\cos\Delta mt)\,|\langle f\,|H|\,\bar{B}^0\rangle|^2) \\
&+ (1-\cos\Delta mt)\left|\frac{p}{q}\right|^2 |\langle f\,|H|\,B^0\rangle|^2) \\
&- 2\sin\Delta mt\cdot\mathcal{Im}(\left|\frac{p}{q}\right| |\langle f\,|H|\,B^0\rangle|\cdot|\langle f\,|H|\,\bar{B}^0\rangle|^*)].
\end{aligned}
$$

2.3.2 The oscillation frequencies: Δm_d and Δm_s.

- Time evolution in plots:

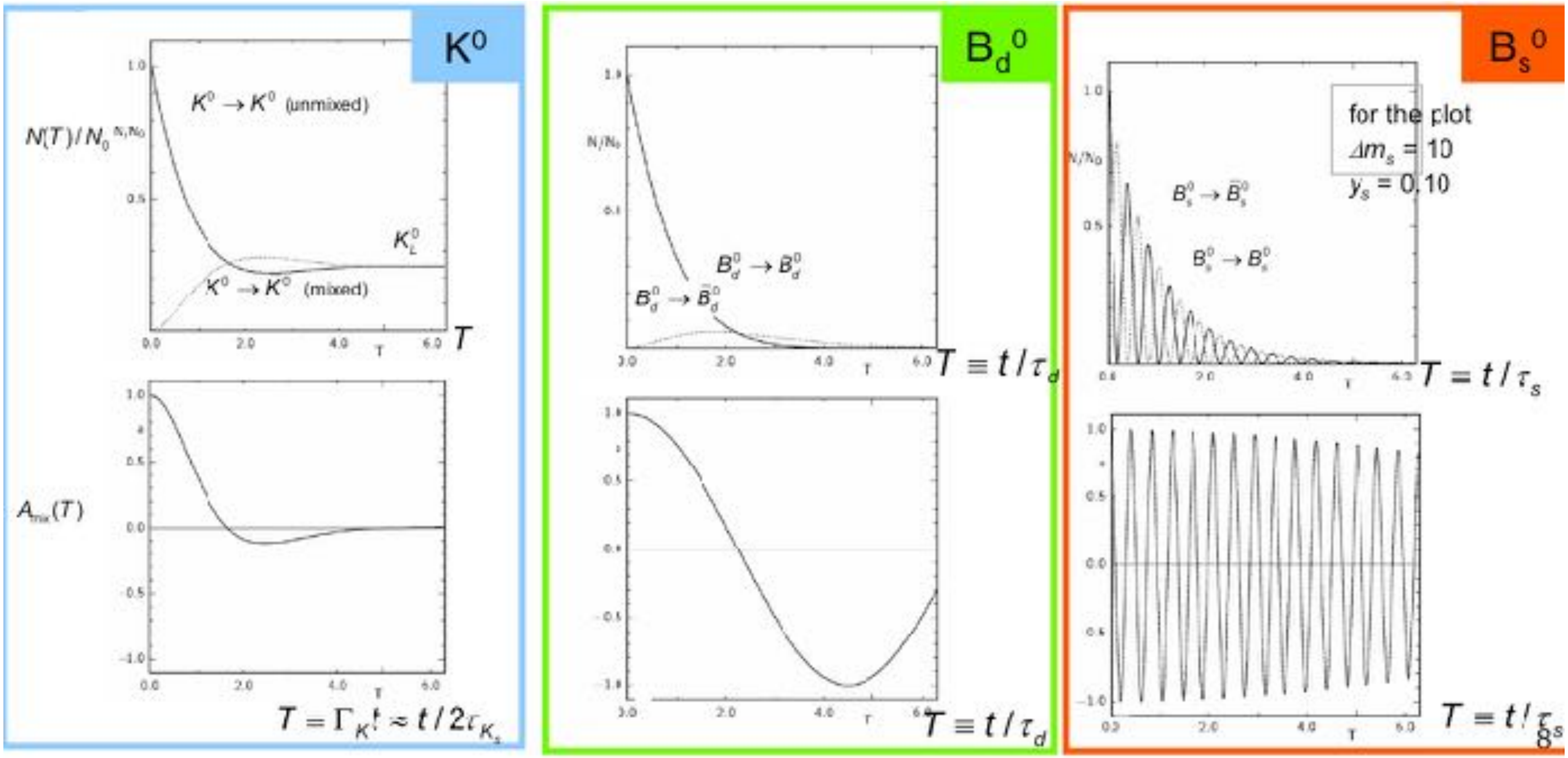

2.3.2 The oscillation frequencies: Δm_d and Δm_s.

- Which observable in order to look at the time evolution ?

- If we only consider the B^0 mixing in absence of *CP* violation (remember that it is so tiny in the *B* mixing that it has not been observed yet):

$$\left|\langle B^0 \,|H|\, \bar{B}^0(t)\rangle\right|^2 = \frac{e^{-\Gamma t}}{2}(1 + \cos\Delta m t)$$

$$\left|\langle \bar{B}^0 \,|H|\, B^0(t)\rangle\right|^2 = \frac{e^{-\Gamma t}}{2}(1 - \cos\Delta m t)$$

- We want to compare the number of mixed and unmixed events along the evolution. Define the time-dependent asymmetry:

$$A_{\rm mix} = \frac{N(B^0 \to B^0) - N(B^0 \to \bar{B}^0)}{N(B^0 \to B^0) + N(B^0 \to \bar{B}^0)} = \cos(\Delta m_d t)$$

- Note: in the case of *Bs*, the width difference is no more negligible. Complete treatment in LHCb TDR.

2.3.2 The oscillation frequencies: Δm_d and Δm_s.

- In the Standard Model the short distance contribution is given by the following diagrams dominated in the loop by the top quark contribution.

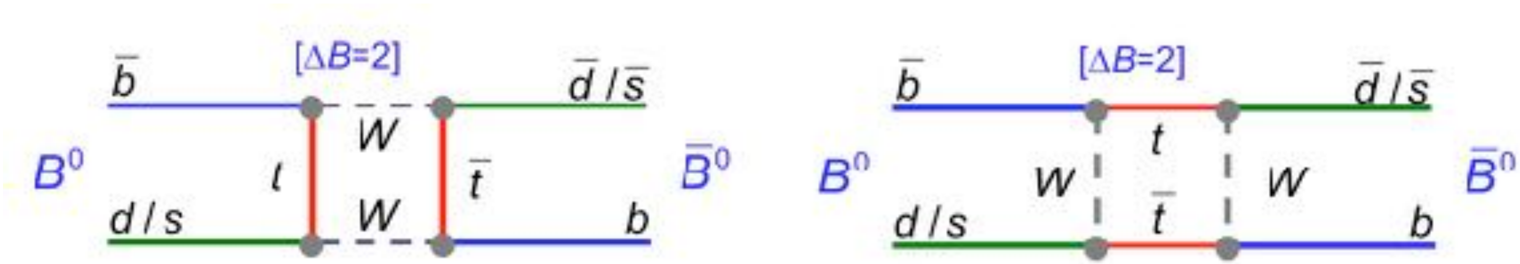

- and Δm_d is given by:

Non pert. QCD correction. Main uncertainty.

The weak part we are searching for.

$$\Delta m_d = \frac{G_F^2}{6\pi^2}\eta_B m_{B_d} f_{B_d}^2 B_d m_W^2 S(x_t)\left|V_{td}V_{tb}^*\right|^2$$

Pert. QCD correction to Inami-Lim function.

Inami-Lim function describing the content of the box. Top quark dominating.

2.3.2 The oscillation frequencies: Δm_d and Δm_s.

The measurements requires several ingredients:

• Reconstruct the flavour at the decay time
Either use a fully flavour specific hadronic mode or tag the charge with direct semileptonic decays.

• Reconstruct the decay time. Requires excellent vertexing capabilities (in particular to reconstruct the fast B_s oscillations).

• Reconstruct the flavour at production time
This is the key ingredient. Made easiest at the *B*-factories where the *B* mesons are coherently evolving. The flavour of one *B* at its decay time gives the flavour of the companion at the same time.

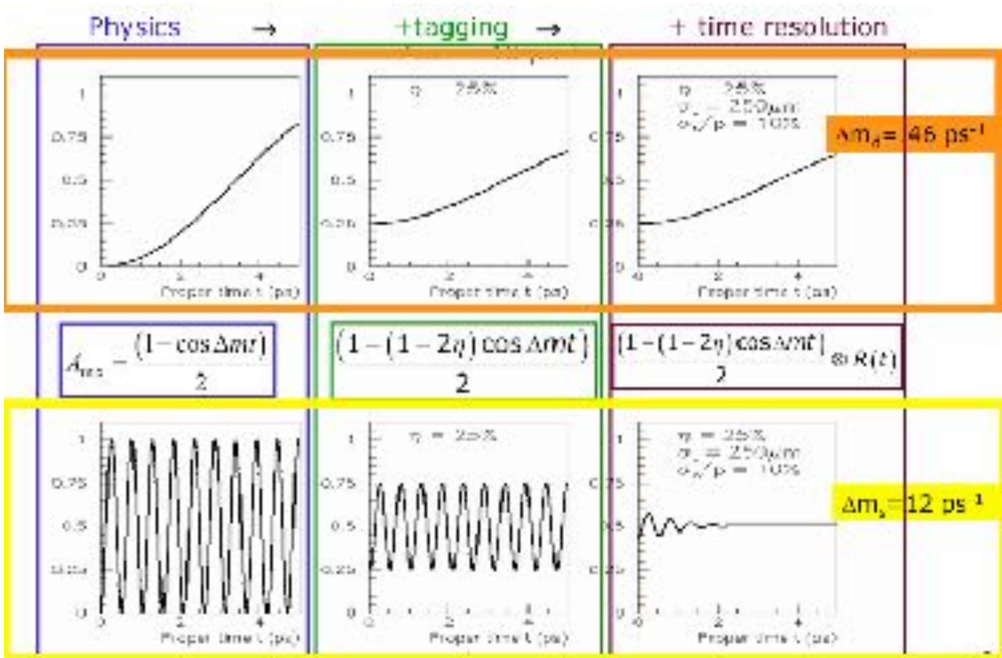

© MH.Schune

2.3.2 The oscillation frequencies: Δm_d.

Results for the oscillation frequency measurements:

- The BaBar example: this is a fantastic measurement among thirty !

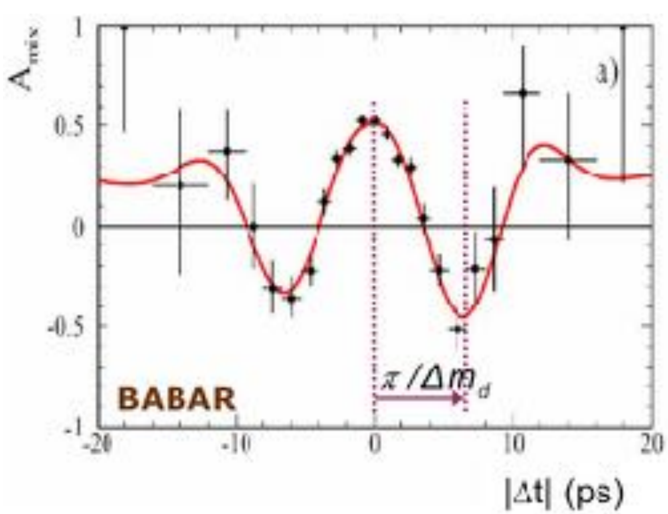

2.3.2 The oscillation frequencies: Δm_d.

Results for the oscillation frequency measurements:

- The BaBar example: this is a fantastic measurement among thirty !

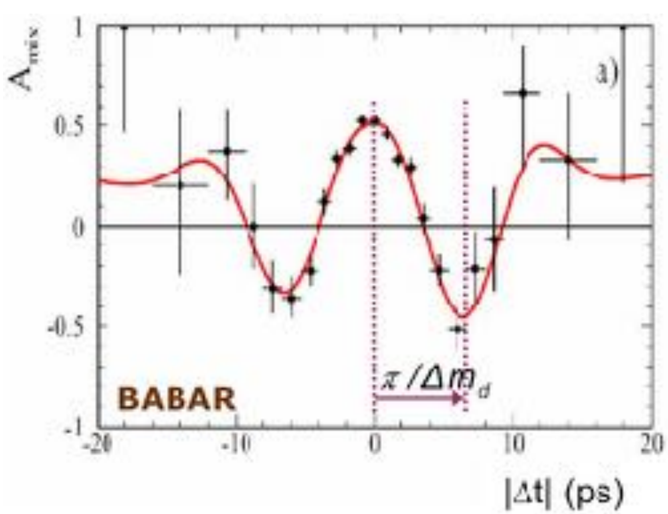

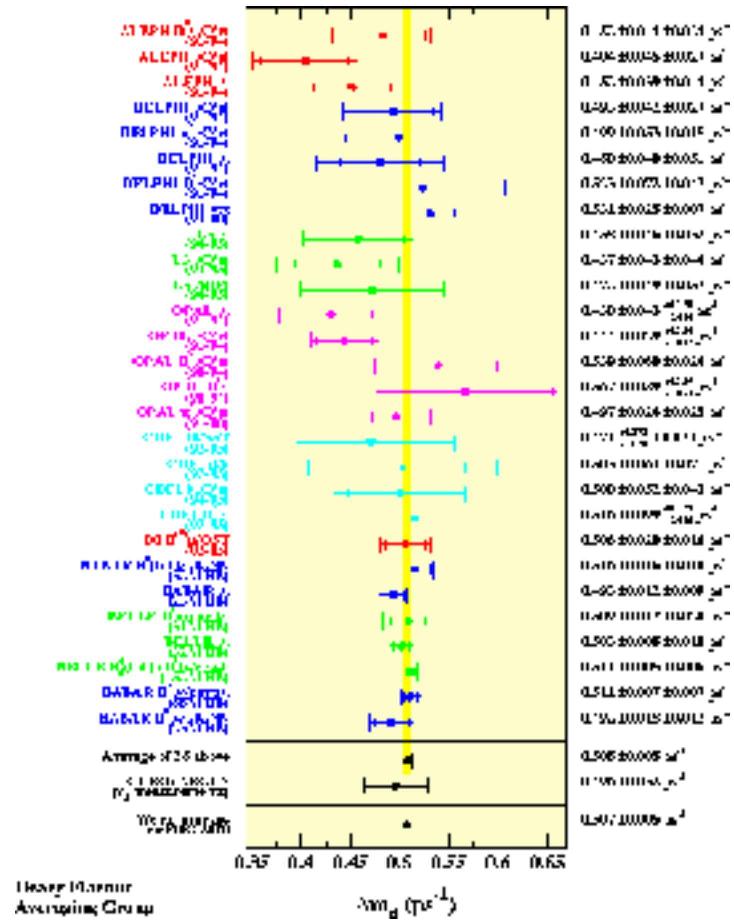

2.3.2 The oscillation frequencies: Δm_d.

Results for the oscillation frequency measurements:

- The BaBar example: this is a fantastic measurement among thirty !

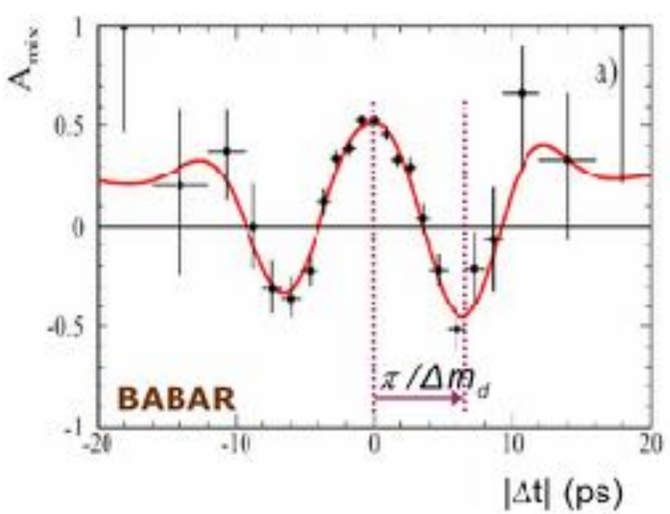

2.3.2 The oscillation frequencies: Δm_d.

Results for the oscillation frequency measurements:

- The BaBar example: this is a fantastic measurement among thirty !

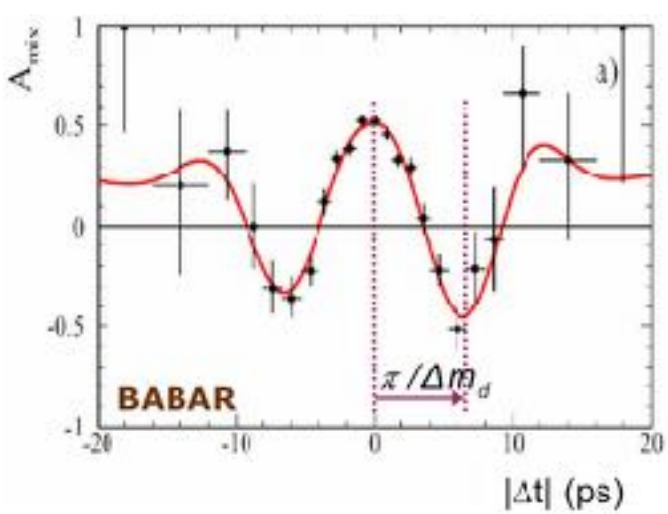

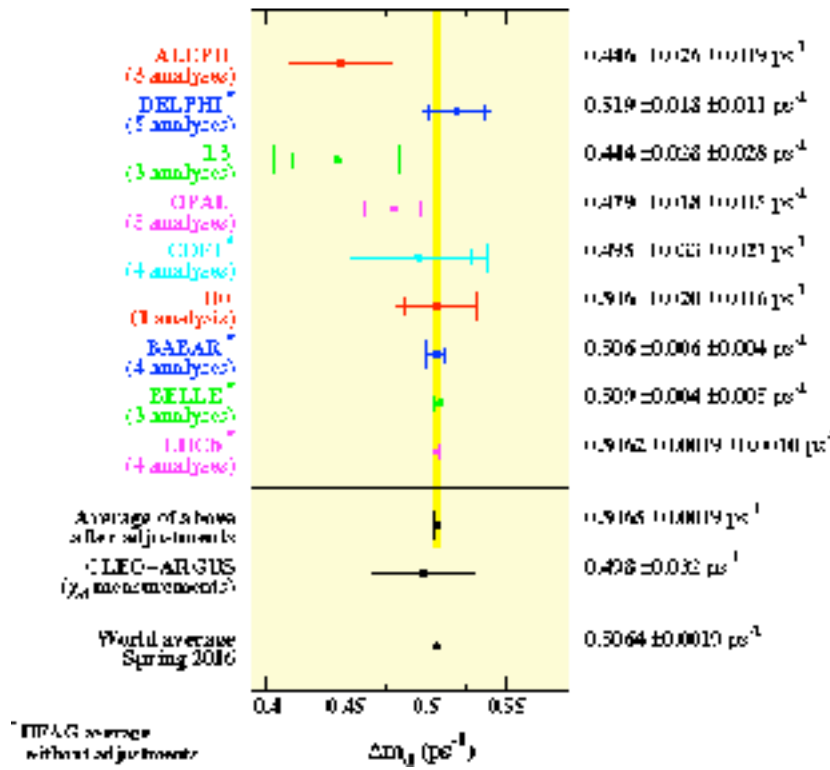

2.3.2 The oscillation frequencies: Δm_d and Δm_s.

Non pert. QCD correction.
Main uncertainty.

The weak part we are searching for.

$$\Delta m_d = \frac{G_F^2}{6\pi^2}\eta_B m_{B_d} f_{B_d}^2 B_d m_W^2 S(x_t)|V_{td}V_{tb}^*|^2$$

Pert. QCD correction to Inami-Lim function.

Inami-Lim function.

$$R_t = \left|\frac{V_{td}V_{tb}^*}{V_{cd}V_{cb^*}}\right| = \sqrt{(1-\bar\rho)^2+\bar\eta^2}\,.$$

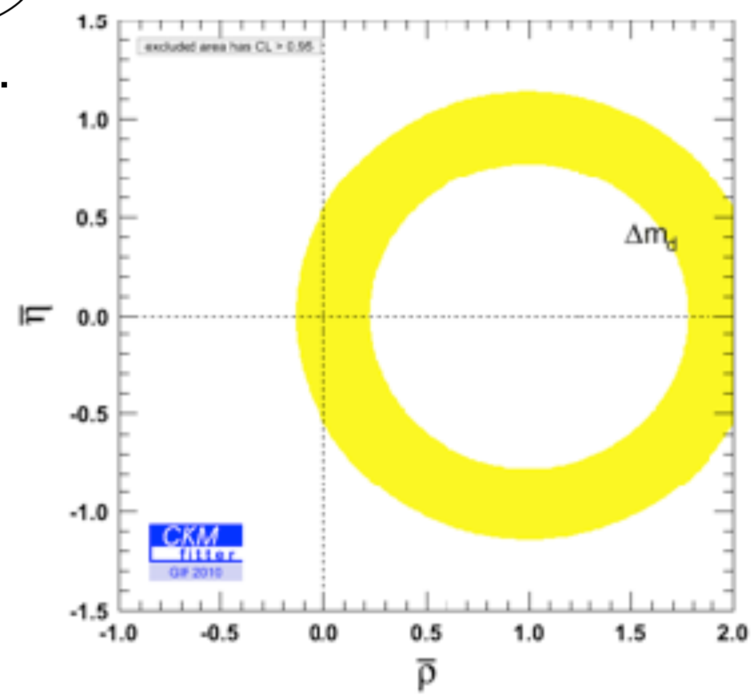

•The constraint on the Wolfenstein parameters is entirely dominated by the calculation on the Lattice of the product decayconstant*bagfactor.

•There is a way out to improve the precision with the *Bs* mixing measurement.

2.3.2 The oscillation frequencies: Δm_d and Δm_s.

• Though Δm_s only depends marginally on the Wolfenstein parameters, it helps a lot in reducing the LQCD uncertainty. Actually, the ratio:

$$\xi = \frac{f_{B_s}\sqrt{B_s}}{f_{B_d}\sqrt{B_d}}$$

is much better determined (better than 5 %) than each of its argument. Δm_s is improving the knowledge we have on the B_d product *decayconstant* X *bagfactor*.

• Note: in the global CKM fit, we don't use anymore the *zeta* parameter but directly the ratios of decay constants and bag factors per species.

2.3.2 The oscillation frequencies: Δm_d and Δm_s.

- The CDF experiment managed to resolve the fast oscillations of the B_s and measured the oscillation frequency Δm_s in 2006 with a remarkable accuracy. It was the end of a long search starting at LEP in the early nineties.

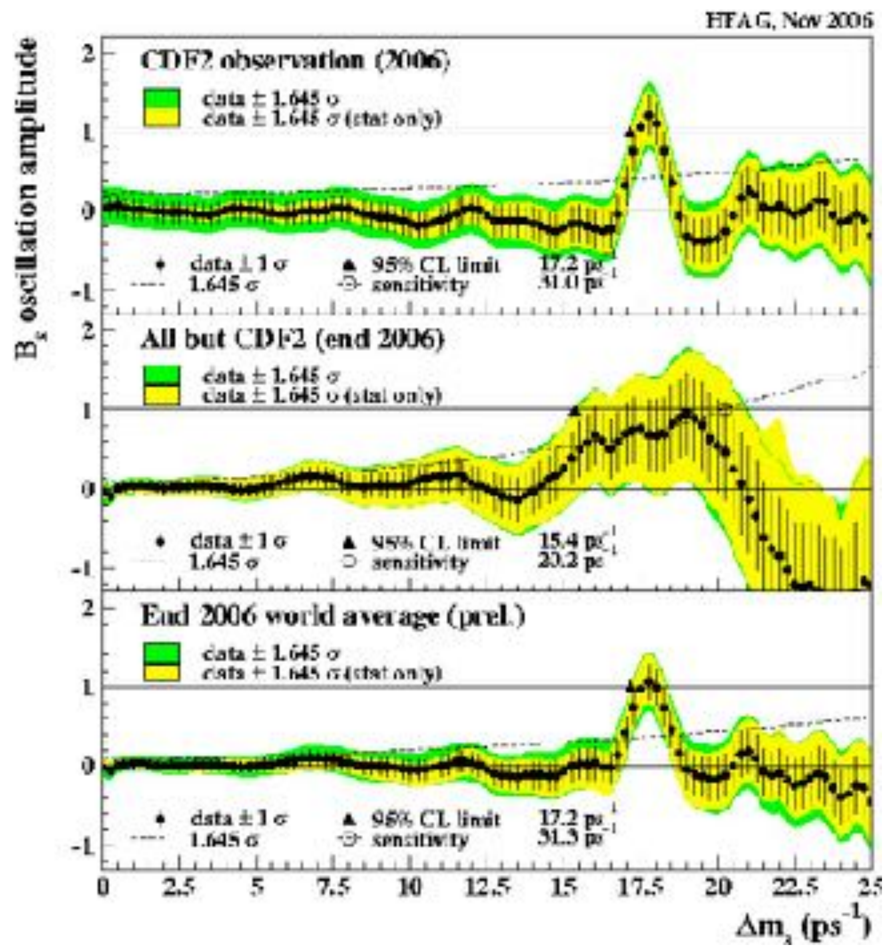

- Amplitude method for combining limits:

$$P(B_s^0 \to \bar{B}_s^0) = \frac{e^{-t/\tau}}{2} \cdot (1 + \mathcal{A} \cos(\Delta m_s t))$$

  - *A* is measured at each Δm_s hypothesis.
  - *A*=0: no oscillation is seen.
  - *A*=1: oscillation are observed.

2.3.2 The oscillation frequencies: Δm_d and Δm_s.

• Digression: looking at the intermediate plot (all experiments but CDF), one sees a structure of the amplitude, yielding to set a limit very close to the CDF measurement.

• This was basically driven by the LEP experiments constraints, very close eventually to resolve the B_s oscillations. It was a 2σ effect which was confirmed … That happens also

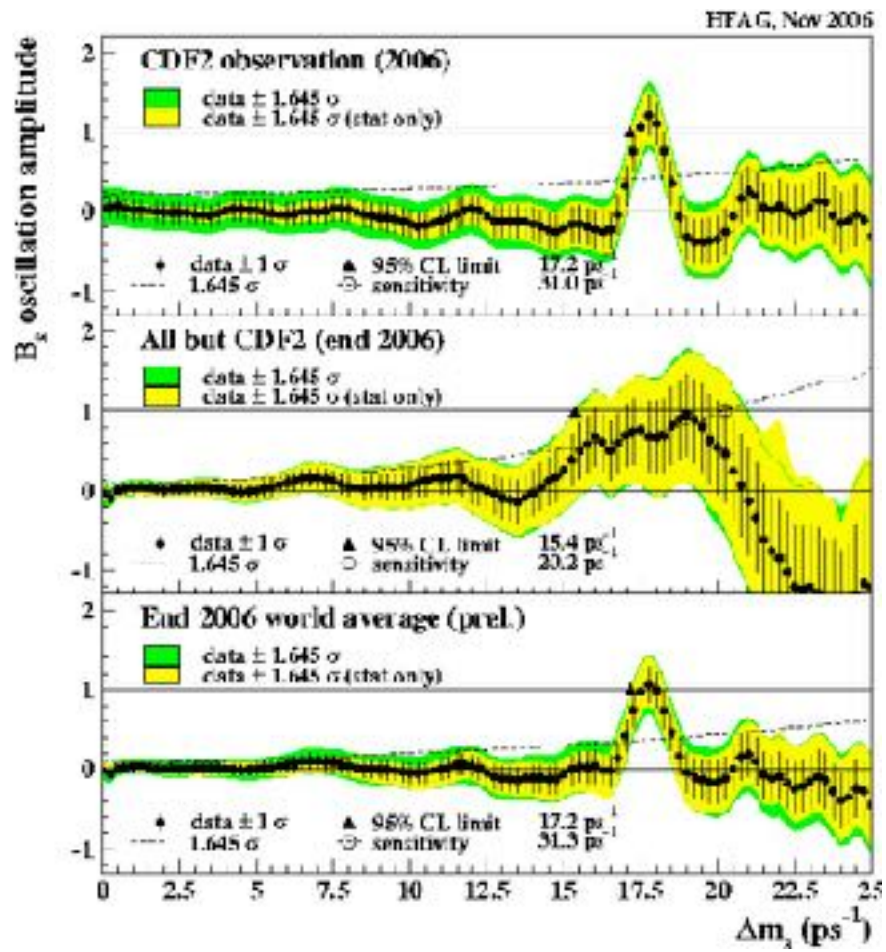

[Never take 2σ effects too seriously !]

2.3.2 The oscillation frequencies: Δm_s nowadays

• Decay time resolution is of utmost importance for such measurements. A textbook illustration of the LHCb performance can be found in the frequency of the B_s mixing, resolved here in the decay $B_s \to D_s\pi$: the textbook picture.

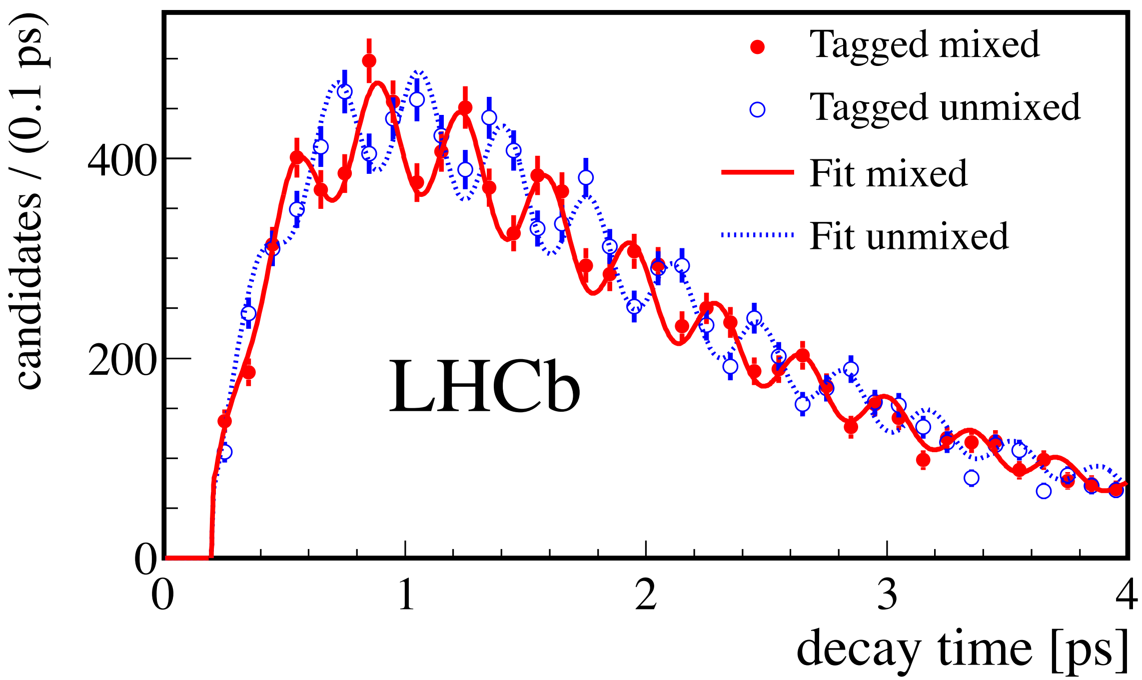

New J. Phys. 15 (2013) 053021 (1 fb^{-1})

2.3.2 The oscillation frequencies: Δm_d and Δm_s.

• The simultaneous fit of the two oscillation frequencies yields a dramatic improvement in the constraint.

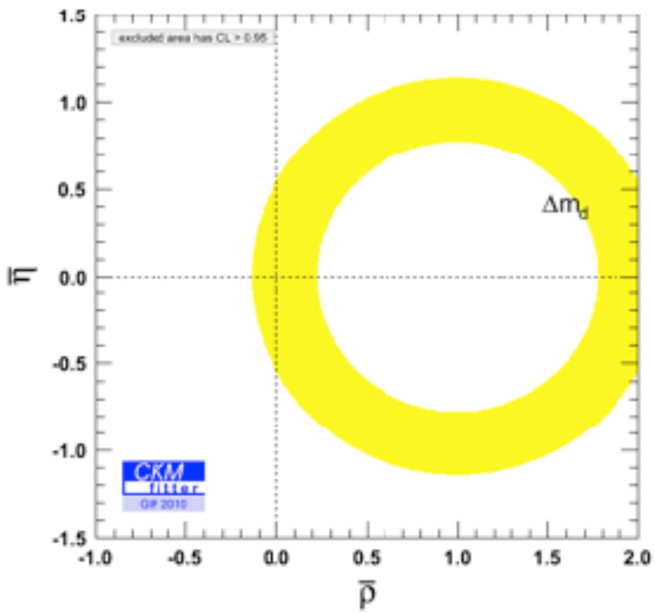

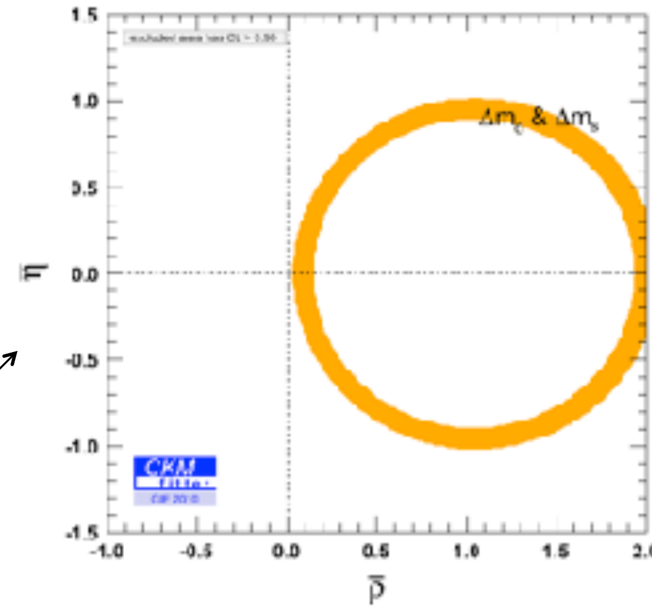

2.3.3 Aparté: anticipating the global fit

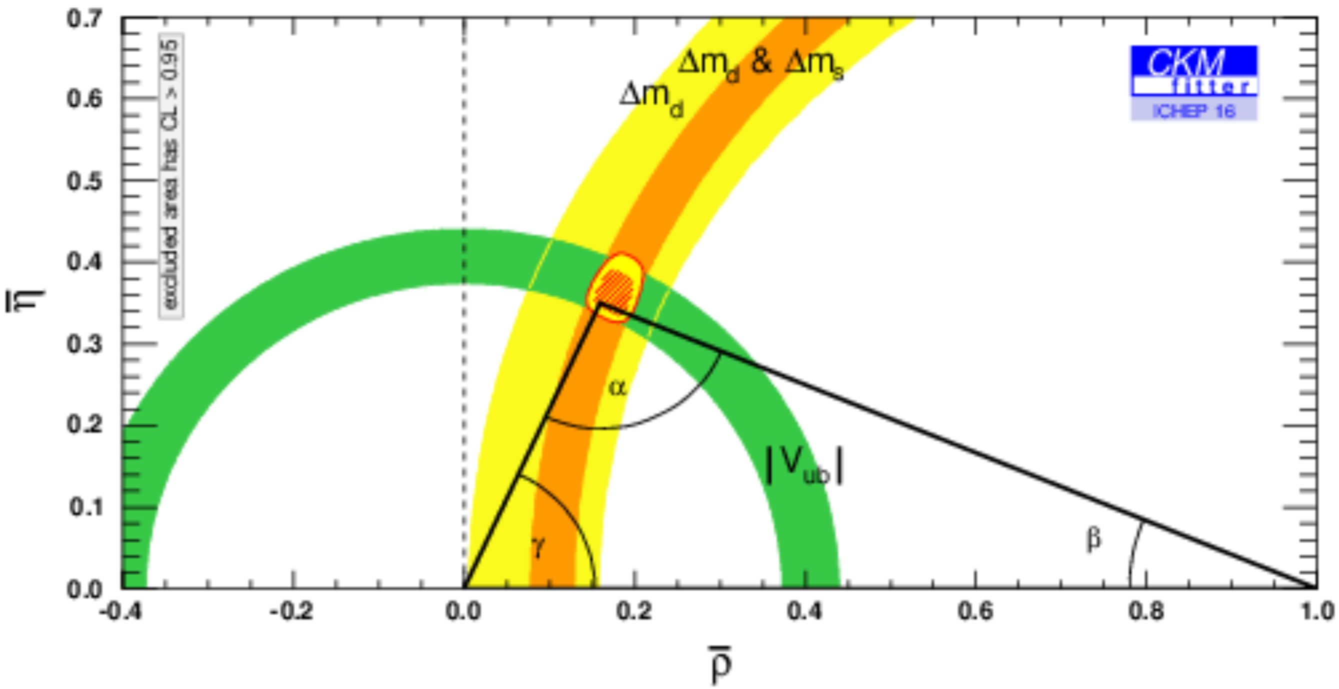

CP violation is predicted with *CP*-conserving observables! Theory limited.

2.4 *CP*-violating Observables

- **2.4.1** Kaon Physics
  - $|\varepsilon_K|$

- **2.4.2** The angle
  - $\sin(2\beta)$

- **2.4.3** The angle
  - $\sin(2\alpha)$

- **2.4.4** The angle γ

The last three observables are measures of phase differences. As such, they are not built under a given theory hypothesis and mostly do not receive any theoretical error in their determination.

2.4.1 The neutral kaon mixing $|\varepsilon_K|$.

$$|\varepsilon_K| = \frac{G_F^2 m_W^2 m_K f_K^2}{12\sqrt{2}\pi^2 \Delta m_K} B_K \Big(\eta_{cc} S(x_c, x_c) \mathrm{Im}\left[(V_{cs}V_{cd}^*)^2\right] + \eta_{tt} S(x_t, x_t) \mathrm{Im}\left[(V_{ts}V_{td}^*)^2\right] + 2\eta_{ct} S(x_c, x_t) \mathrm{Im}\left[V_{cs}V_{cd}^* V_{ts}V_{td}^*\right] \Big) .$$

- Here again the weak interaction part is overwhelmed by theoretical hadronic uncertainties.

- Yet, it deserves some interest as the only kaon observable considered in the KM global fit.

- This *CP*-violating observable yields a complementary constraint to for instance the weak phase of the *B* mixing.

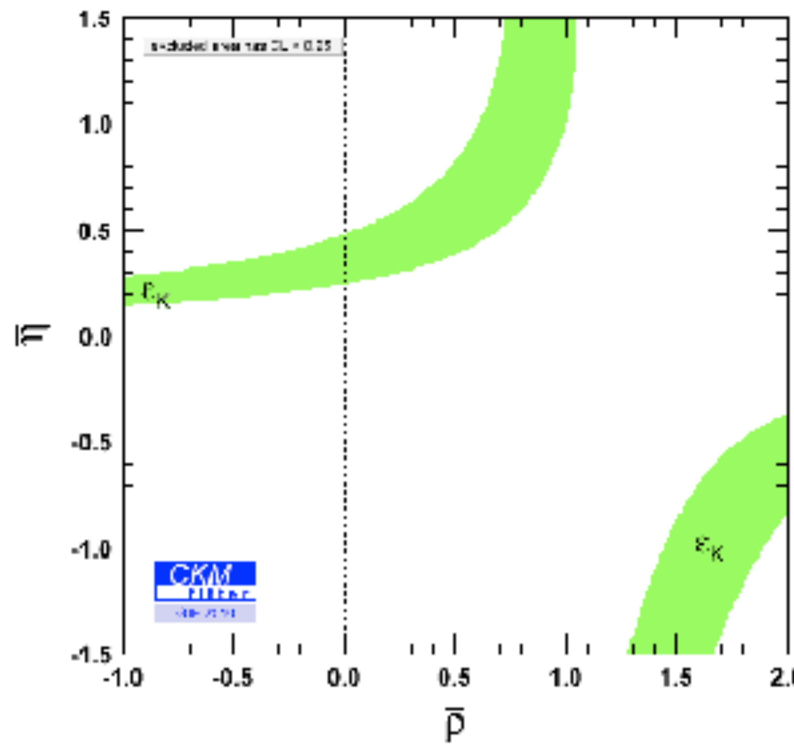

2.4.1 Aparté: direct *CP* violation in *K* decays.

• Not only the *CP* violation in the kaon mixing has been measured but also the direct *CP* violation in the kaon decay.

• Modify slightly the ε_K definition to account for the interference between penguin and tree decays to two pions.

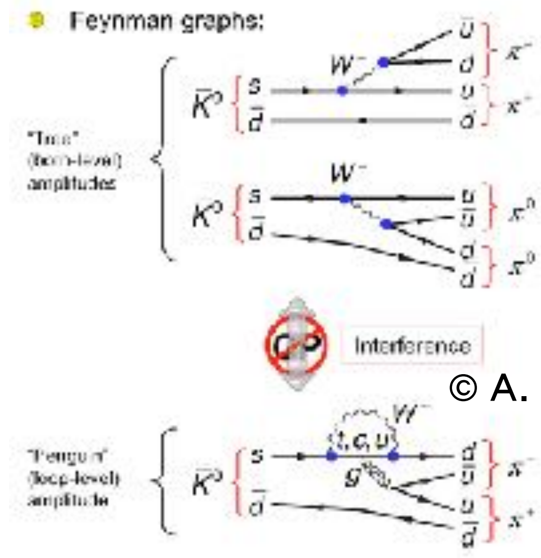

© A. Höcker.

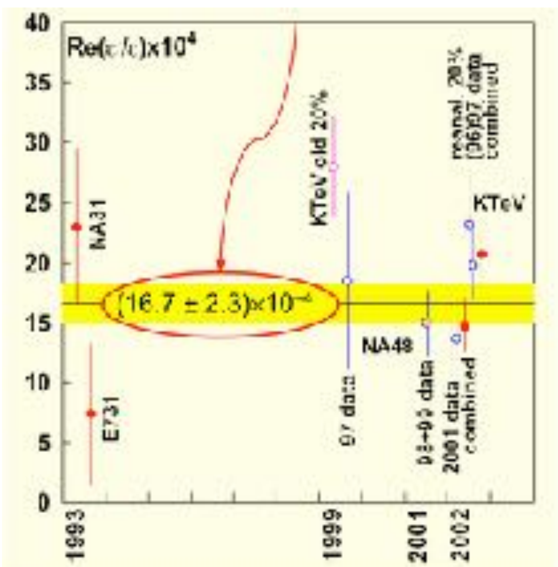

• This is a very small effect and the first observation was reported in 2001 by NA48 and KTeV experiments, after 30 years of efforts.

• The SM prediction is plagued by hadronic uncertainties. It makes unuseful (as of today) for the global fit this (in principle) very valuable information. Disregarded in the following.

2.4.2 The measurement of sin(2β).

$$\beta = \pi - \arg\left(\frac{V_{td}V_{tb}^*}{V_{cd}V_{cb}^*}\right),$$

- Sketch of the method: double slit experiment.

- An interference between processes exhibiting V_{td} and V_{cb} matrix element:

  - The $b \to c$ process: $V^*_{cb}V_{cs}$

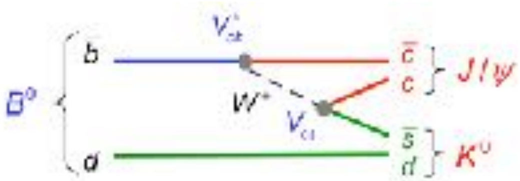

  - The mixing process: $V^*_{tb}V_{td}$

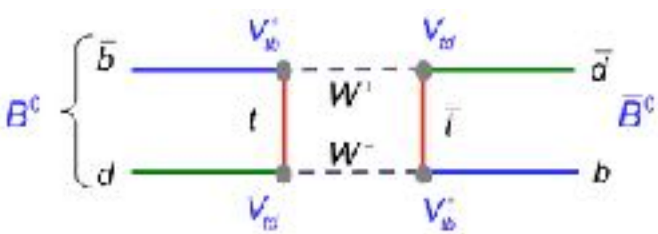

  - And additonally the K^0 mix: $V_{cd}V^*_{cs}$:

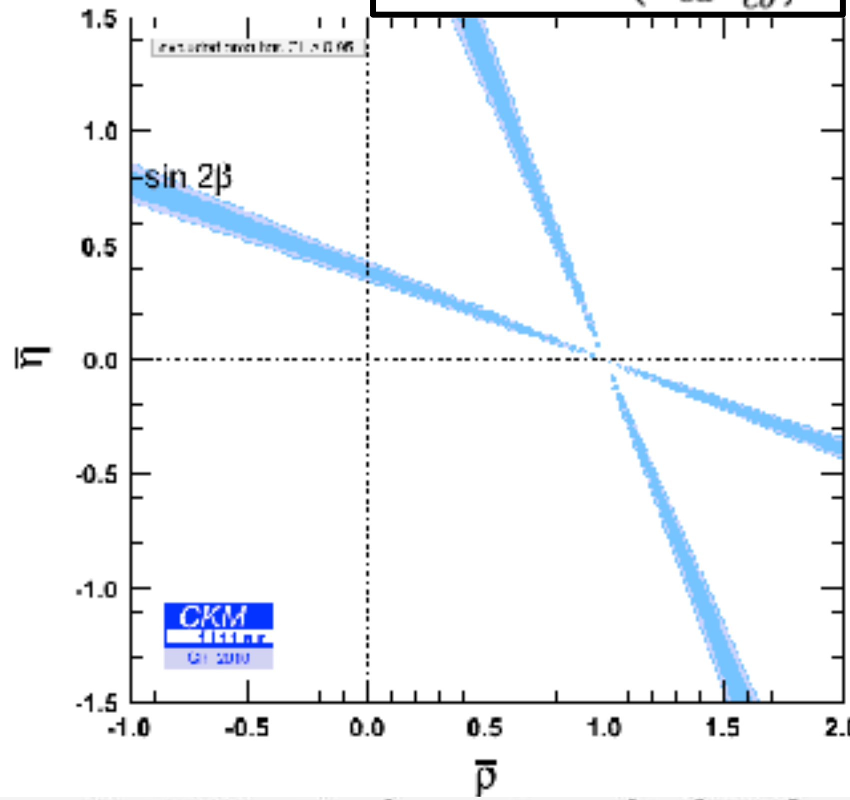

$$\arg\left[\frac{A(B^0 \to J/\psi K^0)}{A(B^0 \underset{mix}{\to} \bar{B}^0 \to J/\psi \bar{K}^0 \underset{mix}{\to} J/\psi K^0)}\right] = \arg\left[\frac{V_{cb}V_{cs}^*}{(V_{td}V_{tb}^*)^2 \cdot V_{cb}^*V_{cs} \cdot (V_{cd}^*V_{cs})^2}\right] = \arg\left[\frac{(V_{cd}V_{cb}^*)^2}{(V_{td}V_{tb}^*)^2}\right] = -2\beta$$

2.4.2 The measurement of sin(2β).

- Sketch of the method: some definitions.

$$\beta = \pi - \arg\left(\frac{V_{td}V_{tb}^*}{V_{cd}V_{cb}^*}\right),$$

- The *CP* asymmetry:

$$A_{CP}(f,t) = \frac{N(B^0(t) \to f) - N(B^0(t) \to f)}{N(\bar{B}^0(t) \to f) + N(B^0(t) \to f)}$$

- Can be expressed as a function of the *S* and *C* observables:

$$A_{CP}(f,t) = S\sin(\Delta m_d t) - C\cos(\Delta m_d t)$$

- which can be related to *CP* violating phase β:

$$\lambda = \frac{q}{p}\frac{A(\bar{B}^0 \to f)}{A(B^0 \to f)} = e^{-i2\beta}\frac{\bar{A}_f}{A_f}$$

$$S = \frac{2\mathcal{I}m\lambda}{1+|\lambda|^2}$$

$$S = -\eta_{CP}\sin(2\beta)$$

- Let's notice that the charmless *CP* final state ππ would receive *S* = sin (2α) in absence of penguin diagrams.

2.4.2 The measurement of sin(2β).

- The experimental method to measure *S* and *C* parameters:

- Fully reconstruct the $b \to c\bar{c}s$ *CP* decay .

- Tag the flavour with the other *B* of the event.

- Reconstruct the time difference between the decays from the vertex separation.

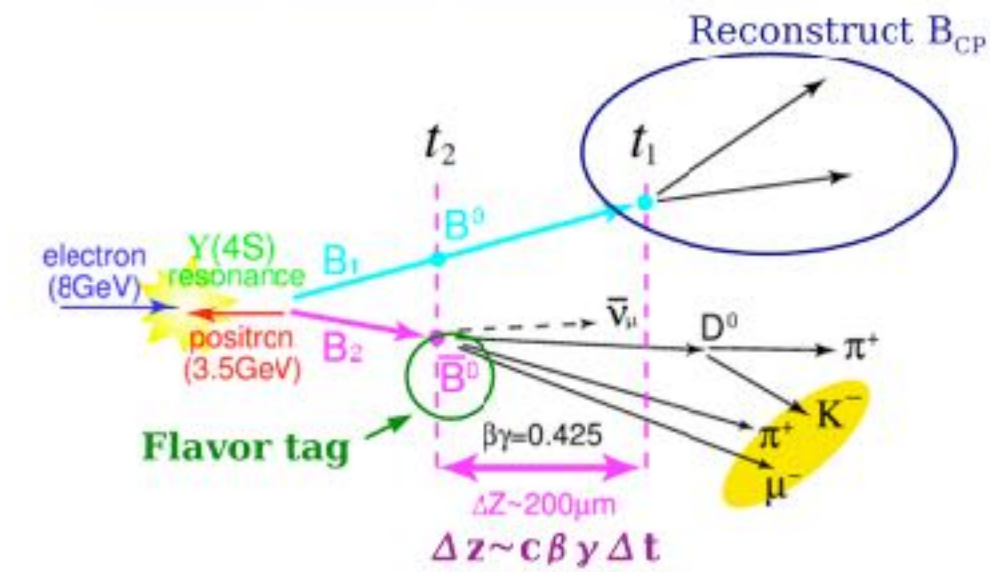

$$\frac{dP_{sig}}{dt}(\Delta t, q) = \frac{e^{-|\Delta t|/\tau_B}}{4\tau_B}\left(1 + q\left(S \sin(\Delta m_d \Delta t) + A \cos(\Delta m_d \Delta t)\right)\right)$$

2.4.2 The measurement of sin(2β).

• Dilution factors: mistag rate and vertexing resolution.

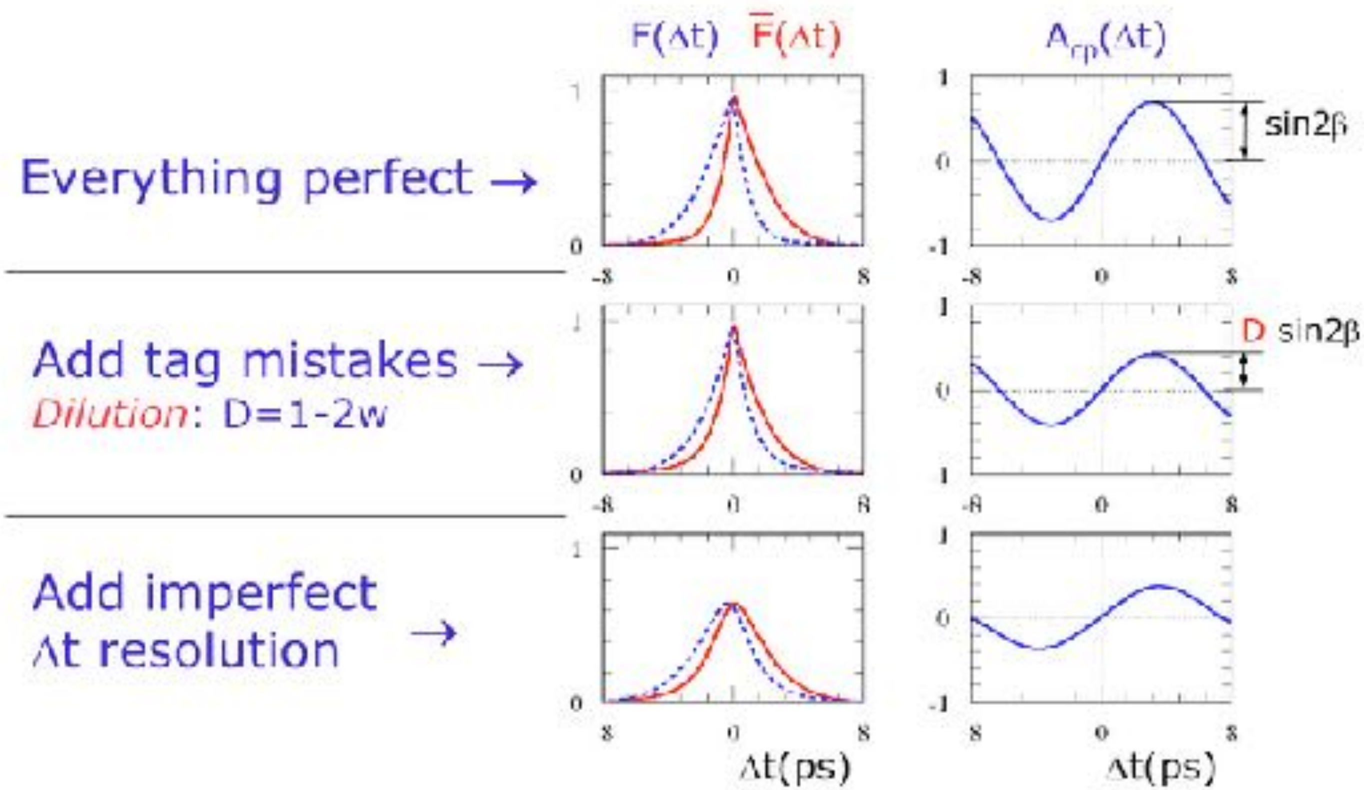

2.4.2 The measurement of sin(2β).

- A selection of Belle results as an illustration of this fantastic achievement.

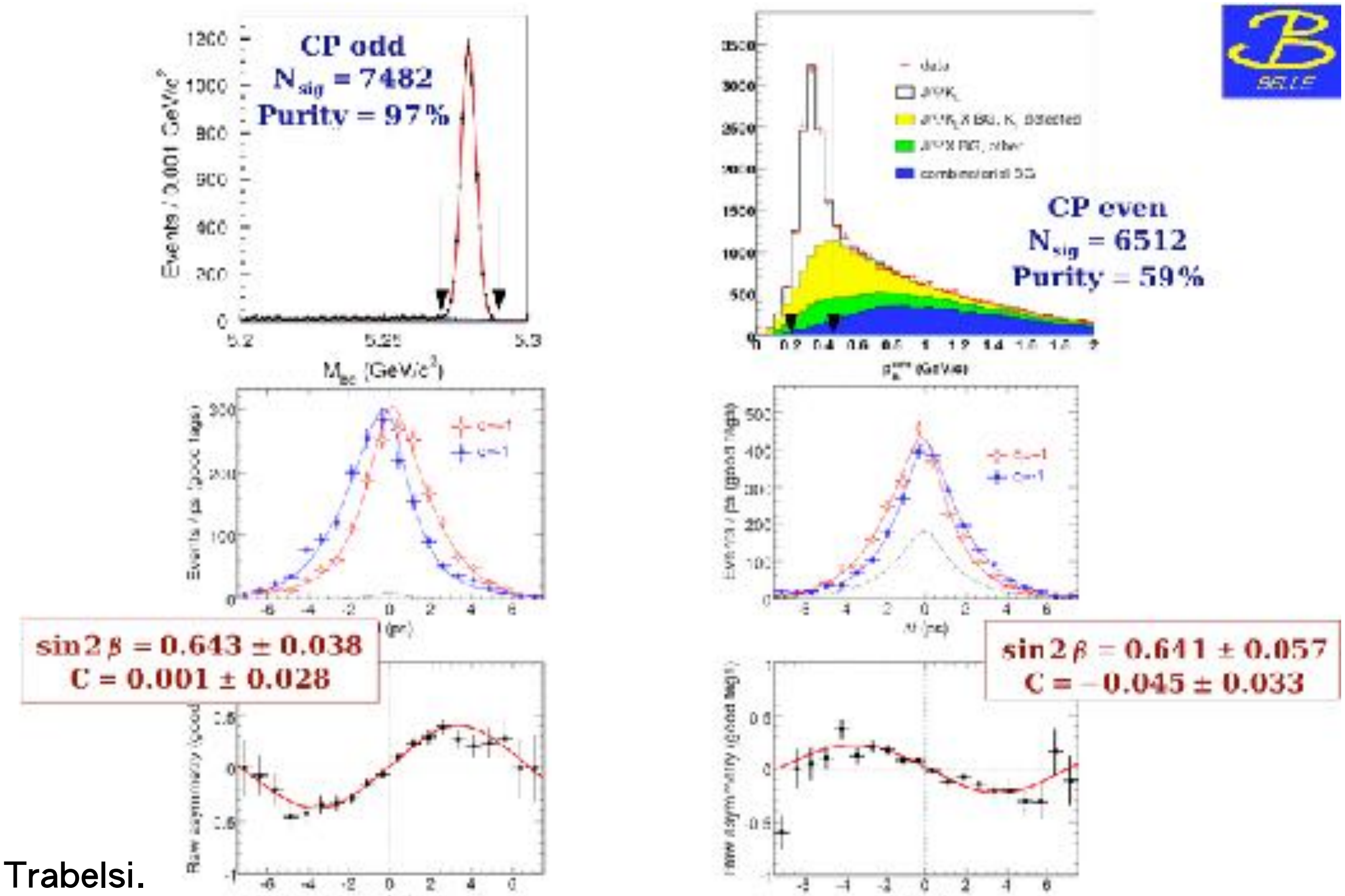

2.4.2 The measurement of sin(2β).

- A selection of Belle results as an illustration of this fantastic achievement.

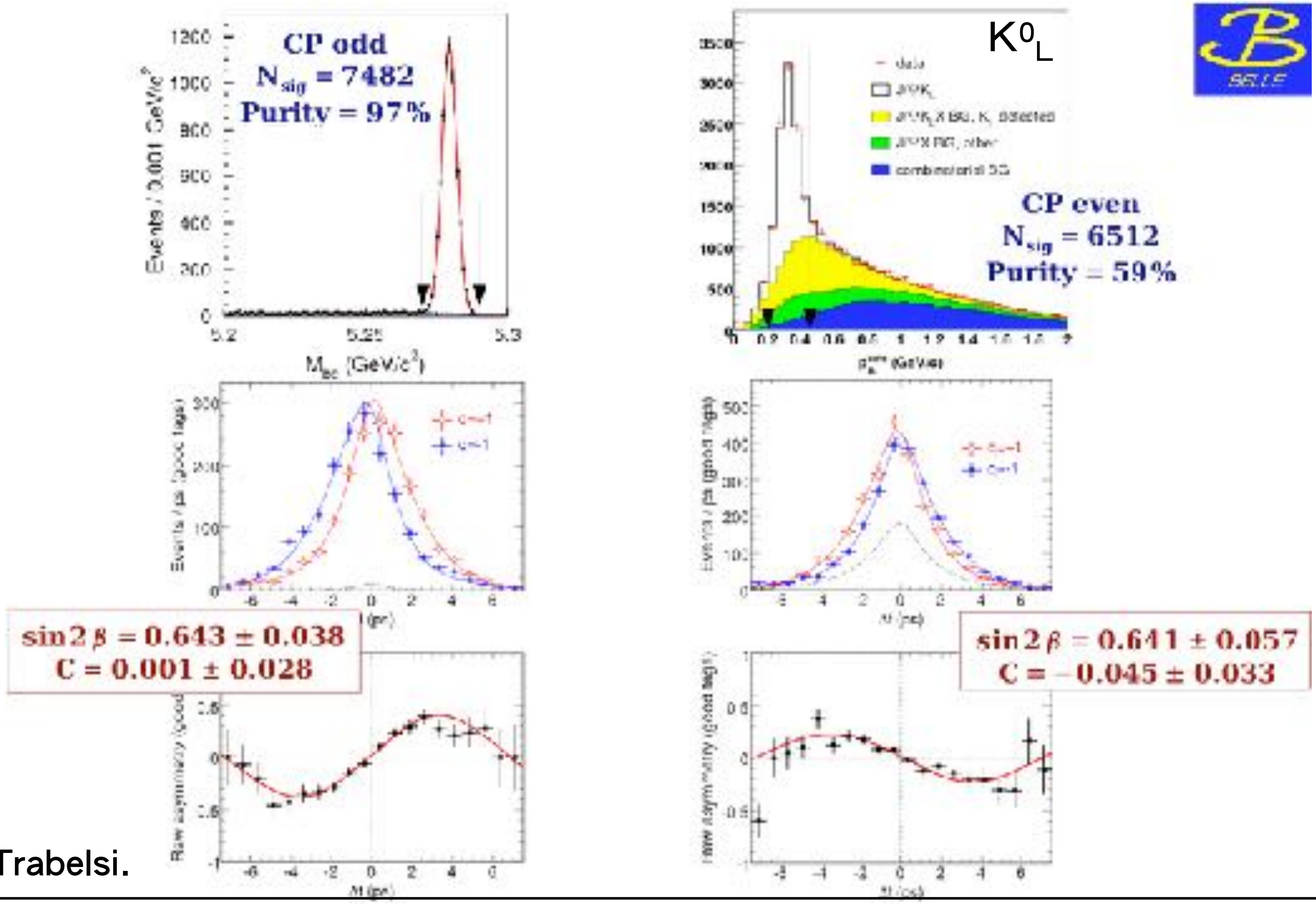

© K. Trabelsi.

2.4.2 The measurement of sin(2β).

- A selection of Belle results as an illustration of this fantastic achievement.

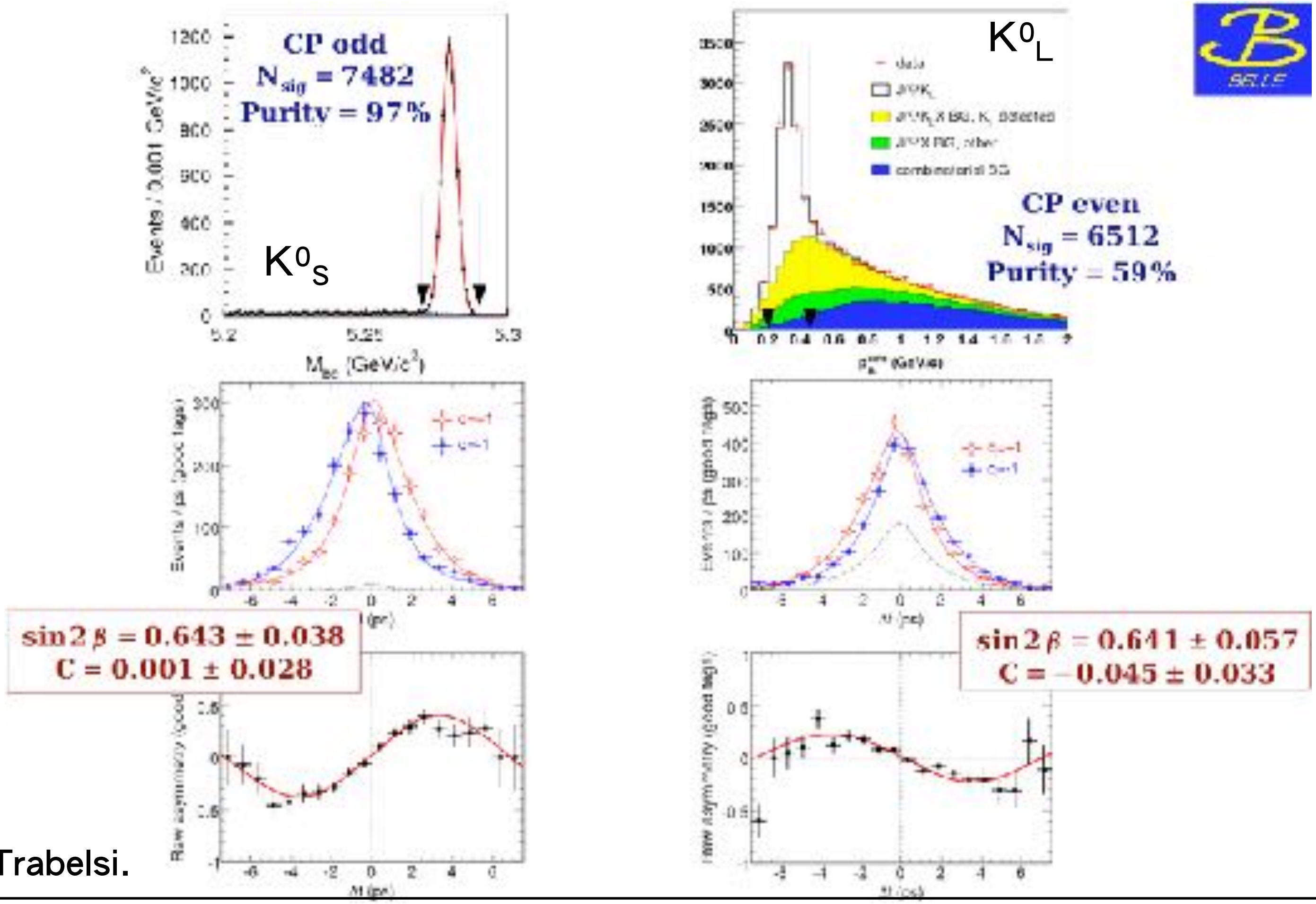

© K. Trabelsi.

2.4.2 The measurement of sin(2β).

This measurement was the *raison d'être* of the *B*-factories and the accuracy of their measurements is a tremendous success…

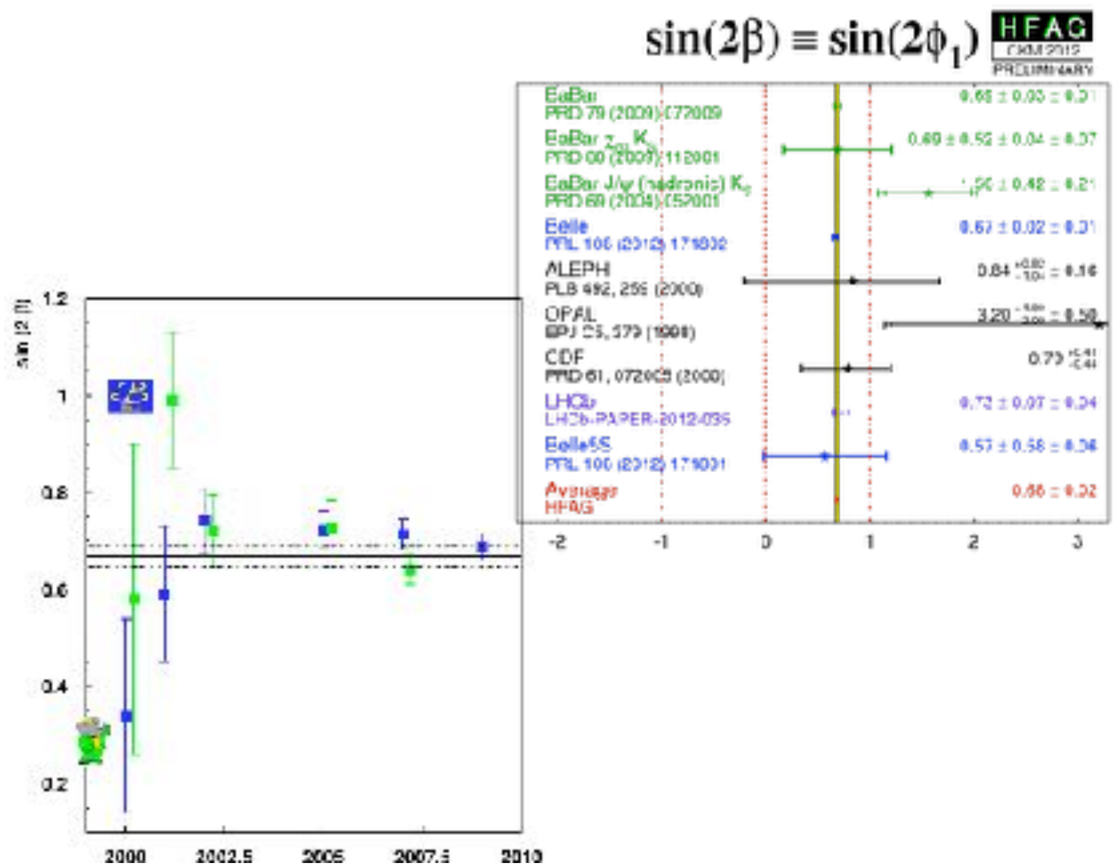

$$\beta = \pi - \arg\left(\frac{V_{td}V_{tb}^*}{V_{cd}V_{cb}^*}\right),$$

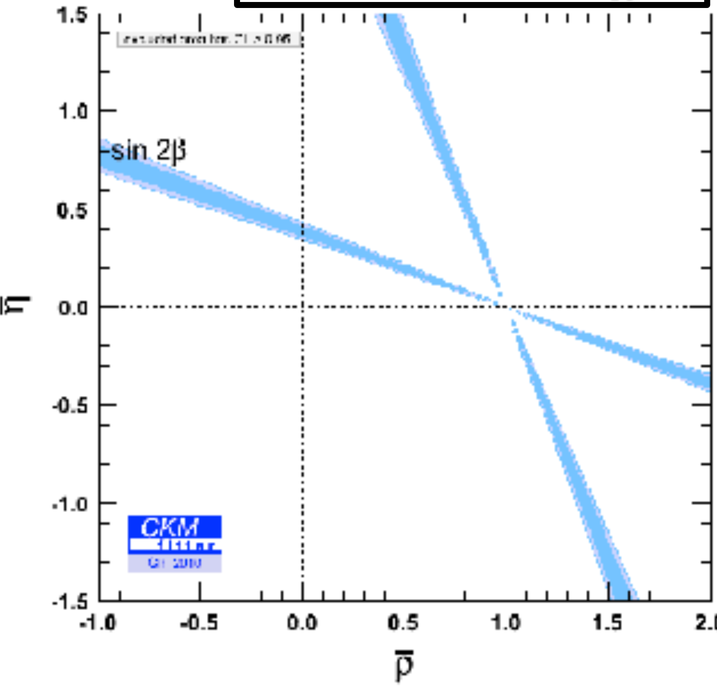

2.4.2 The measurements of sin(2β).

- An active search for β measurements concern the charmless decays proceeding through penguins (*b→s,ss[qq]*).

- Probing a difference with sin (2β) measured in (*b→ccs*) would be an indication of New Physics contributions in the loop diagrams.

- The precision starts to be interesting but more statistics is crucial since each mode receives its own hadronic correction. The consistency is acceptable.

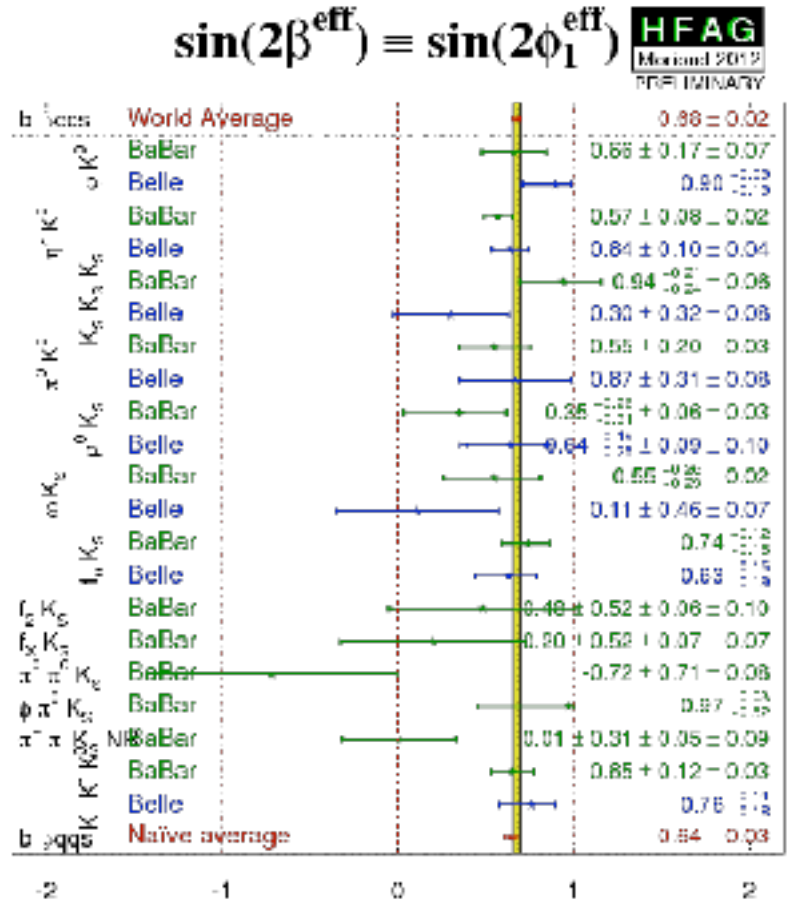

2.4.3 The angle α from $B\to\pi\pi$, $B\to\rho\rho$ (and $B\to\rho\pi$)

• The angle α can be analogously to β measured in the time dependent interference between the mixing and the decay of tree-mediated $b\to uud$ processes.

• The situation is further complicated by the presence of penguin diagram exhibiting a different CKM phase:

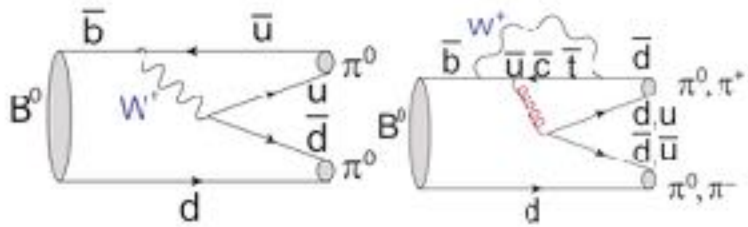

$$A(B^0\to\pi^+\pi^-)=T^{+-}e^{i\gamma}+P$$

• The *CP* asymmetry is modified as:

$$\begin{aligned} A(t) &= S_{\pi^+\pi^-}\sin(\Delta m t)-C_{\pi^+\pi^-}\cos(\Delta m t) \\ &= \sqrt{1-C^2_{\pi^+\pi^-}}\,\sin 2\alpha_{eff}\,\sin(\Delta m t)-C_{\pi^+\pi^-}\cos(\Delta m t)\end{aligned}$$

$$S_{\pi^+\pi^-}=\sin 2\alpha+2r\cos\delta\,\sin(\beta+\alpha)\cos 2\alpha+O(r^2)$$

$$r=|P|/|T|$$

• Additional information is required if you want to make the electroweak interpretation of the measurement.

2.4.3 The angle α from *B*→ππ

- Use companion modes $(\pi\pi)^{+/-/0}$ and isospin symmetry to disentangle penguin contributions:

Gronau, London (1990)

- completely general isospin decomposition

$$A_{+-} = \langle \pi^+\pi^- | H | B^0 \rangle = -A_{1/2} + \frac{1}{\sqrt{2}}A_{3/2} - \frac{1}{\sqrt{2}}A_{5/2}$$

$$A_{00} = \langle \pi^0\pi^0 | H | B^0 \rangle = \frac{1}{\sqrt{2}}A_{1/2} + A_{3/2} - A_{5/2}$$

$$A_{+0} = \langle \pi^+\pi^0 | H | B^+ \rangle = \frac{3}{2}A_{3/2} + A_{5/2}$$

- Tree and EWP contribute to $|\Delta I|=1/2$ and $3/2$ amplitudes
- QCD penguins contribute to $|\Delta I|=1/2$ amplitudes
- $|\Delta I|=5/2$ induced by Isospin Symmetry Breaking (not present in H_W)

- Neglecting $|\Delta I|=5/2$ transition and EWP, A_{+0} is pure Tree.

- Isospin triangular relation :

$$A_{+-} + \sqrt{2}A_{00} = \sqrt{2}A_{+0}$$
$$A_{+-} + \sqrt{2}A_{00} = \sqrt{2}A_{+0}$$

2.4.3 The angle α from $B \to \pi\pi$

- Use companion modes ($\pi\pi$) and isospin symmetry to disentangle penguin contributions.

- In addition to the time-dependent analysis parameters *S* and *C*, consider the Branching Fractions of the companion modes.

- Geometrical resolution:

2.4.3 The angle α from $B \rightarrow \pi\pi$

- Use companion modes ($\pi\pi$) and isospin symmetry to disentangle penguin contributions.

- In addition to the time-dependent analysis parameters *S* and *C*, consider the Branching Fractions of the companion modes.

- Geometrical resolution:

▪ B^{+0} $\rightarrow |A^{+0}| = |\bar{A}^{-0}|$

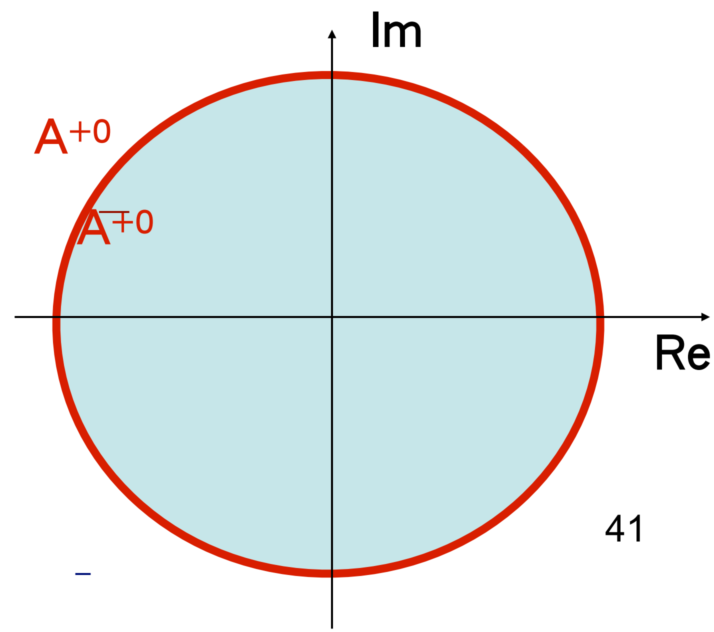

2.4.3 The angle α from $B \rightarrow \pi\pi$

- Use companion modes ($\pi\pi$) and isospin symmetry to disentangle penguin contributions.

- In addition to the time-dependent analysis parameters *S* and *C*, consider the Branching Fractions of the companion modes.

© O.Deschamps

- Geometrical resolution:

- $B^{+0} \rightarrow |A^{+0}| = |\bar{A}^{-0}|$
- $B^{+-}, C^{+-} \rightarrow |A^{+-}|, |\bar{A}^{+-}|$

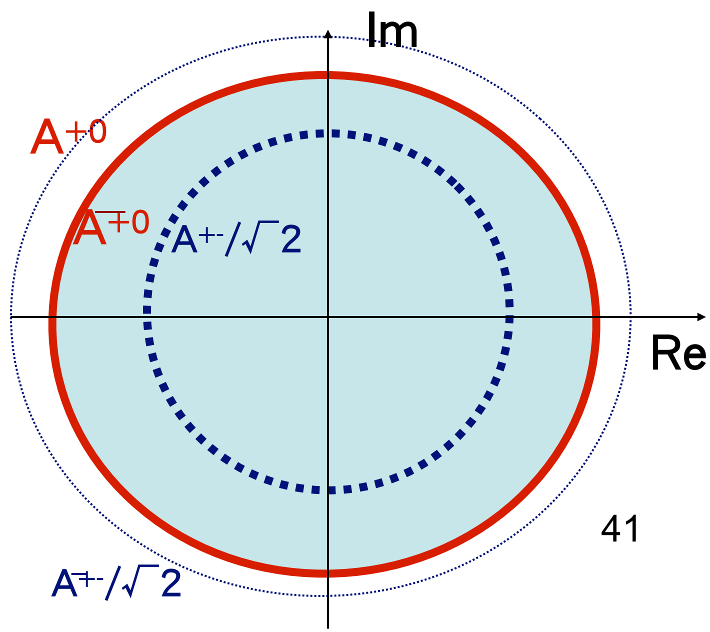

2.4.3 The angle α from $B \rightarrow \pi\pi$

- Use companion modes (ππ) and isospin symmetry to disentangle penguin contributions.

- In addition to the time-dependent analysis parameters *S* and *C*, consider the Branching Fractions of the companion modes.

© O.Deschamps

- Geometrical resolution:

- B^{+0} → $|A^{+0}| = |\bar{A}^{+0}|$
- B^{+-}, C^{+-} → $|A^{+-}|, |\bar{A}^{+-}|$
- S^{+-} → $\sin(2\alpha_{eff})$ → 2-fold α_{eff} in $[0, \pi]$

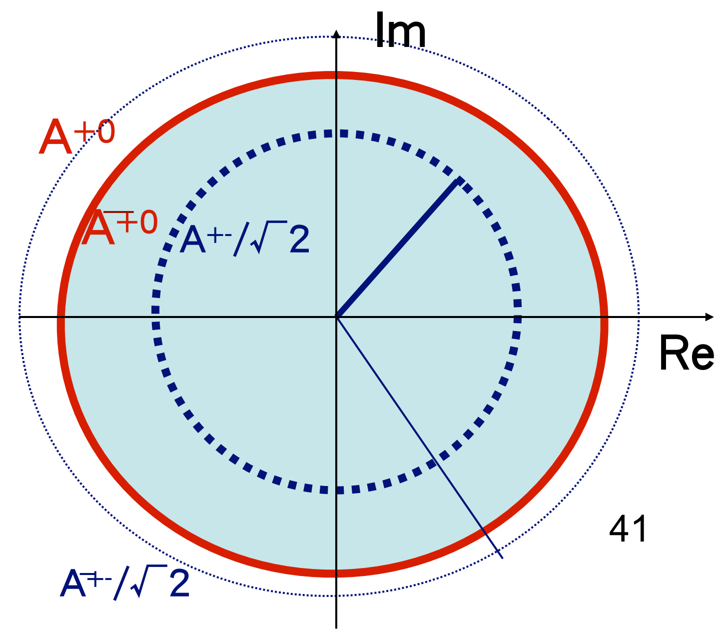

2.4.3 The angle α from $B \to \pi\pi$

• Use companion modes ($\pi\pi$) and isospin symmetry to disentangle penguin contributions.

• In addition to the time-dependent analysis parameters *S* and *C*, consider the Branching Fractions of the companion modes.

• Geometrical resolution:

- B^{+0} $\rightarrow$ $|A^{+0}| = |\bar{A}^{+0}|$
- B^{+-}, C^{+-} $\rightarrow$ $|A^{+-}|, |\bar{A}^{+-}|$
- S^{+-} $\rightarrow$ $\sin(2\alpha_{eff}) \rightarrow$ 2-fold α_{eff} in $[0, \pi]$
- B^{00}, C^{00} $\rightarrow$ $|A^{00}|, |\bar{A}^{00}|$

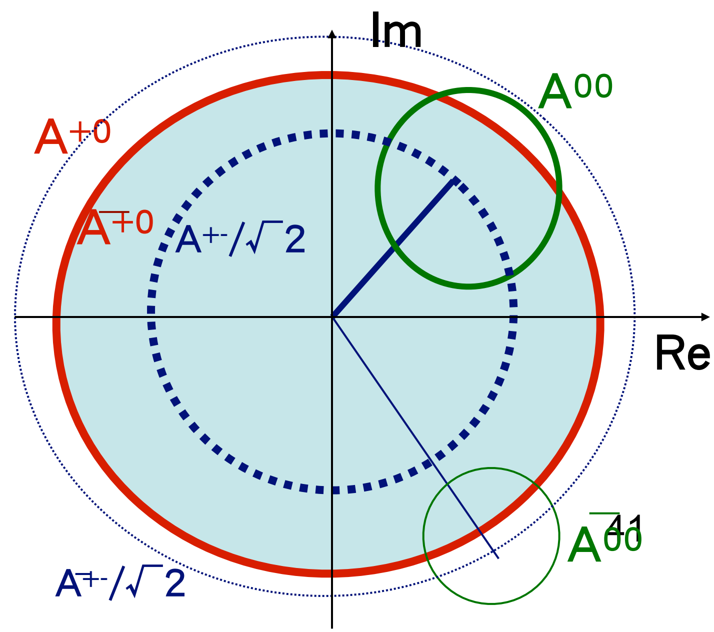

2.4.3 The angle α from $B\to\pi\pi$

- Use companion modes ($\pi\pi$) and isospin symmetry to disentangle penguin contributions.

- In addition to the time-dependent analysis parameters *S* and *C*, consider the Branching Fractions of the companion modes.

- Geometrical resolution:

- B^{+0} → $|A^{+0}| = |\bar{A}^{+0}|$
- B^{+-}, C^{+-} → $|A^{+-}|, |\bar{A}^{+-}|$
- S^{+-} → $\sin(2\alpha_{eff})$ → 2-fold α_{eff} in $[0, \pi]$
- B^{00}, C^{00} → $|A^{00}|, |\bar{A}^{00}|$

• Closing SU(2) triangle → 8-fold α

© O.Deschamps

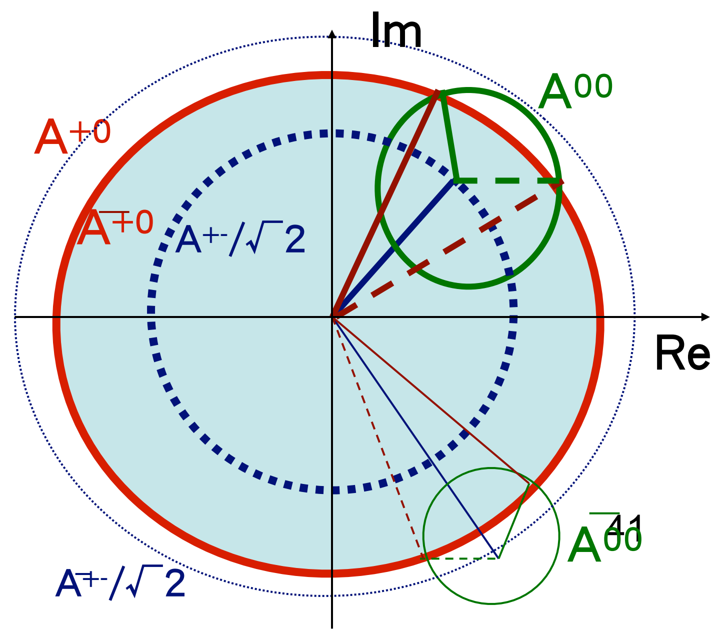

2.4.3 The angle α from $B \rightarrow \pi\pi$

• Use companion modes ($\pi\pi$) and isospin symmetry to disentangle penguin contributions.

• In addition to the time-dependent analysis parameters *S* and *C*, consider the Branching Fractions of the companion modes.

© O.Deschamps

• Geometrical resolution:

- B^{+0} $\rightarrow |A^{+0}| = |\bar{A}^{+0}|$
- B^{+-}, C^{+-} $\rightarrow |A^{+-}|, |\bar{A}^{+-}|$
- S^{+-} $\rightarrow \sin(2\alpha_{eff}) \rightarrow$ 2-fold α_{eff} in $[0, \pi]$
- B^{00}, C^{00} $\rightarrow |A^{00}|, |\bar{A}^{00}|$

•Closing SU(2) triangle $\rightarrow$ 8-fold α

- S^{00} $\rightarrow$ relative phase between A^{00} & A^{00}

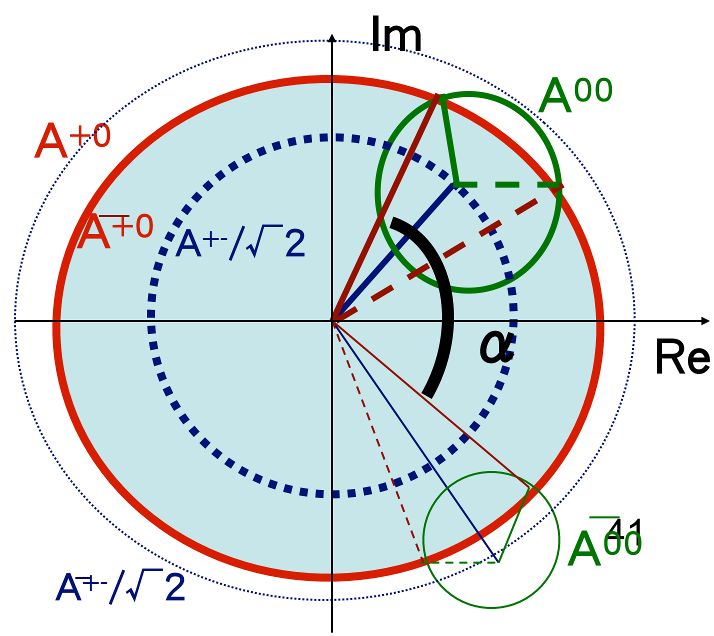

2.4.3 The angle α from $B \to \pi\pi$

- Use companion modes ($\pi\pi$) and isospin symmetry to disentangle penguin contributions.

- In addition to the time-dependent analysis parameters *S* and *C*, consider the Branching Fractions of the companion modes.

© O.Deschamps

- Geometrical resolution:

- B^{+0} → $|A^{+0}| = |\bar{A}^{-0}|$
- B^{+-}, C^{+-} → $|A^{+-}|, |\bar{A}^{+-}|$
- S^{+-} → $\sin(2\alpha_{eff})$ → 2-fold α_{eff} in $[0, \pi]$
- B^{00}, C^{00} → $|A^{00}|, |\bar{A}^{00}|$

- Closing SU(2) triangle → 8-fold α

- S^{00} → relative phase between A^{00} & $\bar{A}^{00}$

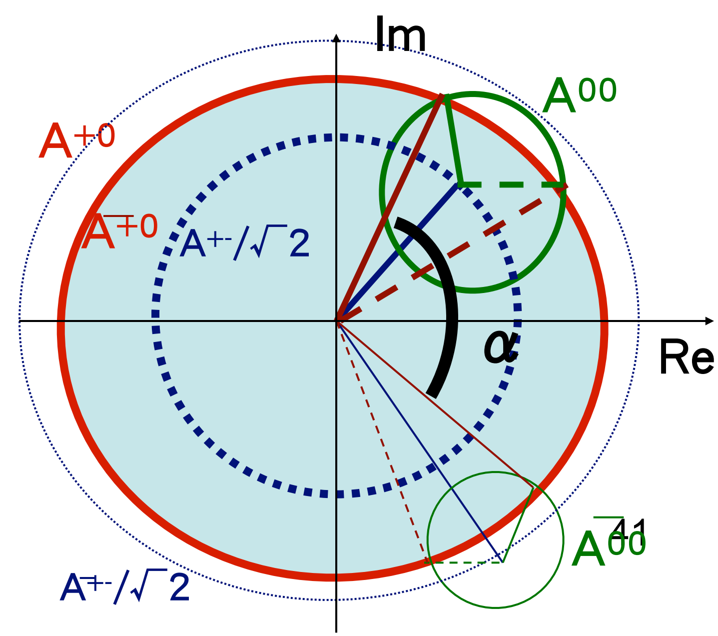

2.4.3 The angle α from $B \to \pi\pi$

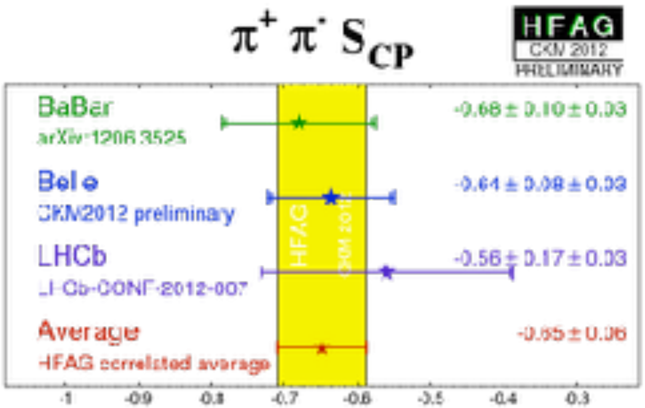

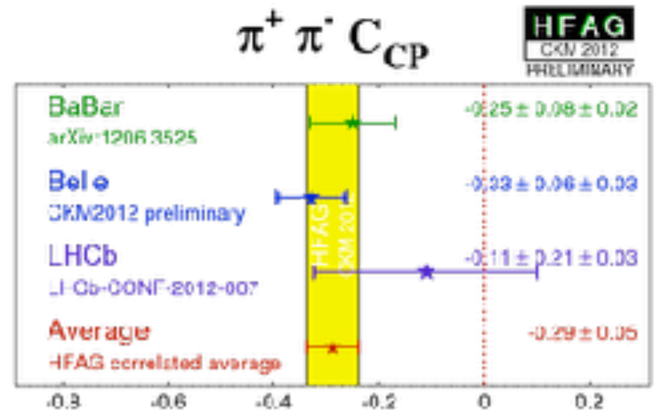

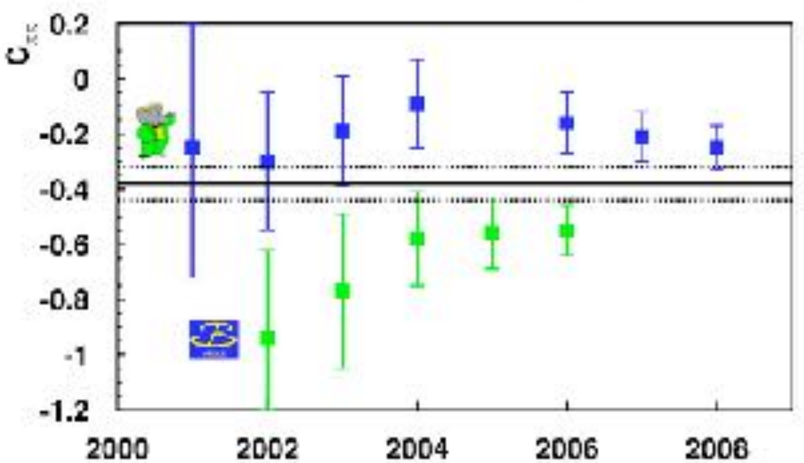

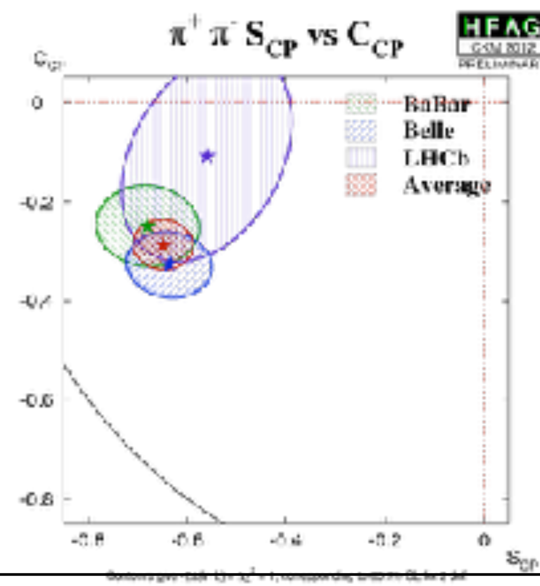

2.4.3 The angle α from $B \to \rho\rho$

- $B \to VV$ process but final state almost pure *CP* state as the decay is saturated with longitudinally polarized ρ's.

- Isospin decomposition same as $B \to \pi\pi$ at first order.

- The inputs of the analysis: $(Br(B \to \rho^+\rho^-), S_{\rho^+\rho^-}, C_{\rho^+\rho^-}, Br(B \to \rho^+\rho^0), Br(B \to \rho^0\rho^0)) + f_L$

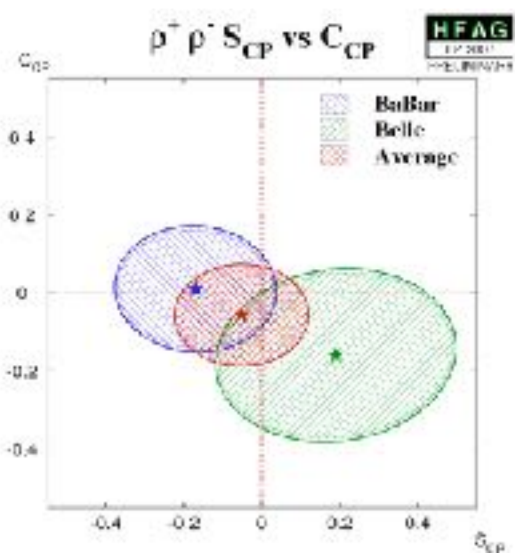

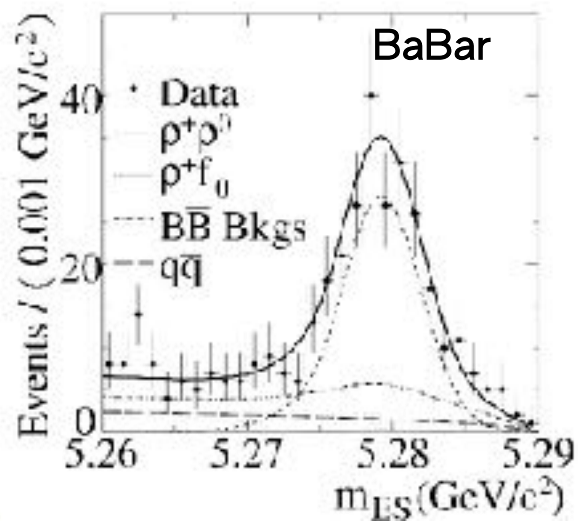

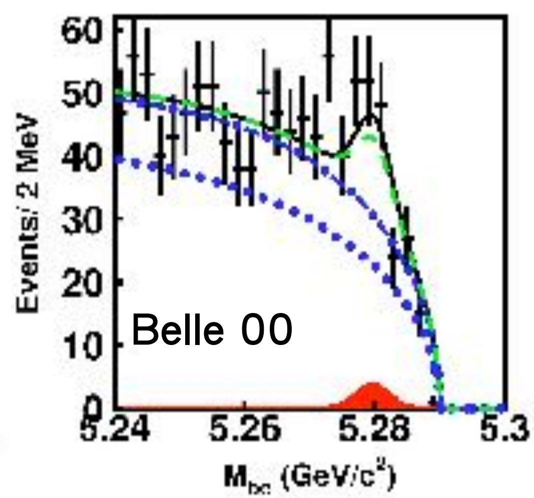

2.4.3 The angle α from $B\rightarrow\rho\rho$

- Inputs :

B^{+-}
B^{0+}
B^{00}
C^{+-}
S^{+-}
C^{00}
S^{00}
f_L^{+-}
f_L^{0+}
f_L^{00}

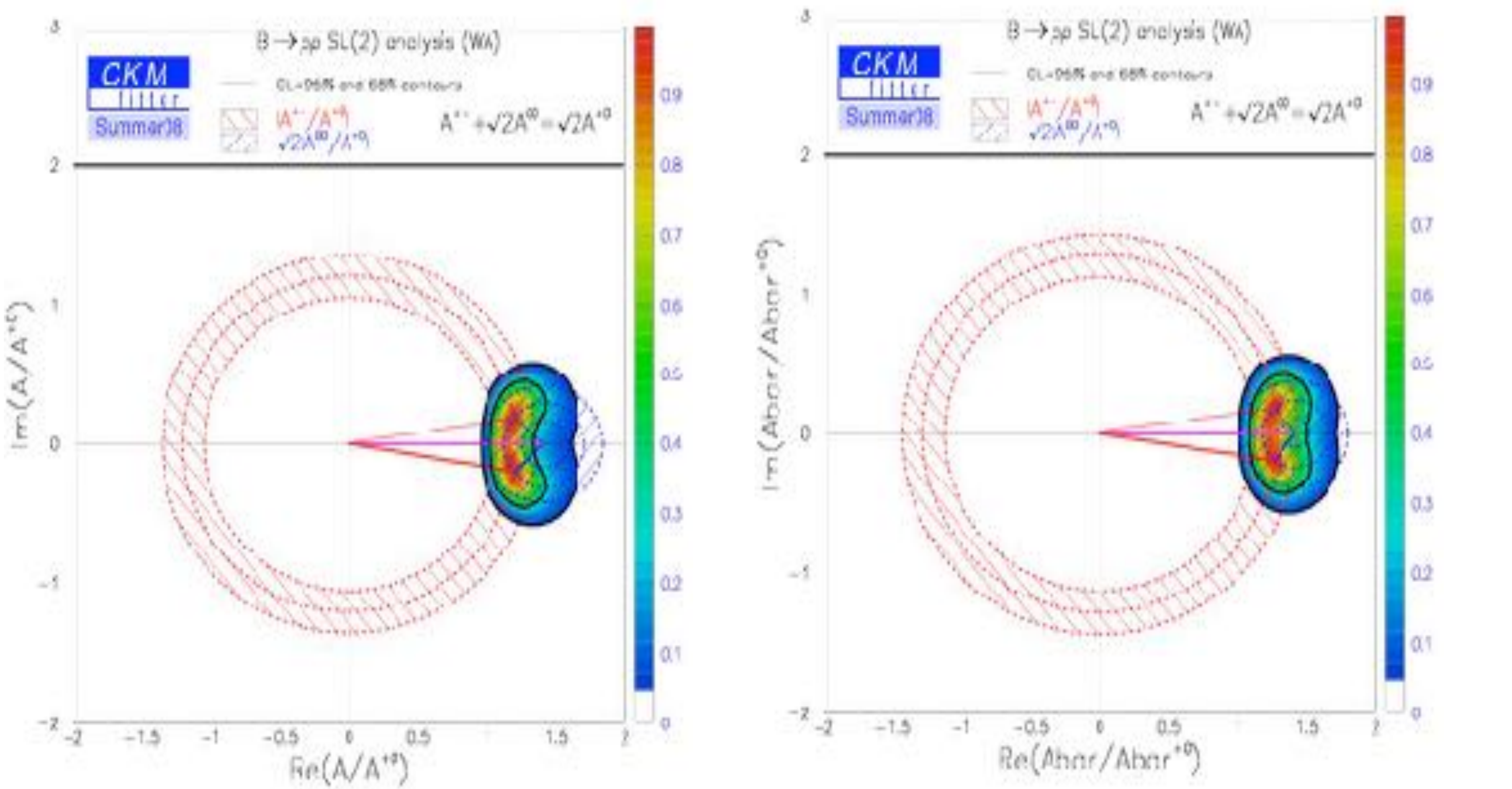

Both triangles (squashed because of the smallness of B^{00}) do close → 8-fold solution for alpha but S^{00} breaks the degeneracy.

2.4.3 The angle α: World Averages

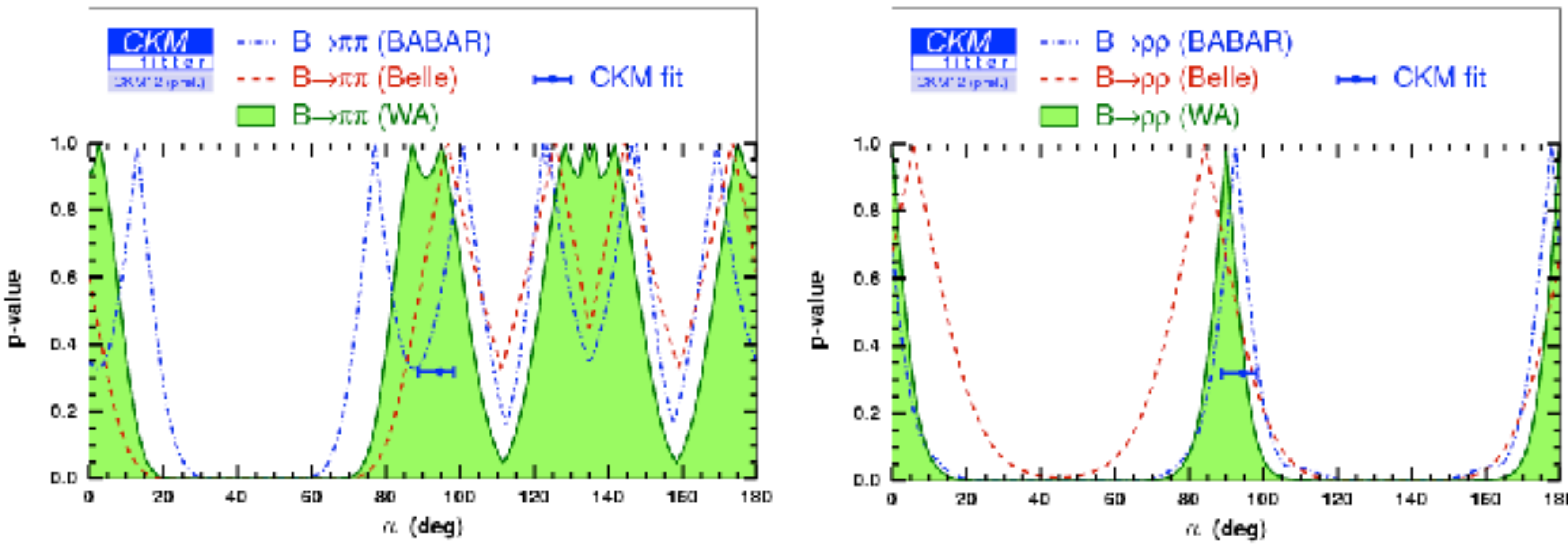

Nice consistency between BaBar and Belle measurements, as well as between $B \to \rho\rho$ and $B \to \pi\pi$.

2.5 The angle α: WA

$$\alpha_{\rm wa} = (88.8 \pm 2.3)^\circ$$

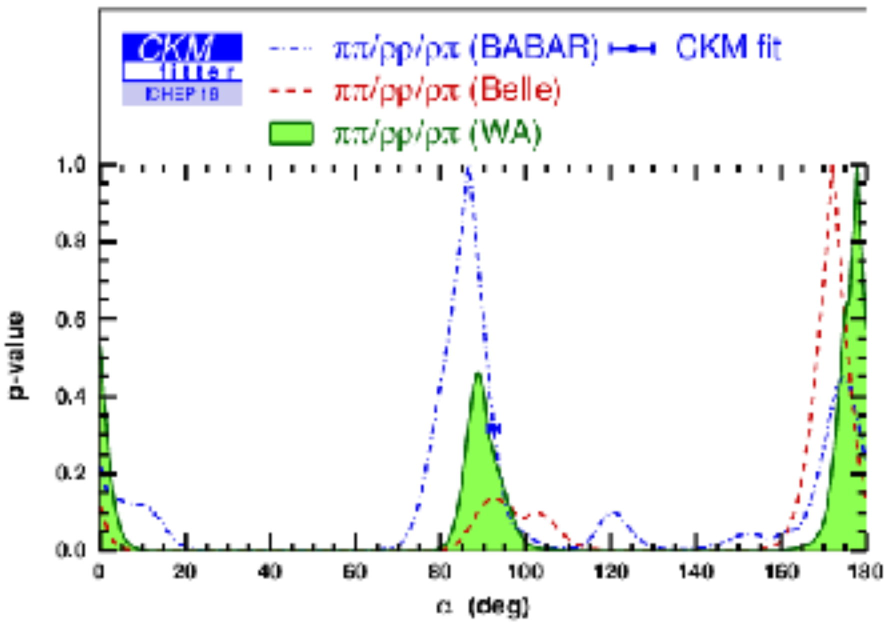

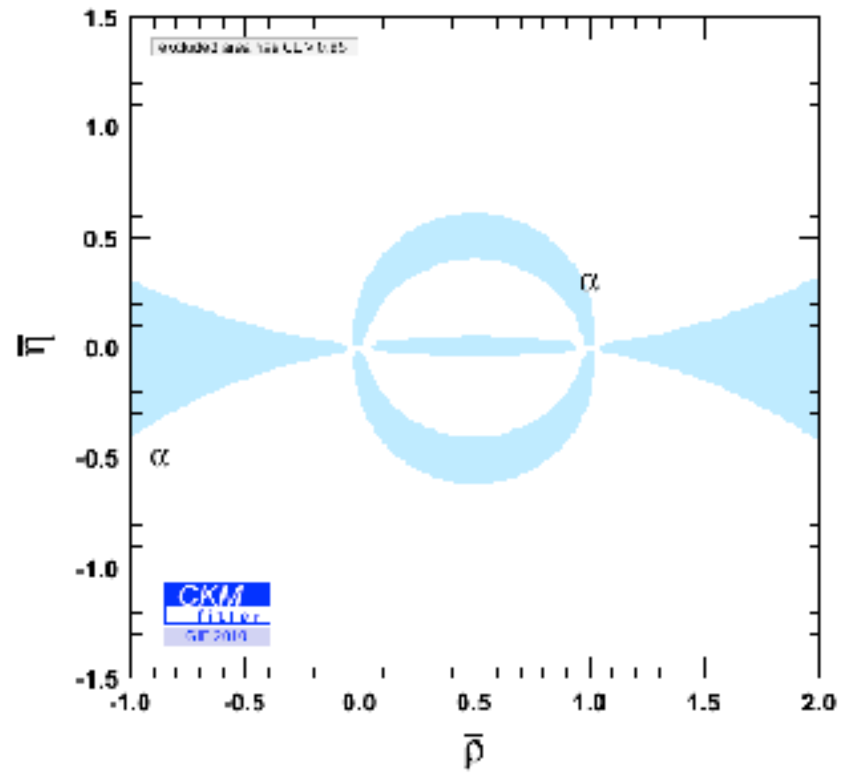

B→ρρ dominates the average. 5% (!) precision measurements.

2.6 The angle γ: principle of the measurement

- The determination of the angle γ requires interferences between charmless b→u transition and another weak phase, say for instance b→c. This interference is realized in decays B→DK.

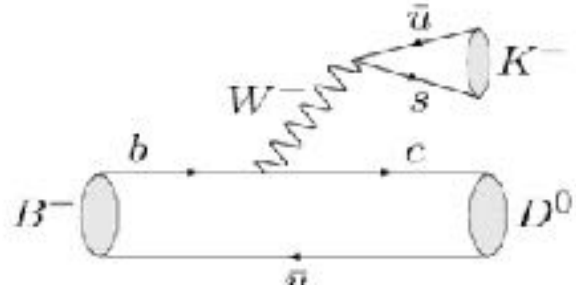

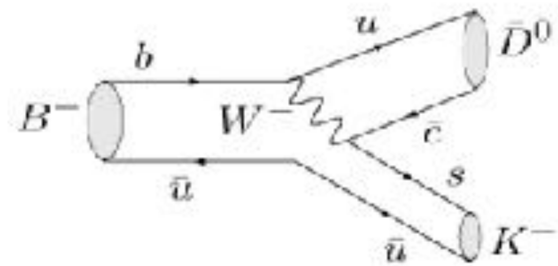

$$A(B^- \to D^0 K^-) = a \qquad \downarrow CP \qquad \bar{A}(B^+ \to \bar{D}^0 K^+) = a$$

$$A(B^- \to \bar{D}^0 K^-) = a e^{-i\gamma} r_B e^{i\delta_B} \qquad \downarrow CP \qquad \bar{A}(B^+ \to D^0 K^+) = a e^{+i\gamma} r_B e^{i\delta_D}$$

- The interference level between b→u and b→c transitions is controlled by the parameter r_B:

$$r_B = \left| \frac{A(B^- \to \bar{D}^0 K^-)}{A(B^- \to D^0 K^-)} \right|$$

- No penguin: theoretically clean. But one has to reach through undistinguishable paths the same final state !

2.6 The angle γ: the methods

- We hence have to reconstruct the *D* mesons in final states accessible to both D^0 and *anti-*D^0. There are three main techniques which have been undertaken at *B* factories:

1. GLW (Gronau, London, Wyler): search for *D* mesons decays into 2-body CP eigenstates, e.g K^+K^-, $\pi^+\pi^-$ (CP=+) or $K_S\pi^0$, ϕK_S (CP=-). Somehow natural but very low branching fractions.

2. ADS (Atwood, Dunietz, Soni): Use *anti-*$D^0 \to K^-\pi^+$ for $b \to u$ transitions (Cabibbo allowed) and $D^0 \to K^-\pi^+$ (Doubly Cabibbo suppressed) for $b \to c$ transitions. Again low branching fractions and additionally one has to know the strong phase of the *D* decay.

3. GGSZ (Giri, Grossman, Sofer, Zupan): use quasi 2-body CP eigenstates of the *D* to be resolved in the Dalitz plane. $D \to K_S\pi^+\pi^-$. So far the most precise gamma determination.

   Note: I used D^0K for illustration. The same stands for D^*K and DK^*. The hadronic factors (r_B, δ_B) are however different in each case.

2.6 The angle γ: a closer look to ADS

©Faye Cheung @ Beauty 2016

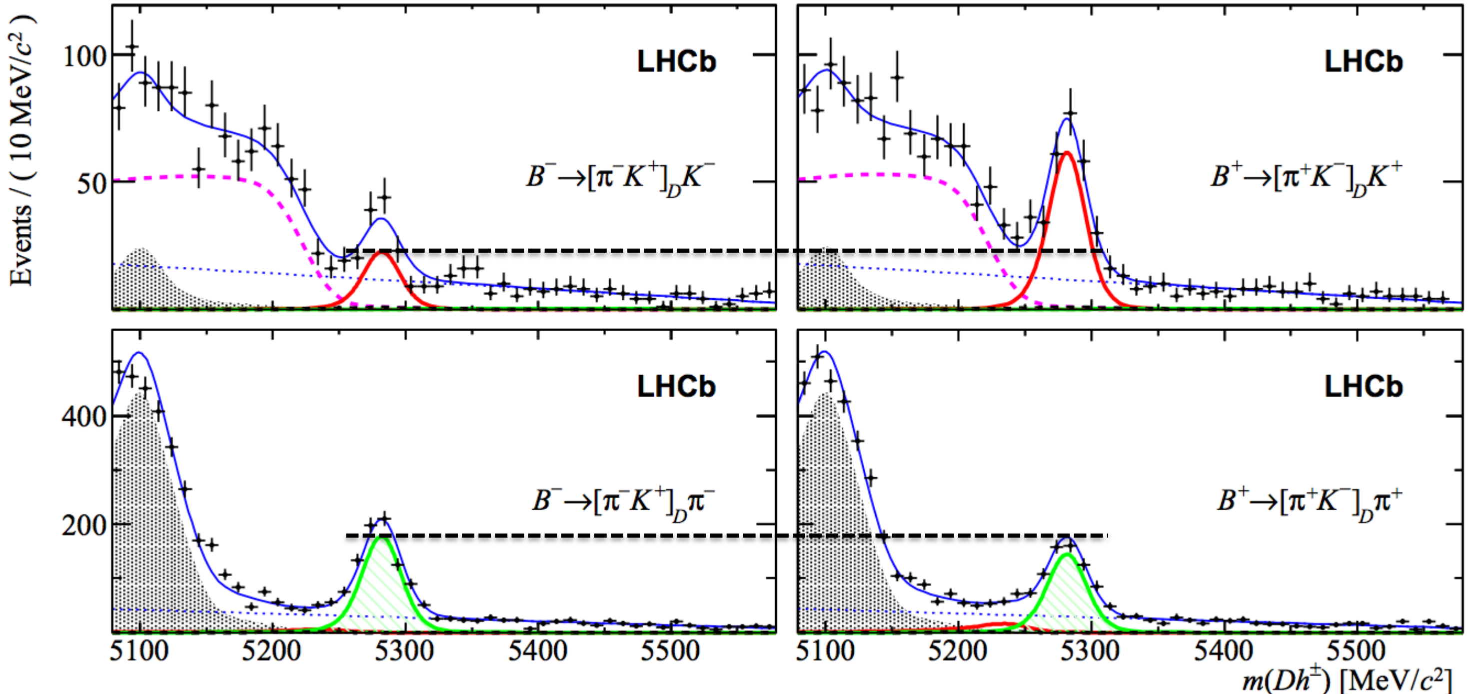

$$A^{\pi K}_{\mathrm{ADS}(K)} = -0.403 \pm 0.056 \pm 0.011$$

8σ First observation of CPV in single $B \to Dh$ decay mode

$$A^{\pi K}_{\mathrm{ADS}(\pi)} = \quad 0.100 \pm 0.031 \pm 0.009$$

2.6 The angle γ: a closer look to GGSZ

- The comparison of the Dalitz planes (DP) of the decays $D^0 \to K_s^0\pi^+\pi^-$ or $K_s^0K^+K^-$ for the transitions $B^+ \to DK^+$ and $B^- \to DK^-$ contains information on γ angle.

- Constrain from CLEO-c measurements the strong phase variation in DP. (Phys. Rev. D 82 (2010) 112006)

- DP binned in regions of similar strong phase:

- Defining:

$$
\begin{aligned}
x_\pm &= r_B\cos(\delta_B \pm \gamma),\\
y_\pm &= r_B\sin(\delta_B \pm \gamma).
\end{aligned}
$$

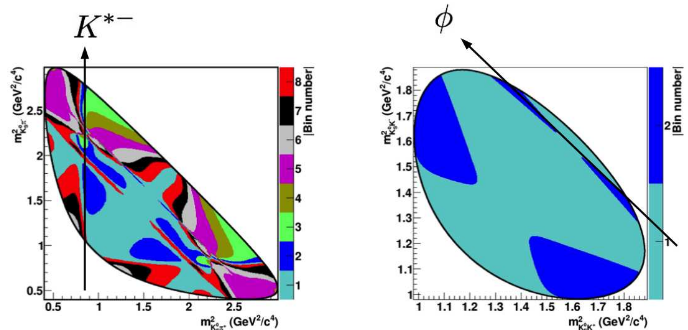

$D \to K_S^0\pi^+\pi^-$ $D \to K_S^0K^+K^-$

- One counts the number of events in each bins *i* for B^+ and B^-:

$$
\begin{aligned}
N^+_{\pm i} &\propto K_{\mp i} + (x_+^2 + y_+^2)K_{\pm i} + 2\sqrt{K_iK_{-i}}[x_+\cos\delta_D(\pm i) \mp y_+\sin\delta_D(\pm i)],\\
N^-_{\pm i} &\propto K_{\pm i} + (x_-^2 + y_-^2)K_{\mp i} + 2\sqrt{K_iK_{-i}}[x_-\cos\delta_D(\pm i) \mp y_-\sin\delta_D(\pm i)].
\end{aligned}
$$

- And solve for the four unknowns *x* and *y*.

2.6 The angle γ: sensitivity GGSZ

• In the Dalitz plane, the level of interference is controlled by the cartesian coordinates (they are the experimental inputs for gamma extraction):

$$x_\pm = r_B \cos(\delta_B \pm \gamma)$$
$$y_\pm = r_B \sin(\delta_B \pm \gamma)$$

• How does the uncertainty on γ scales with r_B? $1/r_B$ …

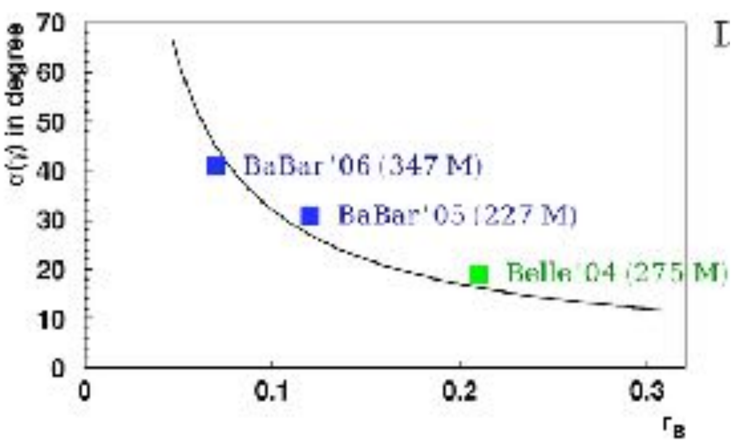

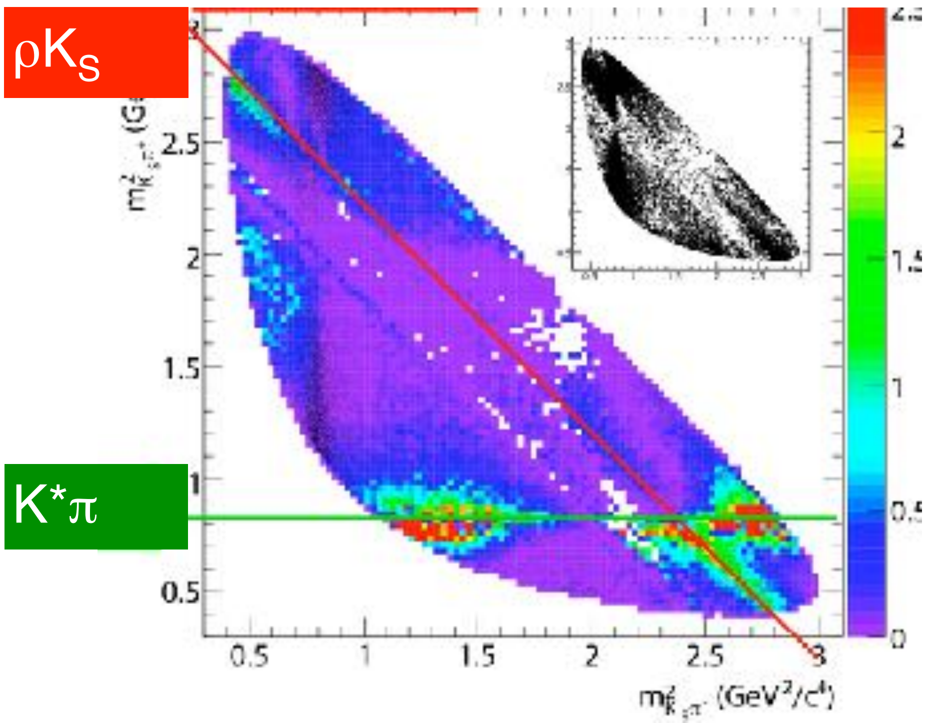

• Sensitivity plot. Which regions of the Dalitz plane do contribute the more to the gamma precision: K*π and ρK$_S$ bands.

2.6 The angle γ: results GGSZ

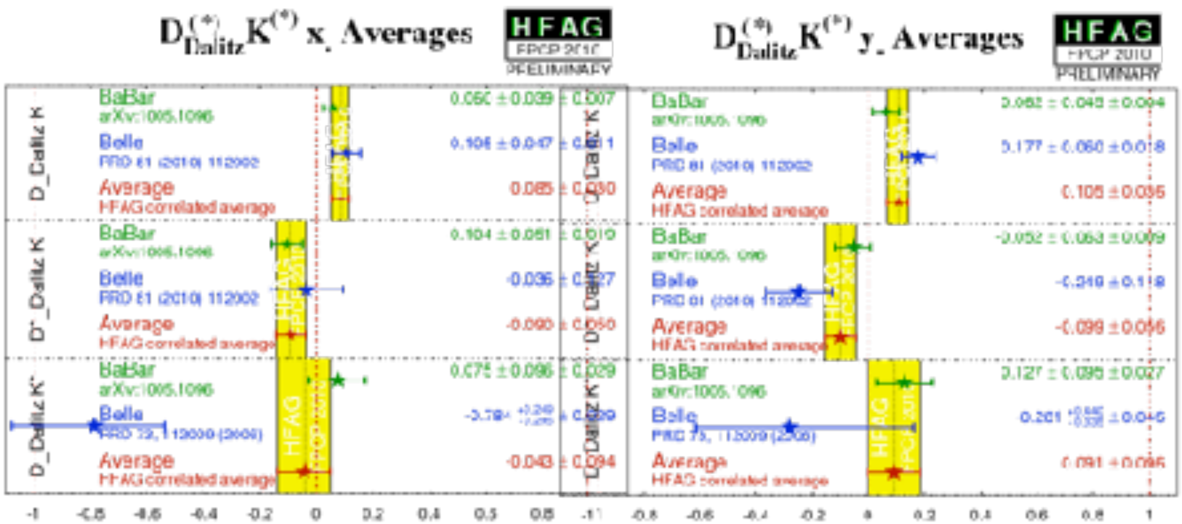

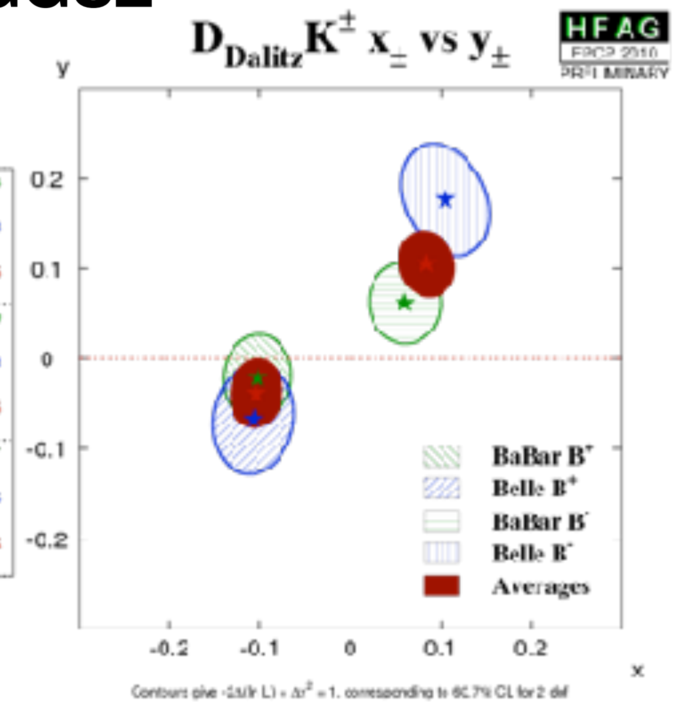

- Best precision for DK mode.

- The BaBar and Belle experiments extracted gamma using a frequentist scheme:

$$\gamma_{\text{BaBar}} = 69\ ^{+15}_{-14}\ (\text{stat.}) \pm 4\ (\text{syst.}) \pm 3(\text{ mod.})\ \text{deg}$$

$$\gamma_{\text{Belle}} = 78\ ^{+11}_{-12}\ (\text{stat.}) \pm 4\ (\text{syst.}) \pm 9(\text{ mod.})\ \text{deg}$$

2.6 The angle γ: results GGSZ LHCb

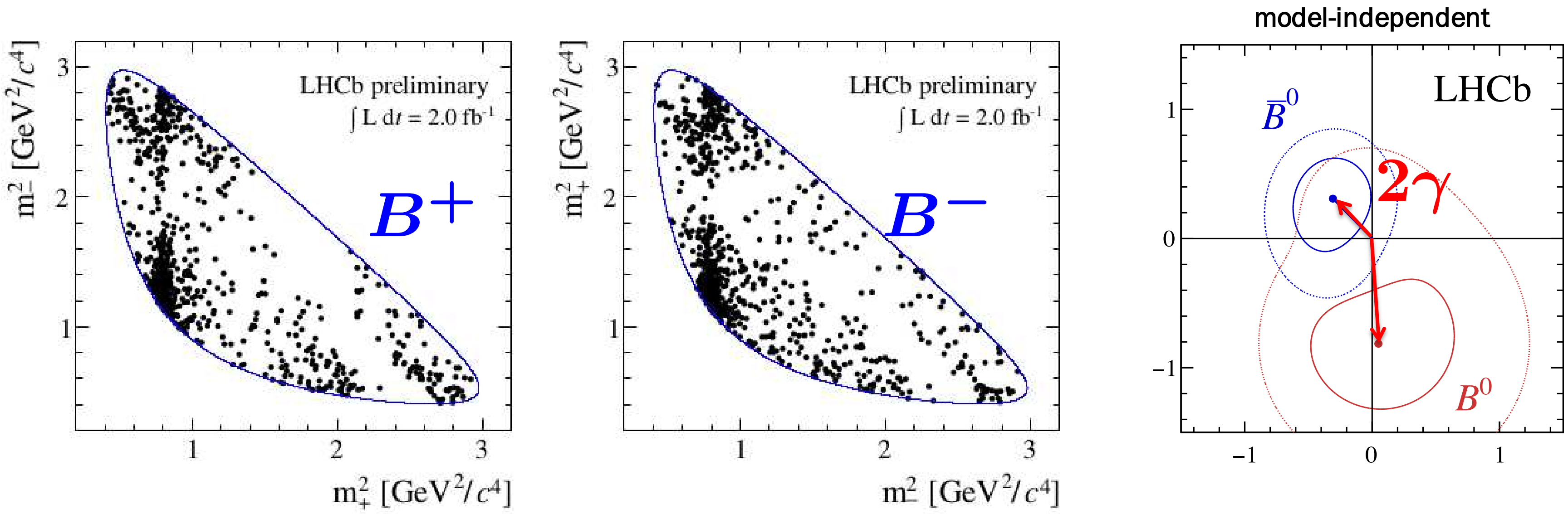

$$r_B = (8.8^{+2.3}_{-2.4})10^{-2},$$
$$\gamma = (57 \pm 16)^\circ$$

(2+1 /fb)

- Best precision for *DK* mode.

2.6 The angle γ: WA

• GGSZ method is nowadays the best way to extract the γ angle. Other methods provide very valuable constraints on r_B and hence contribute to the overall precision.

• The high statistics expected at the LHC will allow to measure the γ angle with a precision comparable to what is achieved with α. LHCb already superseded B-factories precision w/ most of its results obtained w/ 1/fb.

• Though the less well determined angle of the Unitarity triangle, the γ angle measurement is a tremendous achievement of the B factories: was not fully foreseen at the beginning of their operation.

• The γ angle determination makes use of frequentist treatment (MC based) to ensure all the possible values of nuisance parameters (r_B in particular) are tested in the evaluation of the coverage. Significant variation on the global uncertainty w.r.t less sophisticated method. Mandatory for the time being.

2.6 The angle γ: WA

arXiv:1301.2033

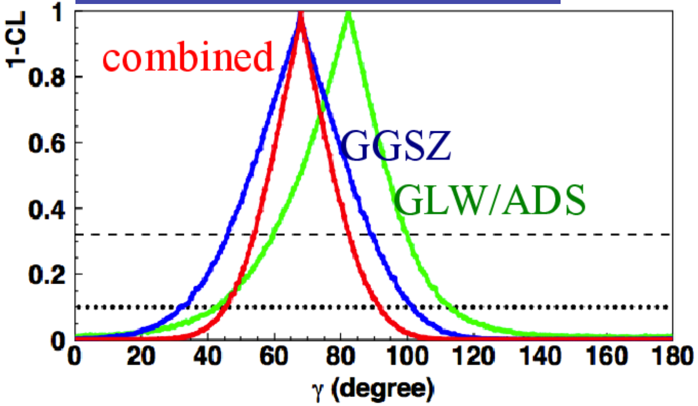

Phys Rev D 87, 052015 (2013)

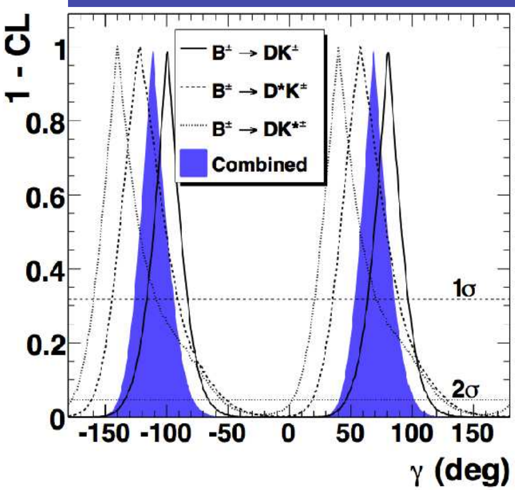

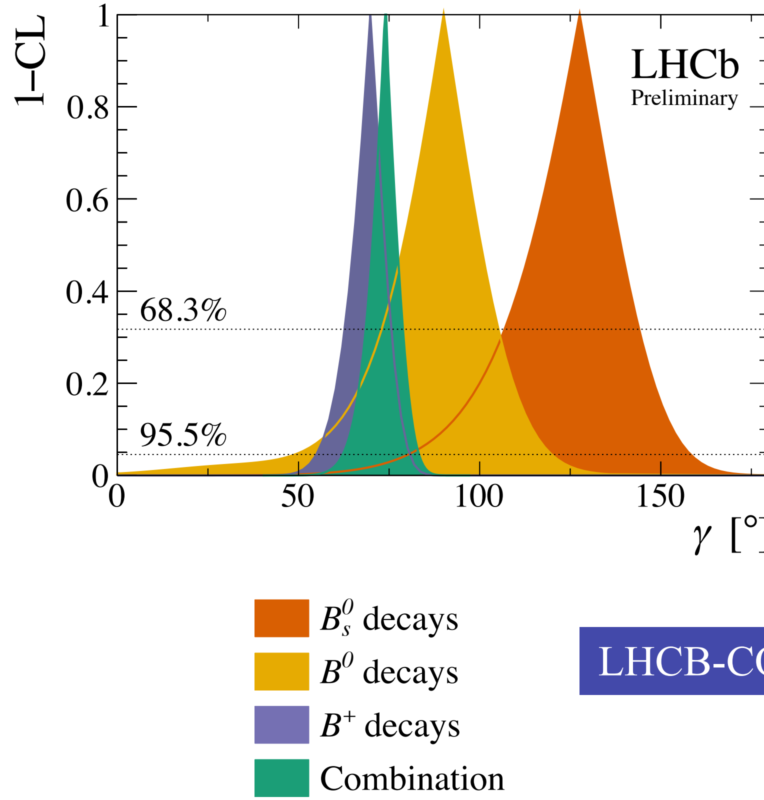

LHCB-CONF-2018-002

$$\gamma_{\mathrm{LHCb}} = (74.0^{+5.8}_{-5.0})^{\circ}$$

2.8 Conclusion of Chapter 2 and introduction to Chapter 3

• We have now all the relevant experimental ingredients to produce the consistency check of all observables in the Standard Model and hence test the KM mechanism. By anticipation, we can produce a unitarity triangle with angles only:

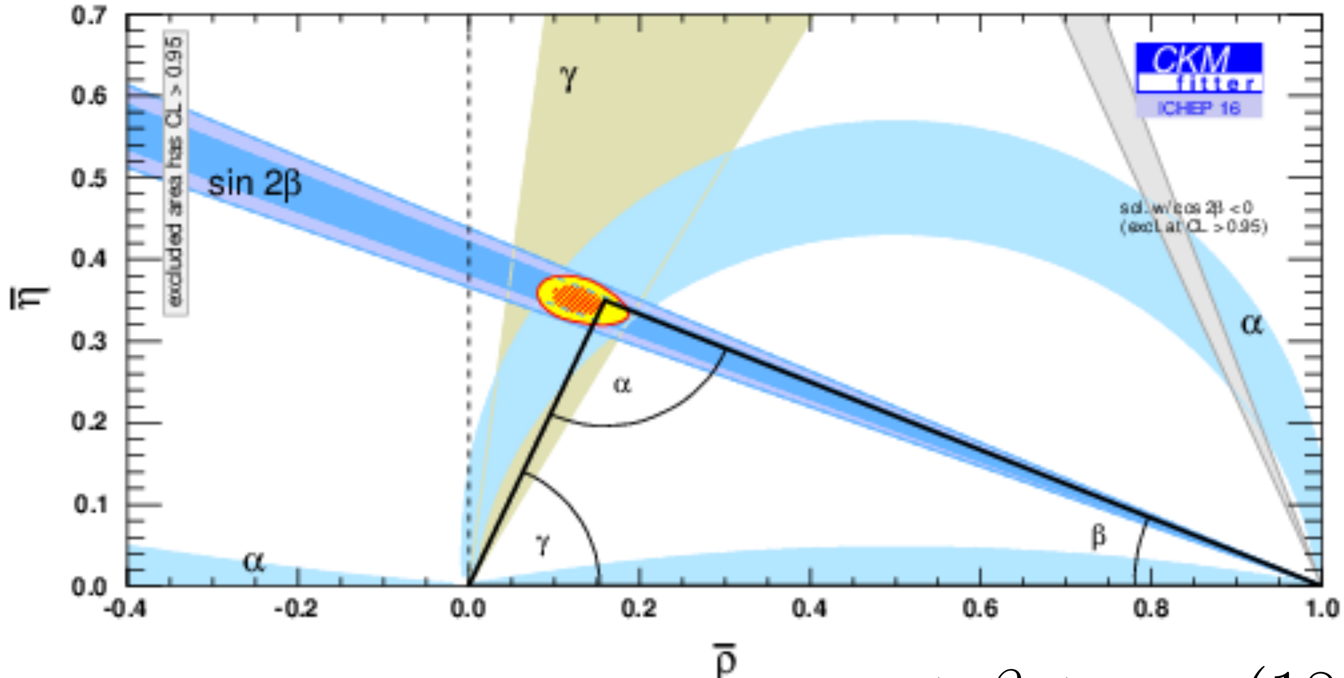

$$\alpha + \beta + \gamma = (186.0 \pm 6.0)^\circ$$